

Dissertation

Expression and function of the chemokine receptor XCR1 on murine CD8⁺ DC

zur Erlangung des akademischen Grades
doctor rerum naturalium
(Dr. rer. nat.)
im Fach Biologie

eingereicht an der Mathematisch-Naturwissenschaftlichen Fakultät I
der Humboldt-Universität zu Berlin

von

Master Biochemiker Ahmed Mora
geboren am 27.12.1978 in Lyon

Präsident der Humboldt-Universität zu Berlin
Prof. Dr. Dr. h.c. Christoph Marksches

Dekan der Mathematisch-Naturwissenschaftlichen Fakultät I
Prof. Dr. Lutz-Helmut Schön

Gutachter: 1. Prof. Dr. Peter-Michael Kloetzel
 2. Prof. Dr. Richard Kroczyk
 3. Dr. Michal Or-Guil

Tag der mündlichen Prüfung: 16-03-2010

Summary

The G protein-coupled receptor XCR1 has been described as the sole receptor for the chemokine ATAC. As contradictory data were published on the expression pattern of XCR1, its role in the immune system has not yet been defined.

In this work, expression of XCR1 was characterized in B6.XCR1-lacZ^{+/+} reporter mice which express β -galactosidase under the control of the XCR1 promoter. In tissue sections, strong expression of XCR1 was only detected in lymphoid organs like spleen, lymph nodes and thymus. In the spleen, XCR1⁺ cells were mainly found in the marginal zones, but also in the red pulp and the T cell zones. Flow cytometric analysis demonstrated exclusive expression of XCR1 on DC, mainly on the CD8⁺ DC subset, but also on a minority of CD4⁻CD8⁻ DC. *In vivo*, these XCR1⁺ cells migrated in response to chemotactic or inflammatory stimuli: application of either an ATAC-expressing cell line or LPS induced within 3 - 9 h the translocation of XCR1⁺ cells to the T cell area of the spleen. When tested for phagocytic capacity, XCR1⁺ CD8⁺ DC, but not other DC subsets, specifically took up injected allogeneic cells, and transfection of these cells with ATAC significantly enhanced their endocytosis by XCR1⁺ CD8⁺ DC. Thus, we could employ allogeneic cells expressing OVA intracellularly to target antigen selectively to XCR1⁺ DC. This antigen targeting induced a strong antigen-specific cytotoxic response by endogenous T cells without a generation of OVA-specific antibodies. In the absence of ATAC, the endogenous cytotoxic activity was markedly diminished. Adoptive transfer and activation of wild type or ATAC-deficient OVA-specific CD8⁺ transgenic T cells confirmed that ATAC is required for the generation of an optimal cytotoxic response. Targeting of antigen to CD8⁺ DC via XCR1 may thus be a promising strategy for the development of new vaccination approaches aimed at optimizing the induction of cytotoxic T cells.

Keywords:

XCR1, ATAC, CD8⁺ DC, cytotoxic T cells.

Zusammenfassung

Der G-Protein-gekoppelte Rezeptor XCR1 ist der einzige Bindungspartner für das Chemokin ATAC. Da die publizierten Daten über das Expressionsmuster von XCR1 widersprüchlich sind, konnte seine Funktion im Immunsystem noch nicht definiert werden.

In dieser Arbeit wurde die Expression von XCR1 in B6.XCR1-lacZ^{+/+} Reporter-Mäusen charakterisiert, die β -Galaktosidase unter der Kontrolle des XCR1-Promotors exprimieren. In Gewebeschnitten konnten wir zeigen, dass eine starke XCR1-Expression nur in lymphatischen Organen wie Milz, Lymphknoten und Thymus nachweisbar ist. In der Milz fanden sich XCR1⁺ Zellen vor allem in der Marginal-Zone, aber auch in der roten Pulpa und der T-Zell-Zone. Durchflusszytometrische Analysen zeigten, dass XCR1 in der Milz ausschließlich von dendritischen Zellen (DZ) exprimiert wird, hauptsächlich von der CD8⁺ DZ Subpopulation aber auch von einer Minderheit der CD4⁻ CD8⁻ DZ. In vivo migrierten diese XCR1⁺ Zellen nach Applikation von chemotaktischen oder inflammatorischen Substanzen: Die Injektion sowohl einer ATAC-sezernierenden Zelllinie als auch von LPS lösten nach 3 - 9 h eine Translokation der XCR1⁺ Zellen in die T-Zell-Zone der Milz aus. Untersuchungen der Phagozytose-Aktivität ergaben, dass nur XCR1⁺ CD8⁺ DZ, aber keine anderen DZ Subpopulationen, injizierte allogene Zellen aufnahmen, und dass eine Transfektion dieser Zellen mit ATAC diese Phagozytose signifikant verstärkte. Daher konnten wir allogene Zellen, die intrazellulär Ovalbumin (OVA) exprimierten, für die selektive Applikation von Antigen auf XCR1⁺ DZ verwenden. Diese selektive Antigen-Applikation induzierte eine starke antigenspezifische zytotoxische Antwort von endogenen T-Zellen, ohne dass es zur Produktion von OVA-spezifischen Antikörpern kam. In Abwesenheit von ATAC war diese endogene zytotoxische Aktivität verringert. Durch adoptivem Transfer und Aktivierung von Wildtyp- oder ATAC-defizienten OVA-spezifischen transgenen CD8⁺ T-Zellen konnten wir bestätigen, dass ATAC für die Erzeugung einer optimalen zytotoxischen Antwort benötigt wird. Die selektive Applikation von Antigen auf CD8⁺ DZ stellt daher eine vielversprechende Strategie dar, um optimierte Vakzinierungs-Ansätze für die Auslösung einer zytotoxischen Immunantwort zu entwickeln.

Schlagwörter:

XCR1, ATAC, CD8⁺ DZ, zytotoxische T-Zellen.

Table of Contents

Table of Contents	I
List of Figures	V
List of Tables	VII
1 Introduction	1
1.1 Dendritic cells	1
1.1.1 Murine DC subsets	1
1.1.2 Dendritic cells in peripheral tissues	3
1.1.3 Localization and migration of DC	4
1.1.4 Antigen uptake by DC	4
1.1.5 Antigen presentation by DC	6
1.2 Chemokines and chemokine receptors	7
1.2.1 Structure and subclasses	7
1.2.1.1 Chemokines	7
1.2.1.2 Chemokine receptors	8
1.2.2 Chemokine functions	8
1.3 ATAC and ATAC-receptor (XCR1)	9
1.3.1 ATAC	9
1.3.2 ATAC-receptor (XCR1)	11
1.4 In vivo antigen targeting models to enhance immune responses	12
1.5 Objective	14
2 Materials and methods	15
2.1 Equipment, chemicals and consumables	15
2.1.1 Equipment	15
2.1.2 Chemicals and consumables	16
2.2 Buffers, reagents and cell culture media	16

Table of Contents

2.3	Mice	17
2.4	Cell biology	18
2.4.1	Cell culture	18
2.4.2	Transfection of 300-19 cells	19
2.4.3	Isolation of cells from lymph nodes or spleens	19
2.4.4	Enrichment of murine dendritic cells by density gradient centrifugation	19
2.4.5	Cell Labeling with CFSE	20
2.4.6	In vivo CTL activity assessment	20
2.5	Generation of a monoclonal antibody directed against murine XCR1	21
2.5.1	Immunization against the XCR1 receptor	21
2.5.2	Hybridoma fusion with polyethylenglycol (PEG) and selection	21
2.5.3	Screening of positive clones expressing an antibody directed against XCR1	22
2.6	Molecular biology	22
2.6.1	Generation of a XCR1 expression vector	22
2.6.2	Cloning of the delta-OVA protein	23
2.6.3	Polymerase chain reaction (PCR)	23
2.6.4	Transformation of <i>E. coli</i>	23
2.6.5	Plasmid preparation	24
2.7	Flow Cytometry	24
2.7.1	Monoclonal antibodies & fluorochromes	24
2.7.2	Surface staining	25
2.7.3	Detection of β -galactosidase activity in single cell	26
2.7.4	Annexin V apoptosis assay	27
2.7.5	Detection of ATAC expression	27
2.8	Histology	27

2.8.1	Tissue preparation and cryosections	27
2.8.2	Immunohistochemistry analysis	28
2.8.3	X-gal (LacZ) histochemistry staining	28
2.9	Animal experimental methods	29
2.9.1	Immunization	29
2.9.2	Adoptive transfer	29
2.9.3	In vivo uptake of cells in the spleen	29
2.9.4	In vivo depletion of Natural Killer cells	29
2.10	Immunological methods	30
2.10.1	Analysis of Ova-specific antibodies using ELISA	30
2.11	Statistics	30
3	Results	31
3.1	Characterization of XCR1 expression	31
3.1.1	Generation of monoclonal antibodies against murine XCR1	31
3.1.2	Detection of XCR1 expression using B6.XCR1-LacZ ^{+/+} reporter mice	33
3.1.2.1	XCR1 expression in murine tissues	33
3.1.2.2	XCR1 expression in murine cell subsets	36
3.1.2.2.1	Histochemical staining using X-gal combined with immunohistology	36
3.1.2.2.2	Analysis of XCR1-LacZ expression in spleen and LN cell subsets by flow cytometry	38
3.2	Migration of XCR1 ⁺ cells in the spleen	42
3.2.1	LPS induces translocation of splenic XCR1 ⁺ cells to the T cell areas	42
3.2.2	localization of XCR1 ⁺ cells after ATAC application	44
3.3	Uptake of allogeneic cells by APC	45
3.3.1	In vivo uptake of allogeneic splenocytes or cell line	45
3.3.2	Kinetics of the uptake of an allogeneic cell line by CD8 ⁺ DC	46

Table of Contents

3.3.3	NK cell depletion has no effect on the uptake of allogeneic cell lines	46
3.3.4	Only XCR1 ⁺ CD8 ⁺ splenic DC take up live allogeneic cell	48
3.3.5	ATAC/XCR1 interaction increases the uptake of allogeneic cells by CD8 ⁺ DC	49
3.3.6	ATAC binds to the cell membrane of apoptotic cell lines	50
3.4	Antigen targeting to CD8 ⁺ DC leads to cellular but not to humoral immunity	51
3.5	Influence of ATAC secretion on the development of cytotoxicity	54
3.5.1	Induction of cytotoxicity after adoptive transfer	55
3.5.1.1	ATAC/XCR1 interaction increases the cytotoxicity activity of CD8 ⁺ T cells	56
3.5.2	Induction of endogenous cytotoxicity	59
4	Discussion	61
4.1	Detection of XCR1 expression in murine tissues and cell subsets	61
4.2	Localization and migration of CD8 ⁺ DC expressing XCR1	63
4.3	XCR1 and the uptake of allogeneic cells	64
4.4	ATAC binds to the cell surface of late apoptotic cells	66
4.5	Antigen targeting to CD8 ⁺ DC using an allogeneic cell line in vivo	67
4.6	Role of ATAC/XCR1 interaction in the induction of cytotoxic CD8 ⁺ T cells	68
	Reference List	71
	Abbreviations	81
	Acknowledgements	84
	Publications	85
	Eidesstattliche Erklärung	86

List of Figures

Fig. 1:	DC subtypes	2
Fig. 2:	Live cells gating strategy	26
Fig. 3:	XCR1 transfected cell line coexpressing YFP	31
Fig. 4:	Screening of clones producing a mAb against murine XCR1	32
Fig. 5:	Analysis of hybridoma supernatant using enriched DC	33
Fig. 6:	XCR1 expression in murine tissues	35
Fig. 7:	Steps of the newly established double-staining protocol for X-gal staining and IHC	37
Fig. 8:	Double staining of X-gal and CD8 or CD11c in axillary lymph nodes	38
Fig. 9:	XCR1 expression in spleen and LN	39
Fig. 10:	Correlation of XCR1 and CD205 expression in the spleen and the LN	41
Fig. 11:	CD8 ⁺ DC translocate to the T cell zone in the spleen after LPS injection	43
Fig. 12:	ATAC induce expansion of XCR1 signal in the T cell area	44
Fig. 13:	Uptake of allogeneic cells by CD8 ⁺ DC	45
Fig. 14:	Uptake kinetics of the allogeneic cell line 300-19-wt	46
Fig. 15:	NK cell depletion has no effect on the uptake of allogeneic cells by CD8 ⁺ DC	47
Fig. 16:	300-19 allogeneic cells are selectively taken up by XCR1 ⁺ CD8 ⁺ DC	48
Fig. 17:	Increase in the uptake of the 300-19 cell line expressing ATAC by CD8 ⁺ DC	49
Fig. 18:	ATAC binds on the cell surface to apoptotic cell	51
Fig. 19:	delta OVA-YFP transfected cell line	52
Fig. 20:	Model of the immune response using an allogeneic cell line that targets antigen to CD8 ⁺ DC	52
Fig. 21:	OVA-specific immunoglobulin production	53
Fig. 22:	<i>In vivo</i> CTL activity against SIINFELK-loaded B6 splenocytes	54
Fig. 23:	Presentation of intracellular OVA to OT-I but not OT-II transgenic T cells	55

Fig. 24: Overview of the adoptive transfer system used to test the influence of ATAC/XCR1 interaction on the induction of CTL.	56
Fig. 25: Influence of ATAC/XCR1 interaction on the differentiation of CD8 ⁺ T cells into effector cells	57
Fig. 26: Overview of the adoptive transfer system used to test CTL induction in the same recipient mice.	57
Fig. 27: CTL induction in B6 recipient mice after transfer of B6 OT-I versus B6.OT-I/ATAC-KO	58
Fig. 28: The development of endogenous OVA-specific cytotoxic activity.....	60

List of Tables

Tab. 1:	Equipment list	15
Tab. 2:	List of buffers and reagents.....	16
Tab. 3:	Cell lines and appropriate cell media.....	18
Tab. 4:	Used monoclonal antibodies	24
Tab. 5:	Flurochromes overview	25
Tab. 6:	Summary of tissues examined for β -galactosidase activity	34
Tab. 7:	Percentages of FDG ⁺ cDC subtypes in spleen and LN.....	40
Tab. 8:	Immunization for the induction of endogenous cytotoxicity	59

1 Introduction

1.1 Dendritic cells

Dendritic cells (DC) are bone-marrow-derived leukocytes first observed in 1970s studies carried out by Steinman on cultured cells purified from lymphoid organs (Steinman and Cohn, 1973). Immature DC present in peripheral tissues are known for antigen uptake by various mechanisms, but have a low expression of MHC (Major Histocompatibility Complex) molecules and can not efficiently activate T cells. After interaction with microbial products (e.g. LPS or CpG) through Toll-like receptors (TLRs) (Iwasaki and Medzhitov, 2004) or cell-damage products through C type lectin receptors (Engering et al., 2002), immature DC migrate towards secondary lymphoid organs where they develop into mature DC. Mature DC strongly up regulate T-cell co-stimulatory molecules (e.g. CD80 and CD86), present antigen on MHC I or II complexes, and efficiently induce T cell responses (Shortman and Liu, 2002; Wilson et al., 2004).

1.1.1 Murine DC subsets

The two main categories of mouse DC are plasmacytoid DC (pDC) and conventional DC (cDC). pDC present in the peripheral blood and lymphoid organs were recognized as potent producers of interferon α and β upon viral infection. They can be distinguished from the conventional DC by expression of the cell surface markers B220, Ly6C, CD45RA and intermediate level of CD11c (Nakano et al., 2001; Villadangos and Young, 2008). cDC present in spleen, thymus and lymph nodes (LN) can be further sub-grouped into two categories: “migratory” or “resident” DC. Migratory DC contain two further subtypes: interstitial and Langerhans DC. Interstitial or dermal DC originate from the dermis, while Langerhans DC reside in the skin epidermis. After exposure to activating substances, both can migrate towards subcutaneous LN. Migratory DC are absent in the spleen and thymus. The second cDC group represented by blood-derived or resident DC are present in the spleen, the thymus, and LN. Resident DC are subdivided into three further groups according to the expression of CD4 or CD8: CD4⁺ DC, CD8⁺ DC and double negative CD4⁻CD8⁻ DC (Shortman and Naik, 2007; Villadangos and Schnorrer, 2007).

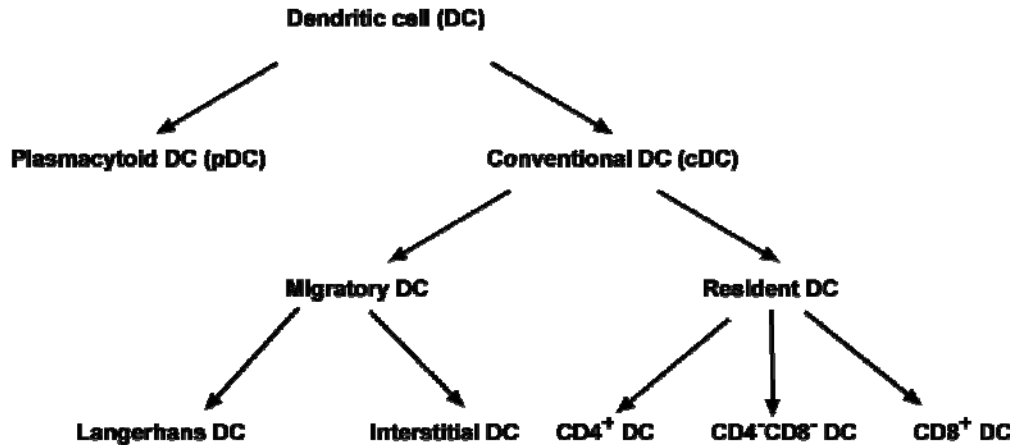


Fig. 1: DC subtypes

Differences in cDC surface marker expression and frequencies in spleen and lymph node are summarized in Tab. 1.

Tab. 1: Mouse DC subtypes in spleen and lymph nodes (Shortman and Naik, 2007; Villadangos and Schnorrer, 2007)

DC subtypes	Resident DC			Migratory DC	
Features	CD4 ⁺	CD8 ⁺	CD4 ⁻ CD8 ⁻	Interstitial	Langerhans
Location/percentage of total DC:					
Spleen	56 %	23 %	20 %	> 4 %	> 1 %
Lymph nodes	4 %	17%	17%	20%	30 %
Surface markers:					
CD11c	+++	+++	+++	+++	+++
CD4	+	-	-	-	-
CD8	-	++	-	-	+/-
CD11b	++	-	++	++	++
CD24	+	++	+	?	?
CD205	-	++	+/-	+	+++
CD207	-	+	-	-	+++
Functional features in steady state:	Immature	Immature	Immature	Mature	Mature
Co-stimulation	+	+	+	++	++
Antigen presentation	+++	+++	+++	+/-	+/-
MHC-II	++	++	++	+++	+++

After infection or inflammation, inflammatory monocytes are recruited from the blood to lymphoid tissues and become inflammatory DC. One example for inflammatory DC are Tip DC that produce Tumor-Necrosis Factor- α (TNF- α) and inducible Nitric-Oxide Synthase (iNOS) after the infection with *Listeria monocytogenes* (Serbina et al., 2003; Shortman and Naik, 2007).

1.1.2 Dendritic cells in peripheral tissues

DC are found in all organs and constitute a complex system of professional APC. In the liver, CD11c conventional DC are subdivided into 4 subgroups according to the expression of CD8 or CD11b into CD8⁺CD11b⁻, CD8⁻CD11b⁺, CD8^{low}CD11b^{low} and CD8⁻CD11b⁻ (Pillarisetty et al., 2004). The role of cDC in the liver was shown after selective depletion of CD11c⁺ cells when it was found that cDC express high levels of costimulatory molecules and effectively cross-present antigens to T cells (Plitas et al., 2008).

In the lung, two DC subsets were identified according to the expression of CD103: CD103⁺ (CD11c^{high}CD11b^{low}) and CD103⁻ (CD11c^{int}CD11b^{high}). Both subtypes are present in the airway and lung-draining bronchial lymph nodes. It was found that the CD103⁺ subset can cross-present antigen to CD8⁺ T cells while the CD103⁻ subset presents antigen to CD4⁺ T cells after antigen inhalation (del Rio et al., 2007; Jakubzick et al., 2008). In an influenza virus study it was found that respiratory DC, especially CD11c⁺CD103⁺ cDC and CD11c⁺B220⁺ plasmacytoid DC, are targeted by the virus and play a role in responses to the infection (Hao et al., 2008).

In the testis, it was reported that DC express MHC I or II molecules and play a role in the suppression of the immune response and T cell activation. On the other hand it was reported in a study using heat shock proteins as testicular auto-antigens that testis DC induce autoreactive lymphocytes, which led to subsequent damage of testicular tissue by breaking the immune privilege (Fijak and Meinhardt, 2006).

In the intestine, DC are present in the lamina propria of the small as well as the large intestine, Payer's patches (PPs), and mesenteric lymph nodes (MLNs). The intestinal lumen and lamina are primary sites for antigen uptake by CX3CR1⁺ DC and PPs or MLNs are sites of triggering the induction of intestinal T and B cell responses. It was found that DC in the subepithelial dome (SED) are the first targets of *Listeria monocytogenes* in the course of the infection, the same DC were responsible for the phagocytosis of orally administered *Salmonella typhimurium* (Johansson and Kelsall, 2005; Niess and Reinecker, 2006)

1.1.3 Localization and migration of DC

DC migrate via afferent lymph from peripheral tissues to secondary lymphoid organs. DC transport informations that determine the differentiation of the activated T cells. DC in the spleen are of great importance as they are responsible for the central immune response against infections. The spleen consists of the red pulp (site of red blood destruction) interfused with the lymphoid “white pulp”. The white pulp consists of three areas around the central arterioles: marginal zone (MZ, mostly macrophages and DC), B cells follicles and T cell zone (periarteriolar lymphoid sheath (PALS)) (Vondenhoff et al., 2008). Histological analyses of splenic CD11c⁺ DC in non-infected mice show that DC are found in the marginal zone, T cell zones and red pulp. CD8⁺ DC are present in the red pulp, the marginal and T cell zones, while CD8⁻ DC are present in the B cell area in the white pulp (Chaussabel et al., 2003; Ato et al., 2006). After infection of mice with *Leishmania donovani*, splenic DC migrate from the MZ to the T cell area. The migration is regulated by the chemokine gradients of CCL19 and CCL21 recognized by CCR7 on DC. The translocation of the DC allows an optimal interaction with the T cells for optimal protection against *L. donovani* (De et al., 2004; Ato et al., 2006). After malaria infection, the same migration was observed (Leisewitz et al., 2004). TLRs like LPS or CpG were also shown to induce maturation, translocation of splenic DC to the T cell area of the white pulp, and finally apoptosis (De Smedt et al., 1998; De Trez C. et al., 2005).

1.1.4 Antigen uptake by DC

DC capture antigen from peripheral sites like skin and mucosa and then migrate to secondary lymphoid organs to initiate immune responses. Immature DC sample a broad variety of Ags, via macropinocytosis (fluid phase uptake), receptor-mediated endocytosis (e.g. C-type lectins, and Fc receptors). Antigen uptake is followed by antigen processing and the formation of MHC-peptide complexes on the cell surface required for T cell priming. Both the uptake mechanism of the antigen and the DC type determine the resulting load of antigenic peptides onto MHC class II (MHC-II) or on MHC class I (MHC-I) molecules (Lanzavecchia, 1996; Engering et al., 2002).

Several receptors mediating endocytosis expressed by immature DC belong to the C-type lectin family including Langerin (CD207), mannose receptor (MR), DEC205, CLEC9a, and DC-SIGN. These receptors play a major role in the binding and subsequent internalization of pathogenic antigens for direct elimination. Proteins with either mannose or galactose side

chains interact with a carbohydrate recognition domain (CRD) of the C type lectin receptors in a calcium-dependent manner (Engering et al., 2002; Cambi et al., 2005).

Langerin is expressed both on the cell surface and intracellularly as “Birbeck granules” in skin epidermal Langerhans cells (LCs). The MR is highly expressed on immature DC and macrophages and is involved in binding end-standing mannose groups on a variety of pathogens and antigens. DEC205 is expressed on DC and thymic epithelial cells, the ligands recognized by DEC205 remain unknown to date. DC-SIGN is exclusively expressed on DC in contrast to MR and DEC205. The cytoplasmic DC-SIGN binds several viruses, mycobacteria, and other pathogens (Engering et al., 2002; Erbacher et al., 2009).

Many cells of the immune system undergo apoptosis after intracellular infections or during the development of lymphocytes. DC are specialized phagocytic cells that are responsible for the clearance of infected dying cells releasing pathogen-associated molecular patterns (PAMPs, like LPS or CpG) as well as non-infected dying cells releasing intracellular damage-associated molecular patterns (DAMPs). The release of DAMPs (fragments of the extracellular matrix, heat shock proteins, phosphatidylserine (PS), and DNA fragments) by apoptotic cells constructs an “eat-me” signals recognized by multiple receptors on DC (Kono and Rock, 2008; Green et al., 2009). It was demonstrated that human DC acquire antigens from apoptotic cells and stimulate antigen-specific class I-restricted CD8⁺ T cells (Albert et al., 1998).

Recently different phagocytic receptors on DC subset were demonstrated to be involved in the uptake of apoptotic cells. T cell immunoglobulin mucin-3 (Tim-3) receptor was reported to be responsible for the recognition of dying cells by CD8⁺ DC (Nakayama et al., 2009).

It was found that CD8⁺ DC expressing CD103⁺ CD207⁺ localized in the splenic marginal zone endocytose apoptotic cells and migrate to the T cell zone (Qiu et al., 2009).

C-type lectin receptor CLEC9A also known as DNGR-1 expressed by CD8⁺ DC binds to the surface of apoptotic cells (unknown ligand). Blocking of CLEC9A did not impair the endocytosis of apoptotic cells but reduced cross-presentation of dead-cell-associated antigens by CD8⁺ DC (Sancho et al., 2009). Both CD8⁺ and CD8⁻ DC were demonstrated to present soluble ovalbumin captured *in vivo*, however only the CD8⁺ DC subset shows selective uptake of live allogeneic splenocytes or apoptotic cells. It was also observed that both CD8⁺ and CD8⁻ DC are capable to phagocytose latex particles in culture (Iyoda et al., 2002). Soluble or latex bead-associated antigens were shown to be taken up by all three splenic DC subsets (CD8⁺ DC, CD4⁺ DC and CD4⁻ CD8⁻ DC) *in vivo* (Schnorrer et al., 2006).

1.1.5 Antigen presentation by DC

The most important function of DC following antigen uptake discussed above, is the processing and presentation of antigen on MHC molecules. Two distinct antigen presenting pathways were characterized according to the type of antigen: Peptides derived from endogenous antigens (e.g. interacellular viral, bacterial, or self proteins) are loaded onto MHC-I. Peptides derived from exogenous proteins taken up by receptor-mediated endocytosis, pinocytosis or phagocytosis are loaded onto MHC-II. Peptides presented by MHC-I are derived from proteins degraded in the cytosol by the ubiquitin-proteasome pathway whereas peptides presented by MHC-II are derived from proteins degraded in endosomal compartment (Kloetzel and Ossendorp, 2004) (Shortman and Liu, 2002; Villadangos and Schnorrer, 2007). Few DC subtype can present exogenous antigen on MHC-I in a process called cross-presentation. Three different mechanisms of cross-presentation were investigated in several studies: 1) Antigen is first taken up by phagosomes is then transported into the cytosol (unclear mechanism) where it is cleaved by proteases into oligopeptides. Peptides end up in the endoplasmic reticulum (ER) transported via TAP (transporter associated with antigen presentation: TAP1/TAP2) where they are loaded onto newly synthesized MHC-I molecules; 2) The generation of peptides within the phagosome itself by lysosomal proteases which are directly transported by unclear mechanism to the ER. 3) ER-phagosome fusion (ergosomes) mechanism where the entire MHC class I loading machinery is integrated to the phagosomal membrane. As consequence of all three mechanisms, MHC-I molecule-peptide complexes are transported to the cell surface (Lin et al., 2008) (Heath et al., 2004; Rock and Shen, 2005).

Cross presentation by DC were observed with model antigens (soluble OVA) as well as pathogens (viral or intracellular bacterial infections).

Several publications deal with the role of antigen presenting DC, especially CD205⁺ CD8⁺ DC, in T cell activation and the induction of an immune response. It was reported that CD8⁺ DC and not CD8⁻ DC could efficiently cross-present immune complexes to CD8⁺ T cells (den Haan et al., 2000). After immunization with soluble OVA, it was found that CD8⁻ DC were slightly more efficient than CD8⁺ DC in presenting antigen in the context of MHC-II to CD4⁺ T cells. However the CD8⁺ DC subtype was far more effective than CD8⁻ DC in the cross presentation of antigen in the context of MHC-I to CD8⁺ T cells (Pooley et al., 2001).

In viral or intracellular bacterial infections, a dominant role of CD8⁺ DC in class I-restricted

presentation for cytotoxic T lymphocytes (CTL) induction was observed. This was shown in herpes simplex virus (HSV) type 1, influenza, and vaccinia virus or *L. monocytogenes* infection (Smith et al., 2003; Belz et al., 2005).

Recently, the role of CD103⁺ DC as a cross presenting DC were demonstrated in different organs like lung, skin and spleen (del Rio et al., 2007; Bedoui et al., 2009; Qiu et al., 2009).

1.2 Chemokines and chemokine receptors

Surveillance, inflammation or development of the immune response is controlled by a group of small proteins called chemokines and their chemokine receptor network. Chemokines were long known for their major role in leukocytes migration to the sites of inflammation. But only recently it was realized that interaction of chemokines with their respective receptors leads to a cascade of signaling events that also result in lymphocyte development and homing, organogenesis, and neuronal communication (Dorner et al., 2004; Lata and Raghava, 2009).

1.2.1 Structure and subclasses

1.2.1.1 Chemokines

Chemokines are small proteins (70 - 125 amino acids, 8 - 14 KDa) containing many basic amino acids residues. The structures of many chemokines were clarified by NMR and X-ray crystallography analyses. In spite of the low sequence homology, chemokines share a conserved tertiary structure with a flexible long N-terminal segment followed by three antiparallel β -sheets and a C-terminal α -helix (Locati et al., 2002; Dorner et al., 2004). Many chemokines were shown to form dimers or oligomers in solution (e.g. CCL2 and CXCL8) (Allen et al., 2007). Almost all chemokines are secreted proteins, only two chemokines, CXCL16 and CX3CL1, are membrane-bound. Two functionally conserved regions at the N-terminus of almost all chemokines provide binding sites for their ligands. One is a high affinity binding site which interacts with its specific G protein-coupled receptor (GPCRs). The other binding site mediates the binding to glycosaminoglycans (GAGs) present on cell surfaces or on the extracellular matrix. Chemokines binding to GAGs help for the generation of a chemokine-gradient for cell migration (Moser et al., 2004; Johnson et al., 2005; Allen et al., 2007).

Chemokines are classified into four subfamilies according to the number and the relative position of cysteine (Cys) residues: CXC, CC, C, and CX3C. The CXC, CC and CX3C

groups contain four Cys residues forming two disulphide bridges which are either separated by one amino acids (CXC), or three amino acids (CX3C), or which are directly adjacent (CC). The C group contains only two Cys residues forming only one disulphide bridge. The CXC and CC groups encompass almost all chemokines, while the other two groups each contain one chemokine. XCL1/ATAC (activation-induced, T cell derived and chemokine-related molecule) is the only member of the C group, while the CX3C group contains only CX3CL1/fractalkine (Moser et al., 2004; Lata and Raghava, 2009).

Chemokines were previously classified into inflammatory and homeostatic subclasses according to function and expression. Inflammatory chemokines are induced after tissue injury, by tumors, during infection, or by inflammatory stimuli like LPS, TNF- α and IL-1. Inflammatory chemokines control the movement of effector leukocyte during infection and inflammation and target cells of the innate as well as the adaptive immune systems. Most inflammatory chemokines belong to the CXC and CC subclasses. Homeostatic chemokines are responsible for cell migration during haematopoiesis in the bone marrow and the thymus and for homing of immune cells to peripheral tissues (Murphy et al., 2000; Moser et al., 2004)

1.2.1.2 Chemokine receptors

Approximately 20 chemokine receptors are known, individual chemokine receptors can often bind several different chemokines. They are 7-transmembrane (7-TM) protein receptors (340 – 370 amino acids) which belong to the subfamily of GPCRs. The acidic N-termini are located extracellularly whereas the C-termini are intracellular. Chemokine receptors were further subdivided into four subfamilies CXCR, CCR, CR, and CX3CR according to their ligand-binding properties (Olson and Ley, 2002; Lata and Raghava, 2009). Besides these functional chemokine receptors, three 7-TM non-signaling scavenger receptors were also observed to bind chemokines (e.g. Duffy). The structure of chemokine receptors has not been solved to date, but it is believed that chemokine receptors exist both as dimers and oligomers. For CCR2, CCR5, CXCR2, and CXCR4 chemokine receptors formation of both homo or heterodimers has been reported (Springael et al., 2005; Allen et al., 2007).

1.2.2 Chemokine functions

The best defined functions of chemokines are attraction of leukocytes and involvement in angiogenesis or angiostasis (Mackay, 2001). However, it was also found that chemokines contribute to immune processes such as lymphocyte development, initiation of the immune

response, and immune pathology (Zlotnik and Yoshie, 2000).

The migration of circulating leukocytes from the blood into inflamed tissues has been described as follows. First, transient interactions between selectin proteins on the cell surface and their carbohydrate ligands on the epithelium lead to the rolling of leukocytes along the blood vasculature to reduce their speed. Leukocytes are selectively activated by sequestered chemokines on the endothelial cell surface to express integrins so that the cells stop rolling and become firmly adhered, which subsequently leads to extravasation (migration into tissue in response to a chemoattractant gradient) (Mackay, 2001; Olson and Ley, 2002).

It was found that GAGs have an important role in cell migration, since chemokines with defective GAG binding sites diminished the arrest of circulating leukocytes on the endothelial cell surface. CCL2, CCL3, and CCL5 mutants defective in binding to GAG, but still capable to bind to their specific receptor, show no effect on cell migration in an intraperitoneal recruitment assay (Rot and von Andrian, 2004; Allen et al., 2007).

Recently, a potential role of chemokines in lymphocyte (B and T cells) development was reported. CXCL12^{-/-} and CXCR4^{-/-} mice share the same phenotype of perinatal death and a defect in B cell lymphopoiesis. Further, expression of several chemokines was detected during thymic development, e.g. CCL25 produced by thymic DC play a role in the relocation of different thymocytes subsets to specific areas in the thymus (Zlotnik and Yoshie, 2000).

In the past few years, various chemokines were shown to be secreted by DC to recruit lymphocytes, such as CCL3, CCL4, CCL5, CCL22, CCL17, and CCL19. Chemokine receptor CCR7 expressed on mature DC has been shown to have a critical function for their migration to the lymph nodes (Olson and Ley, 2002; Rot and von Andrian, 2004).

Chemokine receptors are associated with a wide range of diseases due to their role in viral internalization, which leads to spreading of the infection through the body. CXCR4 and CCR5 are the main receptors mediating human immunodeficiency virus 1 (HIV-1) transmission (Johnson et al., 2005; Lata and Raghava, 2009).

1.3 ATAC and ATAC-receptor (XCR1)

1.3.1 ATAC

In our laboratory, human ATAC was identified in a DNA library from T cells activated with both phorbol 12-myristate13-acetate (PMA) and Ca²⁺ ionophore A23187 (Müller et al., 1995). Independently, murine ATAC were identified by other groups either as lymphotactin (Kelner et al., 1994; Kennedy et al., 1995) or SCM1 (single cysteine motif-1) (Yoshida et al.,

1995). The gene encoding murine ATAC locates to chromosome 1 and shows a typical chemokine gene structure with three exons (Hautamaa et al., 1997).

ATAC (now officially designated XCL1) is the only member of the C family of chemokines sharing some similarity with the CC family, but without the first and third cysteine residues of the four conserved cysteine residues of CC and CXC family chemokines (Kennedy et al., 1995; Dong et al., 2005). ATAC precursor (114-amino acid polypeptide) is encoded by the open reading frame of ATAC mRNA. The 93-amino acid secreted ATAC protein (10 - 12 kDa) results from proteolytic cleavage between Gly²¹ and Val²². The 15 and 17 - 19 kDa *in vivo* expressed variant of human ATAC is O-glycosylated (Dorner et al., 1997).

ATAC expression was previously reported for activated CD8⁺ T cells, Th1-polarized CD4⁺ T cells, $\gamma\delta$ type T cells, and NK cells, but not for monocytes or macrophages (Kelner et al., 1994; Yoshida et al., 1999; Dorner et al., 2002; Dorner et al., 2004). ATAC expression was also observed in activated mast cells (Rumsaeng et al., 1997).

NMR spectroscopy studies demonstrated that ATAC forms two conformations in solution (Kuloglu et al., 2001). It was found that under physiological conditions (37 °C and 150 mM NaCl) ATAC can be present in equilibrium between the conserved chemokine fold (Ltn 10) and a dimeric structure unrelated to chemokines (Ltn 40) (Kuloglu et al., 2001; Tuinstra et al., 2007). It was reported before that ATAC binds with high affinity to the GAG molecule heparin (Peterson et al., 2004). Later, it was shown that the chemokine-like Ltn 10 conformation activates XCR1, but has no affinity to GAGs. In contrast, the alternative Ltn 40 conformation binds GAGs with high affinity, but fails to activate XCR1 (Tuinstra et al., 2008). ATAC expression was detected in several bacterial and viral infections: During *L. monocytogenes* or MCMV murine infections, ATAC was co-expressed with IFN- γ at the single cell level in activated NK cells, CD8⁺ T cells, and CD4⁺ Th1 cells *in vitro* and *in vivo* (Dorner et al., 2002; Dorner et al., 2004). It was found that ATAC is selectively expressed by Th1 but not Th2 cells during *Leishmania major* infection (Müller et al., 2003). In murine tissues, a weak murine ATAC expression was demonstrated in spleen and thymus, whereas heart, brain, lung, liver, and testis were negative (Stievano et al., 2004).

Concerning ATAC function there are contradictory data dealing with the role of ATAC as a chemoattractant for thymocytes, T lymphocytes and NK cells (Kelner et al., 1994; Kennedy et al., 1995), which could not be confirmed by other groups (Bleul et al., 1996; Dorner et al., 1997; Yoshida et al., 1998). Transfection of tumors with ATAC was reported to result in a potent T cell proliferation and strong cytotoxic T lymphocyte (CTL) reaction against the tumor cells. An enhanced homing of cytotoxic T cells into tumor sites was assigned to the

chemotactic effect of ATAC (Huang et al., 2005). A similar CTL response was observed *in vitro* using murine bone marrow derived DC modified by ATAC adenovirus and fused with H22 cells (Zhang et al., 2004). Double-transfected DC expressing ovalbumin (OVA) and ATAC primed OVA-specific CTL *in vivo* more efficiently than DC expressing OVA alone (Matsuyoshi et al., 2004).

1.3.2 ATAC-receptor (XCR1)

The human gene encoding GPR5 (orphan receptor five) (Heiber et al., 1995) was shown to be the only member of the CR family. It was demonstrated, that only ATAC induces migration of GPR5 transfectants in contrast to other known chemokine receptors or orphan receptors. Accordingly, GPR5 was renamed XCR1 (Yoshida et al., 1998). One year later, the murine XCR1 was characterized and it was shown that ATAC induces migration and calcium-mobilization by XCR1 transfectant cells (Yoshida et al., 1999). Northern blot analyses of XCR1 in human tissues revealed XCR1 expression in spleen, thymus and placenta (Yoshida et al., 1998; Shan et al., 2000). Northern blot analyses of mouse tissues revealed a weak XCR1 signal in spleen and lung. Quantitative reverse transcription polymerase chain reaction (qRT-PCR) of spleen cell subsets showed XCR1 expression in T cells, B cells and NK cells (Stievano et al., 2004). Recently in our group, we could show that RNA samples from highly purified splenic resting or activated CD8⁺ T cells, CD4⁺ T cells, B cells, or NK cells give no signal for XCR1. Strong mXCR1 expression was only detected in RNA samples from CD8⁺ DC, and a very low signal with CD8⁻ DC (Dorner et al., 2009).

Higher expression levels of XCR1 were found in activated mononuclear cells from synovial fluid in rheumatoid arthritis (RA) patients (Wang et al., 2004). The Kaposi sarcoma-associated herpes virus (KSHV) encodes CCL2 and CCL3 viral chemokines, which target the human XCR1 as antagonist and agonist, respectively. Since they do not target murine XCR1, They can not be used to study the role of mXCR1 *in vivo*. Few years ago, the role of XCR1 in the immune system was described to be poorly understood (Lüttichau, 2008). Recently in our group we could show that XCR1 on cross-presenting CD8⁺ DC, in combination with ATAC-secreting CD8⁺ T cells helps to induce efficient CTL responses (Dorner et al., 2009).

1.4 In vivo antigen targeting models to enhance immune responses

As DC are central players of the immune response, many promising strategies for vaccinations or immune therapy through antigen-loading to DC were reported. DC derived from progenitor cells of cancer patients, which were loaded with tumor antigens and then injected back into the patients were one of the immunization strategies used to induce anti-cancer effects. Unfortunately, this strategy showed a limited success and has not been accepted so far as an effective means of treating cancer (Tacke et al., 2007). Reported in vivo models for antigen targeting to DC were performed either with cells loaded with antigen or with antigen coupled to specific mAb.

The possibility of evoking antitumor T cell immune responses with antigen-pulsed live or apoptotic allogeneic cells was examined in many studies. It was shown that the CD8⁺ DC subset is responsible for the uptake of live allogeneic cells in culture and in vivo and has the ability to present cellular antigen to CD4⁺ and CD8⁺ T cells (Iyoda et al., 2002). It was also reported that immunization with allogeneic tumor cells induced specific killing of syngeneic tumors (Toes et al., 1996). Bone-marrow derived DC loaded with irradiated E.G7 tumor cells were reported to be effective stimulators of OT-1 CTLs (Strome et al., 2002). Immunization with antigen-pulsed allogeneic cells undergoing apoptosis activated naive CD4⁺ T cells to differentiate into Th1 cells expressing IL-2 and IFN- γ , whereas immunization with antigen-pulsed syngeneic cells activated naive CD4⁺ T cells to differentiate into Th2 cells expressing IL-4 (Agrewala et al., 2003).

Alternative approaches targeted antigen directly to the DC in vivo using monoclonal antibodies (mAbs) specific for molecules on the DC surface. Several factors have to be taken into account when choosing the optimal target molecule on the DC surface. The expression must be limited to DC to permit reduction of the antigen dose and to avoid side effects (Caminschi et al., 2009; Shortman et al., 2009). It was observed that targeting different receptors on DC surface leads to different processing pathways. Regulation of antigen processing by different DC subtypes were performed by targeting OVA coupled to DEC205 or 33D1 antibodies to CD205⁺ CD8⁺ or 33D1⁺ CD8⁻ respectively. In vivo it was found that OT-I cells were strongly activated after injection of DEC205-OVA, whereas OT-II cells were strongly activated after injection of 33D1-OVA (Dudziak et al., 2007). The potency and the quality of the T cell response were tested in another OVA model where different splenic DC receptors (CD11c, CD205, and MHC-II) were used to deliver OVA antigen to DC. All

three receptors show in vitro a comparably effective targeting of antigen to DC for presentation to T cells. However, in vivo targeting of antigen to CD11c delivers more robust responses of both CD4⁺ and CD8⁺ T cells compared to the other two receptors (Castro et al., 2008).

The aim of DC targeting studies is to induce a strong CTL responses against viral infections and tumors or to improve antibody-dependent vaccines (Caminschi et al., 2009; Shortman et al., 2009). The generation of CTL responses was achieved by delivering antigen to different receptors on DC. Targeting DEC205 receptor on CD8⁺ DC with anti CD40 elicits a strong CD8⁺ T cell dependent CTL response with resistance to tumor and to viral infection (Bonifaz et al., 2002; Bonifaz et al., 2004). A potent CTL response was also observed after targeting CLEC9a (DNGR-1) receptor on CD8⁺ DC (Sancho et al., 2008). CD8⁺ DC primed CD8⁺ T cells into long-term effector CTLs after targeting of antigen to the CD36 scavenger receptor. In contrast to studies targeting other receptors induction of CTL was achieved without addition of maturation stimuli (Tagliani et al., 2008). The role of targeting different receptor on different DC subsets was investigated for its influence on antibody production. It was shown that antibody production after targeting immature CD8[−] DC receptors like FIRE (F4/80-like receptor) or CIRE (C-type lectin receptor) was about 1000-fold higher than in the non-targeting control (Corbett et al., 2005). The same observation for antibody production after antigen targeting via the DEC205 receptor with adjuvant was shown in many studies and was explained by the subsequent activation of CD4⁺ T cells (Boscardin et al., 2006; Soares et al., 2007).

DC are not only known for the initiation of immune responses, but also for the induction of tolerance. There are two types of tolerance: either central tolerance occurring in the thymus and bone marrow or peripheral tolerance occurring in secondary lymphoid organs. DC in the thymus are involved in the negative selection of high affinity self-reactive T cells during development. The role of DC were also observed in the induction of peripheral tolerance in the mature peripheral T cell compartment via different mechanisms (deletion, anergy, and regulatory or suppressor cells) (Shklovskaya and Fazekas de St, 2007). Targeting immature DC with antigen without adjuvant leads to peripheral tolerance. This effect was observed after targeting DC subsets with DEC205 or 33D1 receptors without danger or inflammatory signals (Bonifaz et al., 2002; Boscardin et al., 2006)

Targeting antigen to DC in vivo opens the possibility for developing effective vaccines or immune therapies in the future. To date, all reported surface markers for antigen targeting were expressed on individual DC subsets or other cell subsets (Caminschi et al., 2009;

Shortman et al., 2009). Considering the high functional diversity among the different DC subsets, a marker that is selectively expressed on defined DC subsets may enhance both specificity and efficiency of these vaccination strategies.

1.5 Objective

To date, the role of XCR1 in the immune system is barely understood. Several contradictory publications reported expression of XCR1 on a wide variety of immune cells, while recent PCR data of our laboratory indicated selective XCR1 expression by CD8⁺ dendritic cells. Therefore, the aim of this study was to characterize the *in vivo* expression and the function of XCR1 and XCR1⁺ cells.

The main objectives were:

- 1) Characterization of XCR1 expression by a newly generated mAb against mXCR1
- 2) Alternatively, characterization of XCR1 expression by immunohistological and flow cytometry analysis of B6.XCR1-LacZ^{+/+} reporter mice which express LacZ under the control of the XCR1 promoter
- 3) Investigation of the migratory capacity of XCR1⁺ cells *in vivo*
- 4) Verification of the possible involvement of XCR1 in the phagocytosis of allogeneic and syngeneic cells *in vivo*
- 5) Selective targeting of antigen to XCR1⁺ cells and characterization of the ensuing *in vivo* immune response at the level of CD8⁺ T cells

2 Materials and methods

2.1 Equipment, chemicals and consumables

2.1.1 Equipment

The following equipment was used during my PhD work (Tab. 1)

Tab. 1: Equipment list

Equipment	Model	Company
Binocular microscope	Stemi 2000-C	Carl Zeiss, Jena, Germany
Centrifuges	Rotixa 50RS 5415 D	Hettich Zentrifugen, Tuttlingen, Germany Eppendorf AG, Hamburg, Germany
Cryostat	Cryotom 2800 Frigocut N	Reichert-Jung, Vienna, Austria
ELISA reader	DynatechMR5000	Dynatech Laboratories, Chantilly, VA, USA
ELISA washer	Tecan	Krailsheim, Germany
Flow cytometers	FACSCalibur LSR II	BD Biosciences, San Jose, CA, USA
Guava PCA cell analyzer		Guava Technologies, Hayward, CA, USA
Hemocytometer	Neubauer improved counting chamber	Glaswarenfabrik K. Hecht, Sondheim, Germany
Light microscope	LEICA DMIL LEICA	Microsystems Wetzlar GmbH
Photometer NanoDrop	ND-1000	Wilmington, DE 19810 USA
Thermal cycler	2720	Applied Biosystems Inc.
CO ₂ -incubator	BBD 6220	Heraeus, Waltham, USA
Gene pulser		Biorad , Munich, Germany

2.1.2 Chemicals and consumables

All used chemicals were tested for quality and were obtained from the following companies: AppliChem GmbH (Darmstadt, Germany), Carl Roth GmbH (Karlsruhe, Germany), Merck AG (Darmstadt) und Sigma-Aldrich (St. Louis, MO, USA). Sterile plastic materials were obtained from the following companies: Greiner GmbH (Frickenhausen, Germany), Nunc (Roskilde, Denmark) or Sarstedt (Nümbrecht, Germany)

2.2 Buffers, reagents and cell culture media

All buffers and reagents (summarized in Tab. 2) were used routinely during this work. Special buffers or reagents will be described later in the materials and methods section.

Tab. 2: List of buffers and reagents

Buffer/Reagent	Composition
ACK lysing buffer	0.15 mM NH ₄ Cl, 10 mM KHCO ₃ , 0.1 mM Na ₂ EDTA, pH 7.2 - 7.4
AEC-Stock	1 Tablet AEC (Sigma-Aldrich) in 2.5 ml DMF (N,N Dimethylformami)
AEC-Staining buffer	250 µl AEC-Stock, 50 mM CH ₃ COONa pH 5.0; 30% H ₂ O ₂
CFSE Loading buffer	PBS + 0.1% BSA
FACS-PBS	PBS + 2.5% FCS + 0.1% NaN ₃
iFACS-PBS	FACS-PBS + 0.5% Saponin
10×Fc-Block	1 mg/ml anti-CD16/CD32 (clone 2.4G2), 0.5 mg/ml Rate IgG (Nordic, Tilburg)
MACS-PBS	PBS + 2 mM EDTA + 0.5% BSA (Fraction V, Endotoxin <1 EU/mg, PAA Laboratories GmbH, Cölbe)
PBS	136.89 mM NaCl, 2.68 mM KCl, 1.47 mM KH ₂ PO ₄ , 8.05 mM Na ₂ HPO ₄ , pH 7.3
Peroxidase-Block	1 mM NaN ₃ , 10 mM Glucose, 1 U/ml Glucose oxidase (Sigma-Aldrich) in PBS
SOC-medium	(Peptone from Casein (Merck), Yeast Extract (Merck), 5 M NaCl, 1 M KCl, 1 M MgCl ₂ , 1 M MgSO ₄ , 1 M glucose)
Washing buffer	PBS + 0.05% Tween 20
X-gal staining buffer	1 mg/ml X-gal, 5 mM K ₃ Fe(CN) ₆ , 5 mM K ₄ Fe(CN) ₆ , 2 mM MgCl ₂ , 0.02% NP-40, 0.01% Na-deoxycholate (Sigma-Aldrich) in PBS

Basic medium used for cell culture was RPMI 1640 (Biochrom AG, Berlin) with different additives:

R10F⁻/β-ME: 10% fetal calf serum (FCS, Biochrom), 50 μM β-Mercaptoethanol, 2 mM Glutamine (Invitrogen, Gaithersburg, USA)

R10F⁺/β-ME: R10F⁻/β-ME + 100 μg/ml Penicillin/ Streptomycin (Invitrogen)

R10F⁺/β-ME/AA/Pyr: R10F⁺/β-ME + 1 mM non essential amino acids (Invitrogen), 1 mM sodium-pyruvate (Invitrogen)

R10F⁺/β-ME/AA/Pyr/G418: R10F⁺/β-ME/AA/Pyr + 1 mg/ml Geneticin G418 (Invitrogen)

Hybridoma selection medium: RPMI 1640, 20% FCS, 50 μM β-Mercaptoethanol, 50 U/ml IL-6 (Biosource, Camarillo, CA, USA)

2.3 Mice

C57BL/6 (B6)

BALB/c

B6.ATAC-KO

Mice deficient for ATAC (caused by the deletion of exon 2 and 3 of the ATAC gene) were generated by Dr. B. Dorner, (Dorner et al., 2009). Mice were backcrossed for 10 generations onto the C57BL/6 background.

B6.PL.OT-I (B6.OT-I)

OT-I TCR-transgenic mice specific for ovalbumin peptide (OVA₂₅₄₋₂₆₇) (Hogquist et al., 1994), were crossed with B6.PL mice (Jackson) to allow identification of adoptively transferred cells using the Thy1.1 marker.

B6.PL.OT-I/ATAC-KO (B6.OT-I/ATAC-KO)

B6.PL.OT-I mice were crossed with B6.ATAC-KO to generate B6.PL.OT-I/ATAC-KO mice.

B6.PL.OT-II (B6.OT-II)

OT-II TCR-transgenic mice specific for ovalbumin peptide (OVA₃₂₃₋₃₃₉) (Barnden et al., 1998), were crossed with B6.PL mice (Jackson) to allow identification of adoptively transferred cells using the Thy1.1 marker.

B6.XCR1-LacZ^{+/+} (homozygous) and B6.XCR1-LacZ^{+/-} (heterozygous)

A bacterial LacZ gene was inserted into the XCR1 gene locus such that the endogenous XCR1 promoter drives the expression of β-Galactosidase. XCR1-LacZ knock-in reporter mice were obtained from the Jackson Laboratories and backcrossed to the C57BL/6 background for 10 generation.

All mice used in experiments were 8 to 10 weeks old. All mice were bred under specific pathogen-free (SPF) conditions in the animal facility of the Federal Institute for Risk Assessment (Berlin, Germany); experiments were performed according to state guidelines and approved by the local ethics committee.

2.4 Cell biology

2.4.1 Cell culture

Cell lines and hybridomas were cultured in a 5% CO₂ incubator at 37 °C. All cells were maintained in R10F⁺/β-ME. Cell culture flasks (Greiner) and different culture well plates (Nunc) were used. A summary of the cell lines used in this work is given in Tab. 3.

Tab. 3: Cell lines and appropriate cell media

Cell line	Media R10F ⁺ /βME plus	Source	References	Strains
300-19-wt (pre-B cells)	AA/Pyr	Moser, University Bern, Switzerland	(Alt et al., 1981)	NIH/Swiss
300-19-ATAC	AA/Pyr/G418	C. Opitz, Robert Koch- Institut, Berlin	Not published	NIH/Swiss
300-19- XCR1-YFP	AA/Pyr/G418	In this work		NIH/Swiss
300-19-delta OVA	AA/Pyr/G418	In this work		NIH/Swiss
RMA-S (T cell tumor)	AA/Pyr	A. Diefenbach, Albert- Ludwigs-University Freiburg	(Karre et al., 1986)	B6
P3x63Ag8.653 (myeloma)		ATCC	(Kearney et al., 1979)	BALB/c
L1-2-wt (pre-B lymphoma)	AA/Pyr	C. Gerard, Harvard Medical School, Boston, USA	(Gallatin et al., 1983)	C57L
ATAC-R-L1-2	AA/Pyr/G418	O.Yoshie, Kinki University School of Medicine, Osaka, Japan	(Yoshida et al., 1999)	C57L

Cells were counted by using a hemocytometer or a Guava PCA cell counting device. Aliquots of cells were frozen and stored in liquid nitrogen.

2.4.2 Transfection of 300-19 cells

For transfection, 300-19-wt cells used at a cell density between $0.8 - 1.5 \times 10^6$ per ml. After centrifugation at 380 g for 8 min at RT, 10×10^6 cells were resuspended in 800 μ l buffer 42 (65 mM Na_2HPO_4 , 24 mM NaH_2PO_4 , 5 mM KCl, 24 mM Na-succinate, 20 mM HEPES, pH 7.2) into a 1.5 ml tube and mixed carefully with 50 - 70 μ g of defined plasmid DNA (20 - 40 μ l). Mixtures of cells and DNA were transferred into a 0.4 cm electroporation cuvette (Biorad) and transfection was performed at 450 V and 500 μ F in a gene pulser apparatus (Biorad). After electroporation the cell suspensions were transferred from the cuvette into a new 1.5 ml tube using a Pasteur pipette and centrifuged at 300 g for 5 min at RT. The cell pellets were resuspended in 10 ml 37 °C pre-warmed R10F⁺/β-ME/AA/Pyr medium, transferred into a culture flask and incubated at 37 °C overnight. Thereafter, cells were plated out onto 96 well culture plates with a density of one cell per well in selection medium containing 1 mg/ml Geneticin G418 (Invitrogen). After 7 to 14 days, growing cells were tested to identify stable transfectants using flow cytometry.

2.4.3 Isolation of cells from lymph nodes or spleens

For organ preparations all mice were killed by cervical dislocation. Lymph nodes were lacerated and passed through 70 μ m nylon cell sieves (BD Falcon, Bedford, MA, USA) into 2 ml MACS-PBS containing DNaseI (20 μ g/ml). Lymph node cells were centrifuged at 380 g for 8 min at 4 °C. Cell pellets were resuspended into R10F⁺/β-ME medium (Biochrom AG) or MACS-PBS. Splenocytes were obtained by mashing dissected spleens through 70 μ m cell sieves (Falcon) into PBS followed by pelleting and erythrocyte lysis using ACK lysing buffer (Invitrogen) for 1 min at RT. After centrifugation splenocytes were resuspended in MACS-PBS. All live cells were counted using a hemocytometer or a Guava PCA cell analyzer with the Via Count Assay (Guava Technologies, Hayward, CA, USA).

2.4.4 Enrichment of murine dendritic cells by density gradient centrifugation

Ten spleens were transferred into a Petri dish and cut into small pieces. The fragmented spleens were transferred to a 50 mL polypropylene tube and incubated with collagenase D

500 µg/ml (Roche, Mannheim) and DNaseI 20 µg/ml (Roche) in 10 ml RPMI 1640 with 2% FCS (low Endotoxin, Biochrom) for 25 minutes at 37 °C in a shaking water bath, 40 µl 0.5 M EDTA were added for further 5 min. The spleen fragments were then mashed and filtered through 70 µm cell sieves (Falcon) and washed twice in ice-cold MACS-PBS at 350 g for 6 min at 4 °C. The digest was then resuspended in 10 ml MACS-PBS and 10 ml ice cold 14.1% Nycodenz (NycoPrep1.077, AXIS-SHIELD, Oslo, Norway) in a 50 mL polypropylene tube for gradient centrifugation at 4 °C for 20 minutes at 764 g without break. The low-density cells were taken up from the interphase layer containing 20 – 40% CD11c⁺ DC (Shortman, 1968; McLellan et al., 2002).

2.4.5 Cell Labeling with CFSE

CFSE (5, 6 Carboxy-Fluorescein-Diacetate-Succinimidyl-Ester) is a fluorescent dye that segregates equally between daughter cells upon cell division. For cell labeling, cells were resuspended to 50×10^6 per ml in CFSE loading buffer containing CFSE (Molecular Probes Europe, Breda, Netherlands). After 15 min of incubation in a water bath at 37 °C, the cells are washed twice with PBS, counted, and resuspended to the desired concentration for *in vivo* transfer experiments. In this work, cells were labeled for different purposes with different CFSE concentrations. Cell labeling for uptake experiments was performed with 10 µM CFSE, while for *in vivo* cytotoxicity assays cells were labeled with 1.5 µM or 15 µM for CFSE (Low and High), respectively. Labeling with 5 µM CFSE was used to label transgenic T cells for adoptive transfer experiments.

2.4.6 In vivo CTL activity assessment

Erythrocyte-depleted splenocyte suspensions from naïve B6 mice were resuspended at 30×10^6 cells per ml in R10F⁺/β-ME medium and incubated for 2 h at 37 °C, 5% CO₂ with 10 µM SIINFEKL (Apara Bioscience GmbH) peptide or without peptide. After incubation, cells were washed and labeled for 10 min at 37 °C in the dark with CFSE (Molecular Probes) either at 1.5 µM CFSE (CFSE^{low}, unpulsed peptide) or 15 µM CFSE (CFSE^{high}, peptide-pulsed cells). Cells were washed and resuspended in PBS at 100×10^6 cells per ml containing a 1:1 mixture of CFSE^{low} to CFSE^{high} cells. The cell mixture was adoptively transferred into the different recipient mice groups. 18 h later mice were sacrificed and spleen cells were prepared as described. Cells were resuspended in PBS for determination of the CFSE signal using flow cytometric analysis. To evaluate the percentage of specific lysis,

the ratio of CFSE^{low} to CFSE^{high} was calculated according to the following formula (Romano et al., 2004; Hernandez et al., 2007):

$$\text{CTL (specific lysis)} = 100 - \left[\frac{\frac{\text{CFSE}_{\text{high_immunized}}}{\text{CFSE}_{\text{low_immunized}}}}{\frac{\text{CFSE}_{\text{high_control}}}{\text{CFSE}_{\text{low_control}}}} \right] \times 100$$

2.5 Generation of a monoclonal antibody directed against murine XCR1

2.5.1 Immunization against the XCR1 receptor

B6 mice were immunized with 20×10^6 heat shocked (46 °C for 15 min) 300-19-XCR1 cells mixed with 27×10^7 *B.pertusis* in 100 µl PBS. Cells were injected i.p. into B6.XCR1-LacZ^{+/+} homozygous mice. After 4 weeks, secondary immunization was performed. After further 4 weeks, 3 separate immunizations were performed in the last 3 days before the fusion.

2.5.2 Hybridoma fusion with polyethyleneglycol (PEG) and selection

On the day of the fusion, 100×10^6 splenocytes prepared from immunized mice were mixed with 50×10^6 myeloma cells (P3x63Ag8.653) and centrifuged at 380 g for 8 min at RT. The supernatant was completely removed by vacuum suction. The tube containing the cell pellets was placed into a 37 °C water bath with continuous swirling. One ml pre-warmed PEG 1500 (Roche) was added to the pellet within 1 min with further gently shaking for 2 min. Cells were diluted with 4 ml RPMI 1640 added within 4 min with gentle shaking. Further 10 ml RPMI 1640 were added slowly within 5 min at 37 °C. Cells were centrifuged at 500g for 5 min at RT without a break. The pellets were resuspended in R10F⁺/β-ME medium at 37 °C water bath. For hybridoma culture, cells were mixed with 100×10^6 BALB/c thymocytes used as feeder cells in hybridoma selection medium. Finally, 2×10^4 hybridoma cells were plated onto 96-well culture plates (200 µl /well) and placed in a 37 °C incubator. After 7 - 14 days supernatant from growing cells was analyzed for antibody production.

2.5.3 Screening of positive clones expressing an antibody directed against XCR1

L1-2 wild type or ATAC-R-L1-2 transfectant cell lines were used to test for hybridoma clones expressing an antibody directed against XCR1. Cells (0.2×10^6 transfectant or wild type) were incubated for 30 min on ice with 50 μ l supernatant collected from different hybridoma clones. After washing of the cells two times with FACS-PBS, cells were incubated with 50 μ l goat-anti-mouse-IgG (Fc γ fragment specific secondary antibody, Jackson coupled with Cy5) for 20 min on ice. Clones giving a positive signal (flow cytometry) with the ATAC-R-L1-2 transfectant and not with the wild type negative control were considered positive. Selected clones giving a positive signal with the ATAC-R-L1-2 cell line were tested with enriched dendritic cells (Chap. 2.4.4) from B6 or B6.XCR1-LacZ^{+/+} (negative control). Enriched dendritic cells (1×10^6) were incubated 30 min on ice with 50 μ l supernatant from hybridoma clones. As mentioned above, splenic DC subtypes stained with hybridoma supernatants were analyzed by flow cytometry.

2.6 Molecular biology

2.6.1 Generation of a XCR1 expression vector

The source of murine XCR1 was a pRmHa3 DS47 plasmid generated by Dr. H Mages (own laboratory).

A full length murine XCR1 cDNA spanning exons 1 and 2 fused to the DNA sequence of the yellow fluorescence protein (YFP) was amplified by PCR using primers containing *Hind*III-*Not*I endonucleases into pcDNA3.1 plasmid to generate XCR1-YFP fusion protein. The integrity of XCR1-YFP cDNA was verified by DNA sequencing.

Forward primer: muATACR+Ex1-*Hind*III (sequence marked grey binds to cDNA)

*Hind*III

5' ATATTATTAAAGCTTACCATGGACTCAGAGTCAGATGC 3'

Reverse primer: YFP-Not-ATACR

*Not*I

5' TTATATATATTAGCGGCCGCGCTCTAGCATTAGGTGACAC 3'

2.6.2 Cloning of the delta-OVA protein

PcDNA3.1-delta-OVA plasmid containing chicken ovalbumin cDNA (amino acids 138 - 386) was obtained from Dr. A. Scheffold (*Miltenyi Biotec GmbH*). The delta-OVA fragment was amplified by PCR using primers containing restriction sites for *EcoRI/XbaI* endonucleases and inserted into the pcDNA3 vector encoding YFP to generate a fusion protein with a C-terminal YFP. The integrity of the delta-OVA-YFP cDNA was verified by sequencing. Primers used for the cloning are shown below:

Forward primer: delta-OVA-YFP_for (sequence marked grey bind to cDNA)

EcoRI

5' ACTCTAGAATTCACCATGGATCAAGCCAGAGAGCTC 3'

Reverse primer: delta-OVA-YFP_rev

XbaI

5' ACTCTATCTAGAGGGGAAACACATCTGCC 3'

2.6.3 Polymerase chain reaction (PCR)

Standard PCR for the cloning of mXCR1 and delta-OVA protein was performed with the Phusion Hot Start High-Fidelity DNA Polymerase (Finnzymes) using the primers described above in a 50 µl volume according to the following reaction conditions: Initial denaturation for 30 sec at 98 °C followed by 35 cycles (98 °C, 10 sec; 58 °C, 20 sec; 72 °C, 30 sec) and a 10 min delay at 72 °C.

2.6.4 Transformation of *E. coli*

E. coli was transformed by heat shock according to standard methods (Hanahan et al., 1991). XL1-Blue competent *E. coli* (200 µl) were transferred into a pre-cooled 14 ml tube with 10 µl of DNA plasmid and after gently shaking, cells were incubated on ice for 30 min. Bacterial cells were subjected to heat shock at 42 °C for 60 sec, then placed immediately on ice. 800 µl of SOC-medium were added. Bacterial culture was done in an incubator-shaker at 37 °C for 60 min at 160 rpm. For selection of colonies containing plasmids of interest, bacteria were plated out on agar-plates containing 100 mg/ml ampicillin (Sigma).

2.6.5 Plasmid preparation

Plasmid preparation was performed using the QIAprep Spin Miniprep and QIAGEN Maxi Kits (Qiagen, Hilden).

2.7 Flow Cytometry

2.7.1 Monoclonal antibodies & fluorochromes

A complete list of all mAbs (Tab. 4) and fluorochromes (Tab. 5) used for flow cytometric analyses can be found in the following.

Tab. 4: Used monoclonal antibodies

Specificity	Clone	Source	Reference
ATAC	MTAC-311	hybridoma	C. Opitz (RKI, unpublished)
CD3	KT3	hybridoma	(Tomonari, 1988)
CD4	GK1.5	hybridoma	(Dialynas et al., 1983)
CD8	53-6.72	hybridoma	(Ledbetter et al., 1980)
CD11b	5C6	hybridoma	(Rosen and Gordon, 1987)
CD11c	N418	hybridoma	(Metlay et al., 1990)
CD19	1D3	hybridoma	(Krop et al., 1996)
CD49b	DX5	eBioscience	(Arase et al., 2001)
CD90 (Thy-1.1)	3A7	hybridoma	(Logdberg et al., 1985)
CD205 (DEC-205)	NLDC-145	hybridoma	(Kraal et al., 1986)
F4/80	F4/80	hybridoma	(Austyn and Gordon, 1981)
Ly-6G/C (Gr1)	RB6-8C5	hybridoma	(Fleming et al., 1993)
MHC class II	M5/114.15.2	hybridoma	(Bhattacharya et al., 1981)
NK 1.1	PK136	BD PharMingen	(Koo and Peppard, 1984)
7/4	7/4	AbD serotec	(Hirsch and Gordon, 1983)

All mAbs were either purified from hybridoma supernatants and coupled to fluorescent dyes or haptens, or were purchased from the indicated companies.

Tab. 5: Fluorochromes overview

Fluorochrome	Absorbance maximum (nm)	Laser used for excitation (nm)	Emission maximum (nm)	BP filter
FITC/CFSE/FDG	495	488	520	530/30
PE	496	488	573	585/42
PerCP/PE-Cy5.5	488/496	488	675/695	695/40
PE-Cy7	496	488	767	780/60
AF647/Cy5/APC	647/649/650	633	665/667/660	670/14
AF700	702	633	723	720/30
APC-Cy7	625-650	633	767	780/60
PacB/DAPI	405/358	405	455/460	440/40
CasY/PacO/DAPI	400/400/358	405	552/551/460	562/40
PI	488	488	620	LP \geq 670

All fluorochromes for flow cytometric analyses with absorbance and emission maxima as well as lasers used for excitation and band pass (BP) filters at the LSRII are listed. Data are from BD Biosciences or Molecular Probes.

2.7.2 Surface staining

Flow cytometry allows analysis of surface and intracellular protein expression on individual cells using specific fluorophore-conjugated mAb (Radbruch, 2000).

Cells ($0.5 - 5 \times 10^6$) per well were distributed in 96-well round-bottomed microtiter plate (Nunc). At first cells were incubated on ice with Fc-block in FACS-PBS for 5 min to reduce unspecific antibody binding. Next, cells were stained either directly with fluorophore-conjugated mAb for 20 min on ice or indirectly with hapten-conjugated primary mAb followed by incubation with the respective hapten-specific fluorophore-conjugated secondary antibody. The haptens used were biotin (BIO) and digoxigenin (DIG), which were detected using fluorophore-conjugated streptavidin and polyclonal anti-DIG,

respectively. All fluorophore-conjugated mAb were titrated to obtain optimal staining quality.

Dead cells increase the fluorescence background by unspecifically binding to antibodies. Therefore, shortly before measuring the sample in flow cytometry, propidium iodide (PI, 0.33 μ M) or 4', 6-diamidine-2-phenylindole (DAPI, 0.33 μ M, Roche), DNA intercalating fluorchromes that selectively penetrate the leaky membranes of dead cells, were added. PI⁺ or DAPI⁺ dead cells were excluded from the analyses. Samples were acquired on a LSRII flow cytometer using FACSDIVA software or on a FACSCalibur flow cytometer using Cell Quest Pro software (BD Biosciences, San Jose, CA, USA). Data were analyzed using FlowJo software (Treestar, Ashland, OR, USA). Primary data are displayed as histograms or dot plots with numbers indicating the percentage of cells in the respective gate. The basic flow cytometric analysis strategy for gating live cells is shown in (Fig. 2).

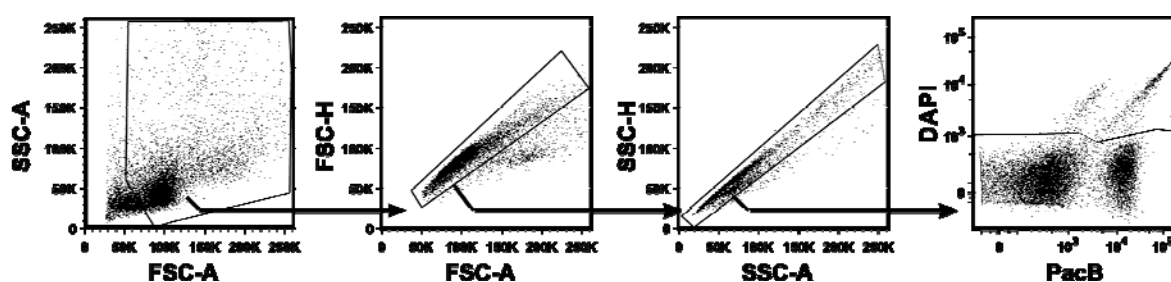


Fig. 2: Live cells gating strategy

Scatter gate of cells acquired by flow cytometry distributed in a dot plot of forward scatter (FSC) versus sideward scatter (SSC). The FSC parameter gives the relative size of each cell while the SSC parameter shows the granularity inside the cells. The scatter gate was set to include all cells but to exclude cellular debris and erythrocytes. Cell doublets were gated out according to height and area of forward and sideward scatter. Finally, autofluorescent cells and dead cells stained with DAPI or PI were gated out. This gating strategy was used for all flow cytometric analyses and will not be shown in the following figures. FSC, forward scatter; SSC, sideward scatter; H, height; A, area.

2.7.3 Detection of β -galactosidase activity in single cell

For detection of β -galactosidase activity in single cells using flow cytometry, the FluoReporter LacZ Flow Cytometry Kits (Invitrogen) was used with fluorescein-di-beta-D-galactopyranoside (FDG) as a substrate. Briefly, a single-cell suspension was prepared and the substrate FDG was loaded into the cells at 37 °C according to the manufacturer. The process was terminated by diluting the cells in ice-cold isotonic medium at 4 °C. Following

FDG-loading a normal surface marker staining with monoclonal antibodies as described was performed.

2.7.4 Annexin V apoptosis assay

Cells that are actively undergoing apoptosis translocate the membrane phospholipid phosphatidylserine (PS) from the inner to the outer leaflet of the plasma membrane. Annexin V (BD Biosciences) is a Ca^{2+} -dependent phospholipid-binding protein that has a high affinity for PS and is used to quantify apoptotic cells. Due to the Ca^{2+} -dependency of Annexin V binding, all incubations were performed in Annexin binding-buffer (10 mM HEPES pH 7.4; 140 mM NaCl; 2.5 mM CaCl_2 and 0.01% NaN_3) at RT. Staining cells simultaneously with Annexin V coupled with Cy5 and the non-vital DAPI allows the discrimination of intact cells (Annexin V⁻ DAPI⁻), early apoptotic (Annexin V⁺ DAPI⁻), late apoptotic or necrotic cells (Annexin V⁺ DAPI⁺) and dead cells (Annexin V⁻ DAPI⁺).

2.7.5 Detection of ATAC expression

Intracellular flow cytometry (iFACS) analysis (Sander et al., 1991) was used to detect ATAC expressed by the transfectant cell line. For detection of ATAC expression, cells were incubated for 3 - 4 h with Brefeldin A (5 $\mu\text{g}/\text{ml}$, Sigma). Brefeldin A prevents intracellular protein transport by inducing the fusion of the Golgi stacks with the endoplasmic reticulum (Rothman, 1994). Cells were subsequently fixed in 2% formaldehyde in PBS for 20 min at RT. Permeabilization of cell membranes was achieved by the addition of 0.5% saponin (Sigma) to FACS-PBS with mAb incubation for ATAC staining. After washing, samples were resuspended in FACS-PBS and measured with a flow cytometer.

2.8 Histology

2.8.1 Tissue preparation and cryosections

Freshly dissected organs were transferred into physiological 0.9% NaCl-solution and immediately shock-frozen in liquid N_2 . Lymph nodes or skin were embedded with TissueTek (Electron Microscopy Sciences, Washington, DC, USA) on aluminium foil, and frozen in liquid N_2 . All tissues were stored at -70°C . For staining, 8 - 16 μm thick cryosections of all tissues were prepared, applied to APES (Aminopropyltriethoxysilan; Sigma) precoated (2%

APES in Acetone, 5 min) microscope slides to prevent tissues sections from being washed off from the slides, dried overnight at RT and stored.

2.8.2 Immunohistochemistry analysis

For immunohistochemistry (IHC) analysis, slides were thawed and fixed in acetone for 10 min at RT. Endogenous peroxidase was blocked by incubation with peroxidase block for 1 h at 37 °C to avoid false-positive signals when using Horseradish peroxidase (HRP)-coupled secondary antibodies. Then, slides were washed two times for 5 min in PBS. All subsequent incubations were carried out in a humid chamber. Tissue sections were incubated with blocking solution (PBS + 10% FCS + 1% tyramide-block (Molecular Probes, T – 20933)) to saturate unspecific binding sites. Subsequently, sections were stained with primary hapten-coupled (BIO, FITC, or DIG) mAb followed by streptavidin, anti-DIG or anti-FITC secondary antibodies coupled to HRP (Roche). The substrate reactions were performed using HRP substrate 3-amino-9-ethylcarbazol (AEC) staining buffer for 5 – 20 min. Nuclei were counterstained with hematoxylin (Merck Chemicals, Darmstadt, Germany) for 5 min. All sections were mounted in Kaiser's glycerol gelatin (Merck), digitized images were captured using an AxioCam HRc CCD camera (Zeiss, Jena, Germany) mounted on an Axioskop microscope (Zeiss), and analyzed using Axiovision LE software (Zeiss).

2.8.3 X-gal (LacZ) histochemistry staining

For the analysis of β -galactosidase activity, frozen tissue sections from B6 mice or homozygous B6.XCR1-LacZ^{+/+} mice were fixed in 0.25% glutaraldehyde in PBS for 10 min at RT, washed 3 times with cold PBS for 5 min, incubated with X-gal staining buffer containing 1 mg/ml 5-bromo-4-chloro-3-indolyl- β -D-galactopyranoside substrate (X-gal Sigma) overnight at 37 °C. After washing 3 times in PBS, sections were counterstained by 1% Neutral Red (ICN Biomedicals, Aurora, OH, USA) for 5 min, excess staining was removed by rinsing in tap water for 5 min (Sanes et al., 1986). For the simultaneous detection of X-gal and surface markers, a double staining protocol was established. Slide sections were fixed with acetone for 10 min at RT. Immunostaining with mAbs against specific surface markers was performed to the point just before substrate reaction. Slides were washed and refixed in 0.25% glutaraldehyde in PBS for 10 min at RT. After washing, X-gal staining was performed as described above. Then the peroxidase substrate was applied to proceed further with IHC.

2.9 Animal experimental methods

2.9.1 Immunization

Immunization with delta OVA transfectant cell line: Recipient mice were immunized i.v. with 3×10^6 300-19-delta OVA, 300-19-wt was used as a negative control. Cells were always washed two times with PBS and OVA-GFP expression was checked by flow cytometry before injection into recipient mice.

Injection of lipopolysaccharide (LPS): 25 μ g LPS from *E coli* O55:B5 (Sigma, Saint Louis, MO, USA, L 6529) was i.v. injected into B6.XCR1-LacZ^{+/+} mice. After 0, 3, 6, 9 and 24 h cryosections from spleen tissue were prepared.

Injection of ATAC transfectant cell line: 300-19-ATAC or 300-19-wt cells (1×10^6) were injected i.v. into B6.XCR1-LacZ^{+/-} heterozygous or B6.XCR1-LacZ^{+/+} homozygous recipient mice. After 6 h cryosections from spleens were prepared.

2.9.2 Adoptive transfer

Splenocytes from OT-I or OT-II OVA-TCR-transgenic donor mice were isolated and the relative frequency of T cell was analyzed by flow cytometry. OT-I spleens contain 12 - 20% Thy-1.1⁺ CD8⁺ T cells and OT-II spleens contain 12 – 18% Thy-1.1⁺ CD4⁺ T cells. Splenocytes containing $1 - 4 \times 10^6$ OT-I CD8⁺ T or OT-II CD4⁺ T cells were i.v. transferred into recipient mice, which were immunized 18 – 24 h later.

2.9.3 In vivo uptake of cells in the spleen

CFSE-labeled cells (10×10^6) were injected i.v. into recipient mice, 12 h after injection the CFSE signal was determined by flow cytometry in the spleen. For this type of experiment, different cell types were injected: Splenocytes from B6 mice, splenocytes from BALB/c mice, RMA-S, 300-19-wt and 300-19-ATAC transfectant.

2.9.4 In vivo depletion of Natural Killer cells

For NK depletion, B6 mice were injected i.p. with 200 μ g PK136 mAb or 50 μ l rabbit anti-mouse asialo-GM1 serum (Wako Pure Chemical Industries Ltd.) on days –1 and –3 before injecting CFSE-labeled 300-19 cell line. Control mice (without depletion) were injected with PBS.

2.10 Immunological methods

2.10.1 Analysis of Ova-specific antibodies using ELISA

First, blood was collected from immunized mice anesthetized with isoflurane (CuraMed Pharma GmbH, Karlsruhe, Germany) by puncture of the retro-bulbar vein plexus using 10 µl minicap capillaries (Hirschmann Laborgeräte GmbH, Eberstadt, Germany). In order to quantify the amount of OVA-specific immunoglobulin (Ig) present in serum of immunized mice, a sandwich Enzyme Linked Immunosorbent Assay (ELISA) was performed. 100 µg/ml OVA in PBS were used to coat 96-well flat bottom MaxiSorp immuno plates (Nunc, Roskilde, Denmark) overnight at 4 °C. Blocking solution (1% BSA in PBS) was added for 1 h at RT, and then the plates were further incubated with serum from the samples diluted in blocking solutions for 1 h at 37 °C. After extensive washing, detection of bound OVA-specific Ig was accomplished using HRP-coupled goat anti-mouse Ig-specific antibodies (Southern Biotech Antibodies, Birmingham, AL, USA) for 1 h at 37 °C. Colour signals were developed using 3, 3', 5, 5'-Tetramethylbenzidine (Sigma, T 3405) as a substrate in phosphate citrate buffer (0.1 M Na₂HPO₄ + 0.05 M citric acid in dH₂O, pH 5.0). 1 M H₂SO₄ was used to stop the colour reaction. ELISA plates were analyzed in a microtiter plate photometer (Dynatech Laboratories, Chantilly, VA, USA) at 450 nm (reference wavelength 630 nm), and data were analyzed using the Revelation software (Dynatech Laboratories)(Porstmann and Kiessig, 1992)

2.11 Statistics

All statistical analyses were performed using Prism software (GraphPad Software Inc., San Diego, CA, USA). Differences between groups of mice were analyzed applying unpaired two-tailed Student's test, a P value of < 0.05 was considered significant.

3 Results

3.1 Characterization of XCR1 expression

3.1.1 Generation of monoclonal antibodies against murine XCR1

Until now, all data on XCR1 expression relied on RNA detection and could not be verified by protein staining. Commercial monoclonal antibodies against murine XCR1 are unavailable and previous attempts in our group to generate mAb in rats using XCR1-transfected cell lines or synthetic XCR1 peptide immunizations failed. We therefore decided to use the B6.XCR1-LacZ^{+/+} reporter mice (Jackson Laboratories) to generate mAb against XCR1, since these mice lack XCR1. To generate a XCR1-expressing cell line, we first constructed an XCR1-YFP-pcDNA3.1 expression vector, which contains the full-length murine XCR1 cDNA (spanning exon 1 and 2) fused to YFP (Chap. 2.6.1). The generated vector was used for the transfection of the murine pre-B cell line 300-19-wt by electroporation. Stable clones were selected by resistance against Geneticin (G418, Invitrogen) and were tested for the expression of YFP using flow cytometry. The B10 clone showed a strong YFP expression and was selected for immunization (Fig. 3).

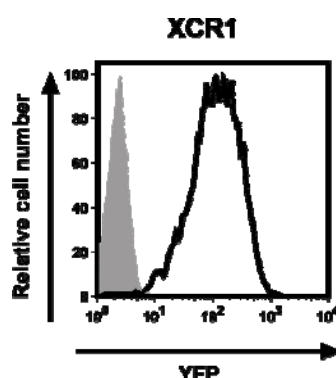


Fig. 3: XCR1 transfected cell line coexpressing YFP

YFP expression in transfected cell lines was analyzed using flow cytometry. 300-19-XCR1-YFP clone B10 (open black curve) and negative control 300-19-wt cell line (filled grey curve).

To generate a mAb against XCR1, B6.XCR1-LacZ^{+/+} mice were immunized with 20×10^6 300-19-XCR1-YFP cells i.p. (Chap. 2.5.1). The two fusion experiments performed resulted in more than 5,000 hybridoma clones. To screen for positive clones, L1-2-wt or ATAC-R-L1-2 expressing YFP were stained using hybridoma supernatants (Chap. 2.5.3) and

analyzed by flow cytometry. L1-2 cells were used to reduce the number of unspecific hybridoma clones expressing mAb that can bind unspecifically to antigen from the immunized cells (300-19). Thirty Clones gave a positive result with ATAC-R-L1-2 but not with L1-2-wt. The brightest staining was observed with the supernatants taken from the clones number 665 and 2406 (Fig. 4).

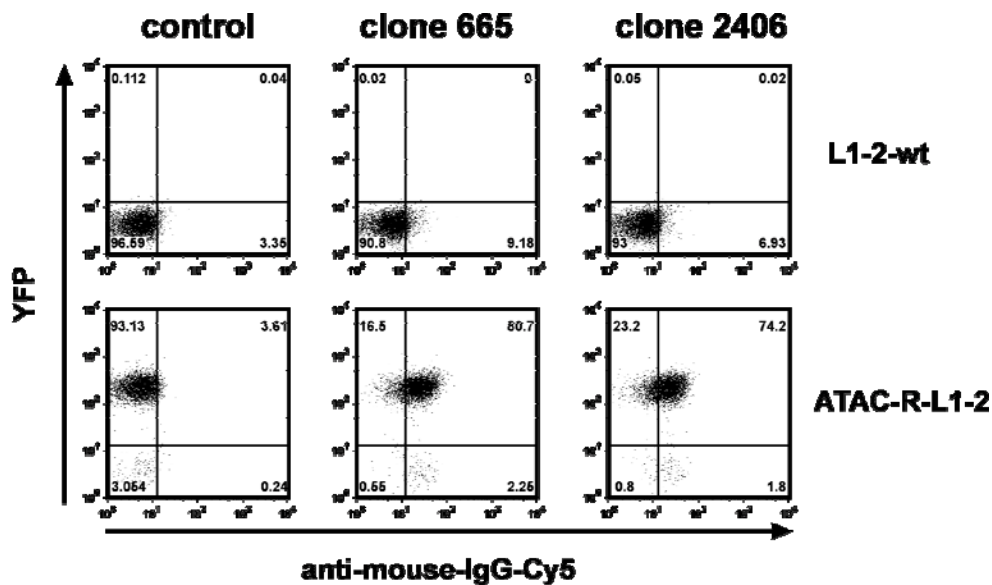


Fig. 4: Screening of clones producing a mAb against murine XCR1

The supernatants of each of the 30 clones were incubated with L1-2-wt or ATAC-R-L1-2 transfectant cell lines. After washing, the cells were incubated with goat-anti-mouse-IgG secondary antibody coupled to Cy5. Samples were analyzed by flow cytometry, as a negative control for the staining background the secondary antibody was used alone. Both 665 and 2406 clones gave a positive signal with the ATAC-R-L1-2 transfectant only.

In our lab it was demonstrated that at the RNA level a strong mXCR1-signal was detected in $CD8^+$ DC, and a very low signal in $CD8^-$ DC. To control the results obtained with the transfected cell line, the selected clones were further analyzed with primary cells from B6 wt or B6.XCR1-LacZ^{+/+}. Hybridoma supernatants taken from clones 665 and 2406 were incubated with enriched DC splenocytes as described before in (Chap. 2.4.4) and analyzed by flow cytometry (Fig. 5 A). No clone gave a positive signal with $CD8^+$ DC from B6 wt or B6.XCR1-LacZ^{+/+} mice (Fig. 5 B). Unfortunately, the new immunization trials to get a mAb against XCR1 did not succeed.

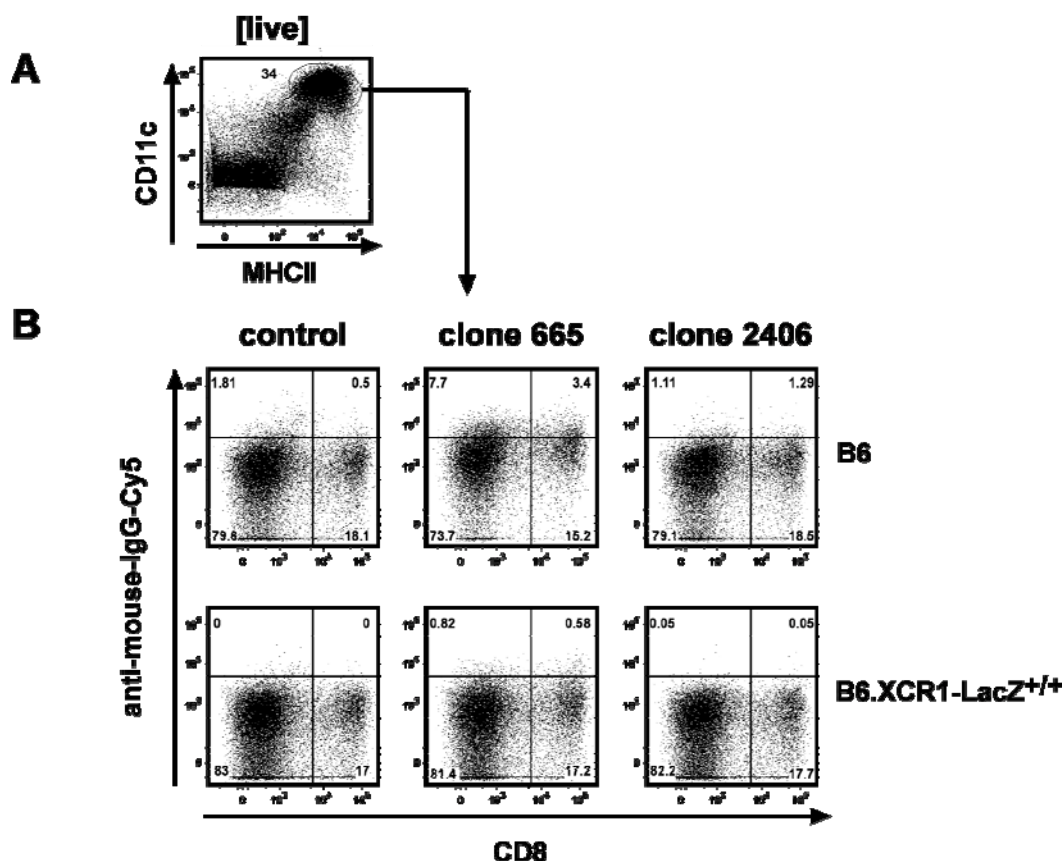


Fig. 5: Analysis of hybridoma supernatant using enriched DC

(A) Splenic DC from B6 wt or B6.XCR1-LacZ^{+/+} mice were enriched to 30 - 40% of live cells using a Nycodenz-gradient. (B) Splenocytes from donor mice were incubated with supernatants from hybridoma clone 665 or 2406. Splenocytes stained with goat-anti-mouse-IgG coupled to Cy5 and CD8 mAb.

3.1.2 Detection of XCR1 expression using B6.XCR1-LacZ^{+/+} reporter mice

Since our efforts to generate a monoclonal antibody against XCR1 were not successful, an alternative approach was used for the detection of XCR1. In the B6.XCR1-LacZ^{+/+} mouse the *E. coli* LacZ gene encoding the enzyme β -galactosidase is expressed under the control of the XCR1 promoter. In these mice, β -galactosidase enzyme activity can be used as a reporter for XCR1 expression. In histology, β -galactosidase activity was detected using X-galactopyranoside (X-gal) as a substrate. For flow cytometry, fluorescein-di- β -D-galactopyranoside (FDG) was used for the detection of β -galactosidase.

3.1.2.1 XCR1 expression in murine tissues

For the detection of XCR1 expression in murine tissues, a LacZ histochemistry staining protocol based on the original published method (Sanes et al., 1986) was established

(Chap. 2.8.3) by using X-gal as substrate (Sigma). Tissue sections positive for β -galactosidase activity were defined according to the blue precipitates. Tissues from B6 mice were used as a negative control for any possible background staining. All histologically examined tissues are listed in (Tab. 6).

Tab. 6: Summary of tissues examined for β -galactosidase activity

Tissues positive for β-galactosidase activity	Tissues negative for β-galactosidase activity
Spleen	Ear
Thymus	Skin
Lymph node	Kidney
Lung	Brain
Liver	Urinary Bladder
Testis	Trachea
Ovary	Pancreas
Placenta	Tongue
Payer's patches	Salivary gland
Small intestine	Uterus
Large intestine	Bone Marrow
	Embryo
	Eyes

Histological sections showing the positive XCR1-signals in blue (Neutral Red was used for counterstaining), are presented in Fig. 6. XCR1 was detected in lymphoid organs like spleen, thymus, and lymph nodes and in non-lymphoid organs like liver, lung, and testis. XCR1 expression was observed in the spleen and LN more frequently than in the thymus or in non-lymphoid organs. Although only few cells stained positive for LacZ in non-lymphoid organs, the XCR1 expression was clear-cut. In the spleen, XCR1 expression was found in the red pulp, the marginal zones and in the T cell zones. In lymph nodes, XCR1 was identified in the subcapsular sinus and in the paracortical area. In the liver, XCR1 signals were observed only in the sinusoidal areas. In the testis, XCR1 was identified in the interstitial spaces of the seminiferous tubules.

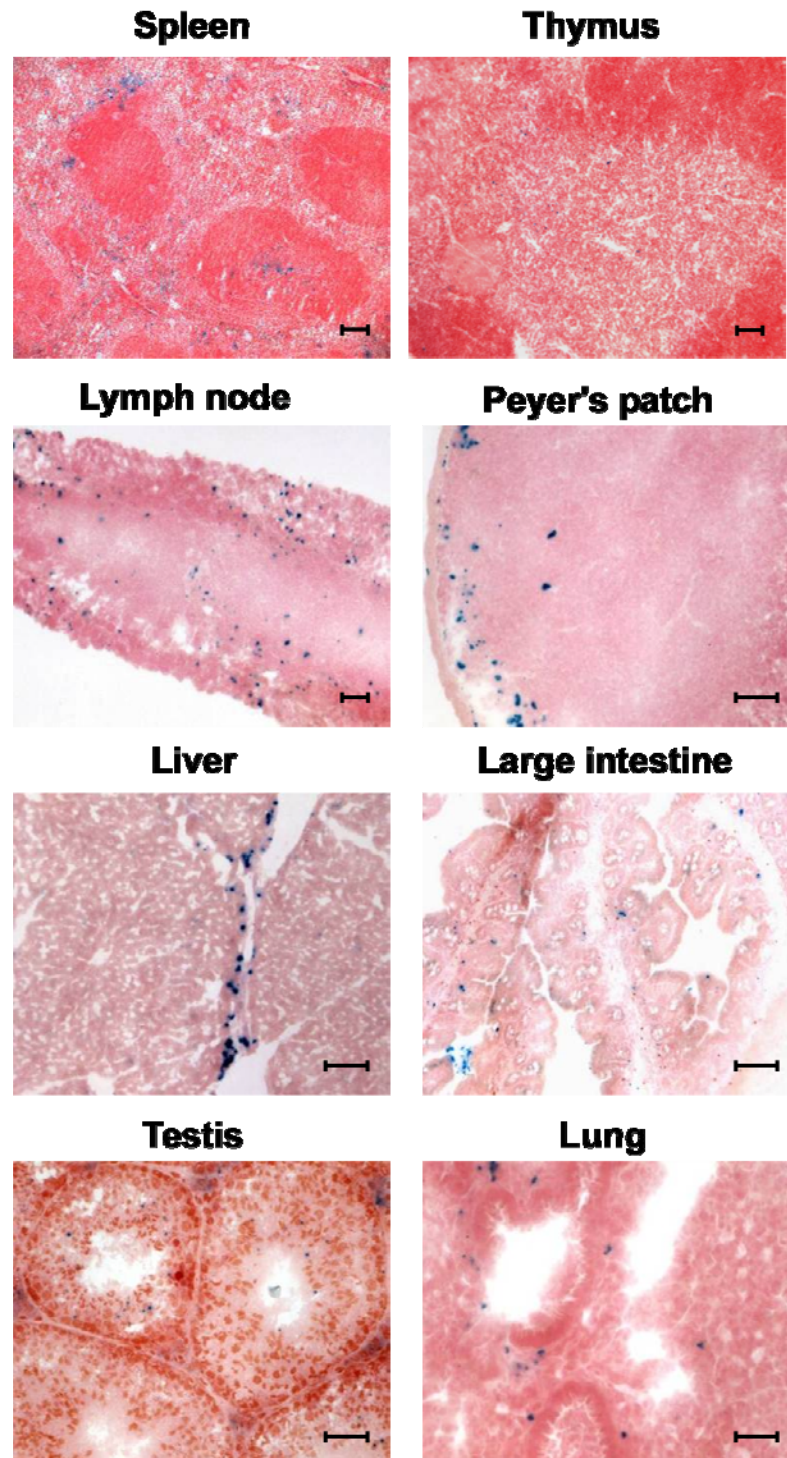


Fig. 6: XCR1 expression in murine tissues

Different tissues from a B6.XCR1-LacZ^{+/+} mouse were histologically examined for β -galactosidase activity using X-gal (a chromogenic substrate for β -galactosidase). Tissues of wild type B6 animals were used as a negative control (not shown). Spleen, thymus, axillary LN, Payer's patches LN, liver, large intestine, testis, and lung. XCR1 signal in blue, nuclear counterstaining with 1% Neutral Red. Scale bar corresponds to 50 μ m.

3.1.2.2 XCR1 expression in murine cell subsets

Previously, many contradictory data were published on the expression of XCR1. Using quantitative RT-PCR, we could not detect XCR1 mRNA in samples from highly purified splenic resting or activated CD8⁺ T cells, CD4⁺ T cells, B cells, or NK cells (Dorner et al., 2009). Strong mXCR1 expression was only detected in RNA samples from CD8⁺ DC, and a very low signal in CD8⁻ DC. To verify these results with a different method, the detection of XCR1 in the different cell subsets was performed in the B6.XCR1-LacZ^{+/+} reporter mouse.

3.1.2.2.1 Histochemical staining using X-gal combined with immunohistology

We were interested in characterizing the phenotype of XCR1 expressing cells in the different lymphoid tissues. To achieve this, we stained for β -galactosidase in combination with different surface markers.

Previously, it has been reported that detection of β -galactosidase using mAb is a sensitive method (MacGregor et al., 1987). For this reason, we first tried to stain β -galactosidase using a commercial mouse mAb (Promega) together with a peroxidase-labeled secondary antibody. This strategy was unsuccessful because of the high level of non-specific staining. Secondly, we tried to establish a double staining protocol to combine X-gal histochemical staining with immunohistostaining. After performing different experiments, we were faced with the problems that cell surface molecules are destroyed by strong fixatives like paraformaldehyde or glutaraldehyde that are necessary for X-gal staining. At the same time no X-gal staining could be obtained with acetone fixation. Finally, we succeeded to establish a new double staining protocol using two different fixations, in which a histochemical staining of X-gal was combined with the standard peroxidase staining protocol for correlation with cell surface markers (Chap. 2.8.3). The staining steps are shown in Fig. 7.

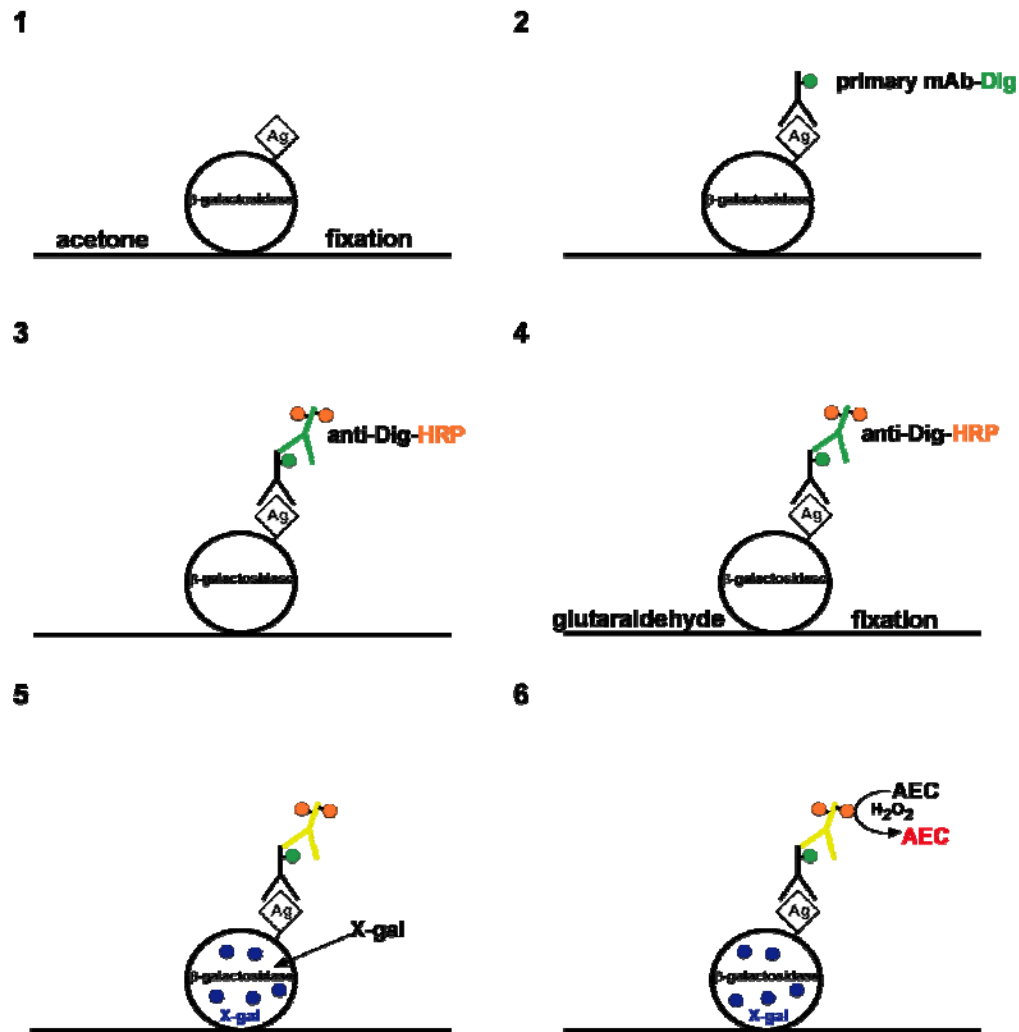


Fig. 7: Steps of the newly established double-staining protocol for X-gal staining and IHC

Cryostat sections were prepared from lymph nodes of B6.XCR1-LacZ^{+/+} mice. The XCR1⁺ signal correlated with the CD8⁺ surface marker on cells in the paracortical area of LN (Fig. 8 A) and all XCR1⁺ signals colocalized with the CD11c⁺ marker (Fig. 8 B). Similar results were also observed in the thymus and the spleen (data not shown). These results indicated that XCR1-expressing cells co-express CD11c and CD8 thus suggesting that these cells are CD8⁺ DC.

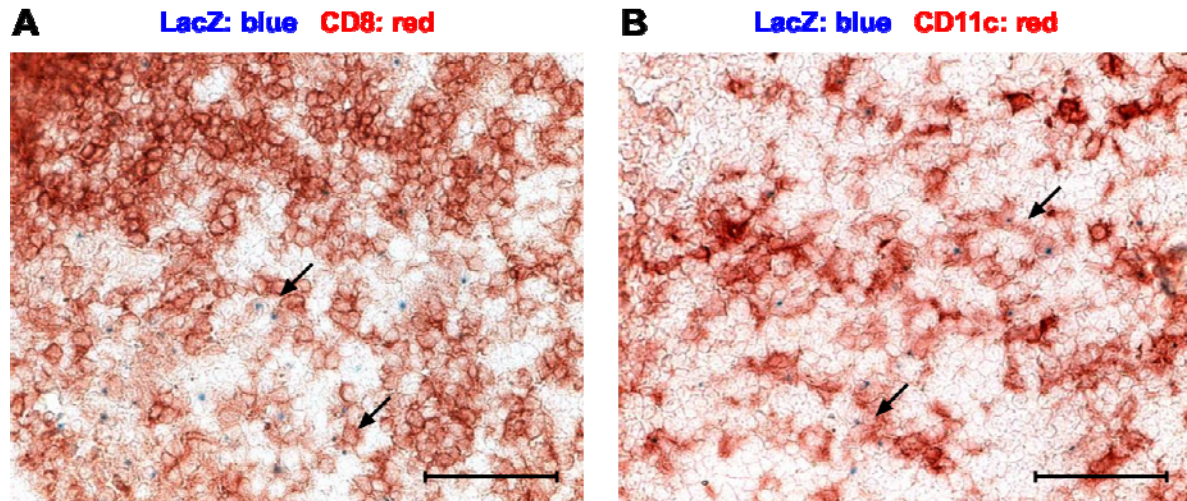


Fig. 8: Double staining of X-gal and CD8 or CD11c in axillary lymph nodes

LN sections from a B6.XCR1-LacZ^{+/+} mouse were immunohistologically examined for double-staining of β -galactosidase and CD8 or CD11c. (A) XCR1 in blue and CD8 in red. (B) XCR1 in blue and CD11c in red. Scale bar corresponds to 50 μ m.

3.1.2.2.2 *Analysis of XCR1-LacZ expression in spleen and LN cell subsets by flow cytometry*

Due to the difficulties in the unequivocal interpretation of histological data shown above, a different approach was used to detect the XCR1 expression in diverse cell subsets using flow cytometry. XCR1 staining of cell subsets was performed with a FluoReporter LacZ Flow Cytometry Kit (Invitrogen) (Chap. 0). In order to characterize XCR1 expression at the level of single cells, spleen and LN cells were prepared from homozygous B6.XCR1-LacZ^{+/+} or B6 mice (negative control). FDG staining was combined with staining for various lineage markers (CD11c⁺ MHC-II⁺ for cDC, CD3⁺ for T cells and CD19⁺ for B cells (Chap. 2.7.2). In the spleen, 70 - 85 % of all CD8⁺ DC were FDG⁺, as well as 10 % of the CD4⁻ CD8⁻ DC, all other cell subsets tested were FDG⁻ (Fig. 9 A). In the lymph node, approximately 50 % of the CD8⁺ DC were FDG⁺. Additionally, a few percent of the CD4⁻ CD8⁻ DC and CD4⁺ DC showed a FDG-signal. All other cell subsets tested were FDG⁻ (Fig. 9 B).

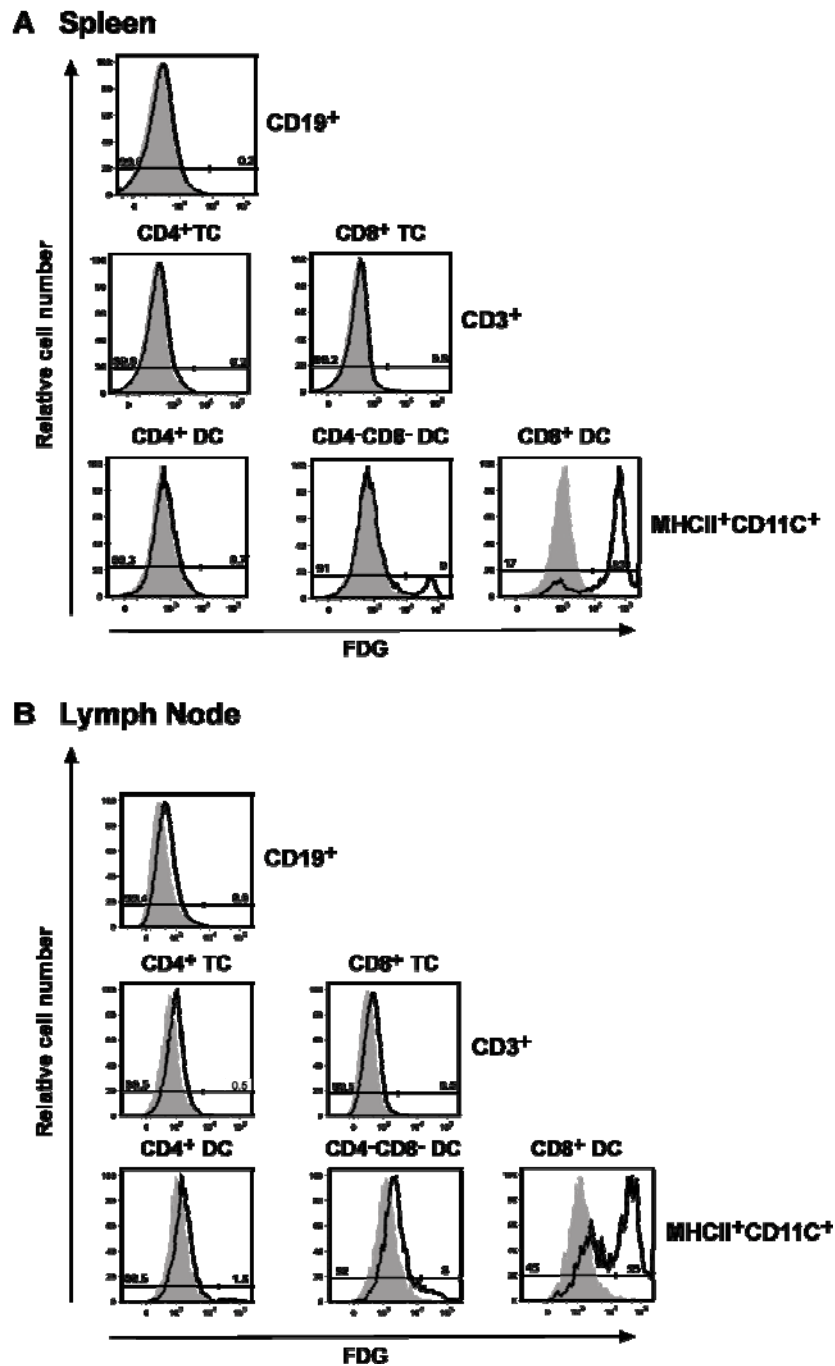


Fig. 9: XCR1 expression in spleen and LN

Spleen or LN cells from homozygous B6.XCR1-LacZ^{+/+} mice were loaded with FDG and analyzed by flow cytometry. FDG-fluorescence was analyzed in various cell subsets defined by staining with mAb against CD19, CD3, CD11c, MHC-II, CD4 and CD8. (A) Percentage of FDG⁺ cells in various cell subsets in the spleen (CD19⁺ B cells, CD4⁺ T cells, CD8⁺ T cells and CD11c⁺ MHC-II⁺ DC subtypes). (B) Percentage of FDG⁺ cells in various cell subsets in the LN. The background signal obtained in wild type B6 mice is depicted as filled grey curves, positive FDG signals obtained with cells from B6.XCR1-LacZ^{+/+} mice are shown as open black curves.

The percentages of FDG⁺ conventional DC subsets in spleen and different lymph nodes are summarized in Tab. 7.

Tab. 7: Percentages of FDG⁺ cDC subtypes in spleen and LN

Organs/ cDC subtypes	FDG⁺ CD4⁺ DC %	FDG⁺ CD4⁻ CD8⁻ DC %	FDG⁺ CD8⁺ DC %
Spleen	0	9	80
Popliteal LN	4	8	46
Inguinal LN	8	15	64
Axillary LN	2	10	41
Mandibular LN	4	12	53
Mesenteric LN	9	21	53

FDG⁺ cells were further characterized for the expression of a surface marker known to be present at high levels on CD8⁺ DC (e.g. DEC205). DEC205 receptor expressed on CD8⁺ DC belongs to the C-type lectin family mediating endocytosis. The correlation between CD205 and XCR1 in spleen and LN was analyzed by flow cytometry. Splenocytes were prepared from B6.XCR1-LacZ^{+/+} or control B6 mice. DC from DAPI⁻ live cells were defined by gating on CD19⁻ CD11c⁺ MHCII⁺ cells and subdivided using CD4 and CD8 expression (Fig. 10 A). In the spleen, all FDG⁺ CD8⁺ DC or FDG⁺ CD4⁻ CD8⁻ DC were at the same time positive for CD205, on CD4⁺ DC no XCR1 or CD205 expression was found (Fig. 10 B). In the LN, the same correlation between XCR1 and CD205 expression was observed (Fig. 10 C). Other surface markers expressed at high level on CD8⁺ DC (e.g. CD103 or CD24) were also tested and were found to be expressed on all FDG⁺ cells (data not shown).

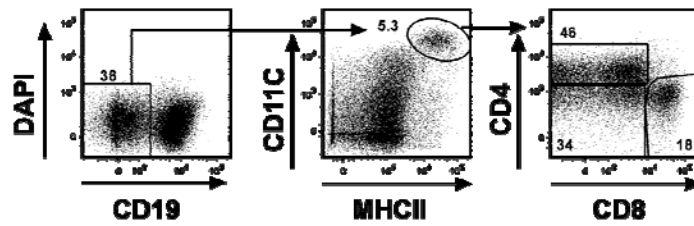
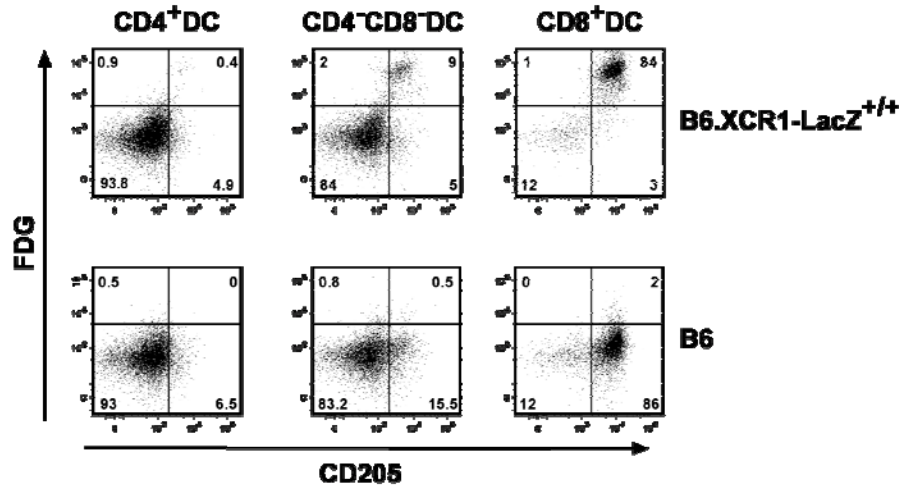
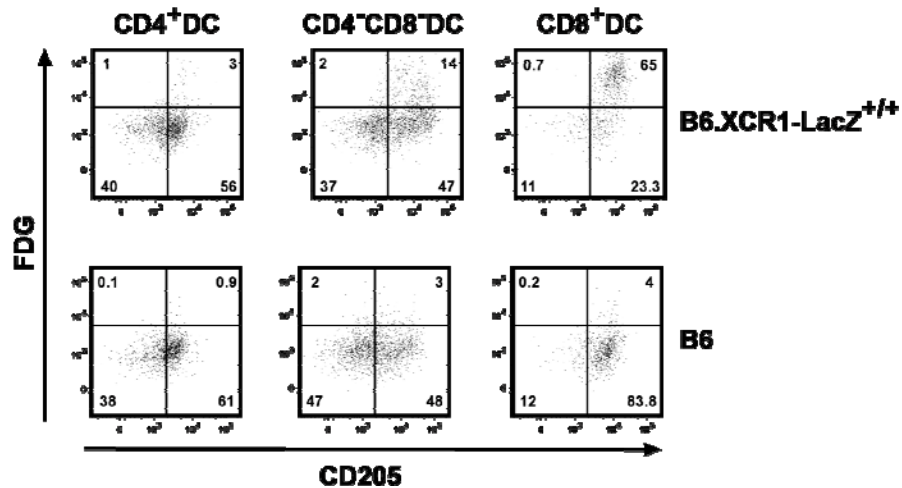
A DC Gateing**B Spleen****C Lymph node**

Fig. 10: Correlation of XCR1 and CD205 expression in the spleen and the LN

Spleen and LN cells from homozygous B6.XCR1-LacZ^{+/+} or B6 wt were stained with FDG. (A) DC subsets were gated using the markers CD19, CD11c, MHC-II, CD4 and CD8. (B) Correlation of FDG and CD205 expression on DC subsets in the spleen. (C) Correlation of FDG and CD205 expression on DC subsets in the LN. In B and C the upper rows represent cells from B6.XCR1-LacZ^{+/+} mice, the FDG background signal obtained with cells from wild type B6 mice is shown in the lower rows.

3.2 Migration of XCR1⁺ cells in the spleen

Many published data demonstrate that TLR-agonists like LPS or CpG induce translocation of splenic DC to the T cell area of the white pulp (De Smedt et al., 1998; De Trez C. et al., 2005). A similar effect was also shown in infection models with *Plasmodium* and *Leishmania* (Ato et al., 2006; Leisewitz et al., 2004). After chracterization of XCR1 expression in the different murine tissues, we were interested to investigate whether XCR1⁺ cells migrate after LPS or ATAC application.

3.2.1 LPS induces translocation of splenic XCR1⁺ cells to the T cell areas

LPS (25 µg) was injected i.v. into B6.XCR1-LacZ^{+/+} mice and spleen cryosections were prepared after different time points (0, 3, 6, 9, and 24 h) (Chap. 2.9.1). The sections were histologically examined using a standard peroxidase protocol for CD11c or CD205 or the established X-gal staining for XCR1. As shown in Fig. 11 A, CD11c⁺ DC start to translocate from the marginal zone and the red pulp into the T cell zone after 3 - 9 h, after 24 h the CD11c signal was still detectable. The XCR1⁺ DC show a similar translocation as CD11c⁺ DC from the marginal zone and the red pulp into the T cell zone, but after 24 h there was no XCR1 signal detected (Fig. 11 B). CD205⁺ cells show similar migration into the T cell zones with up regulation of the CD205 expression at 6 – 9 h after LPS injection (Fig. 11 C).

The injection of LPS into B6.XCR1-LacZ^{+/+} led to a similar translocation of CD11c⁺, CD205⁺ and XCR1⁺ cells in the spleen. This data indicate that CD8⁺ DC translocation into the T cell area after LPS injection is not dependent on XCR1 expression. After 24 h, no XCR1 signal was detected which could either be due to the selective disappearance of CD8⁺ DC or the downregulation of LacZ expression.

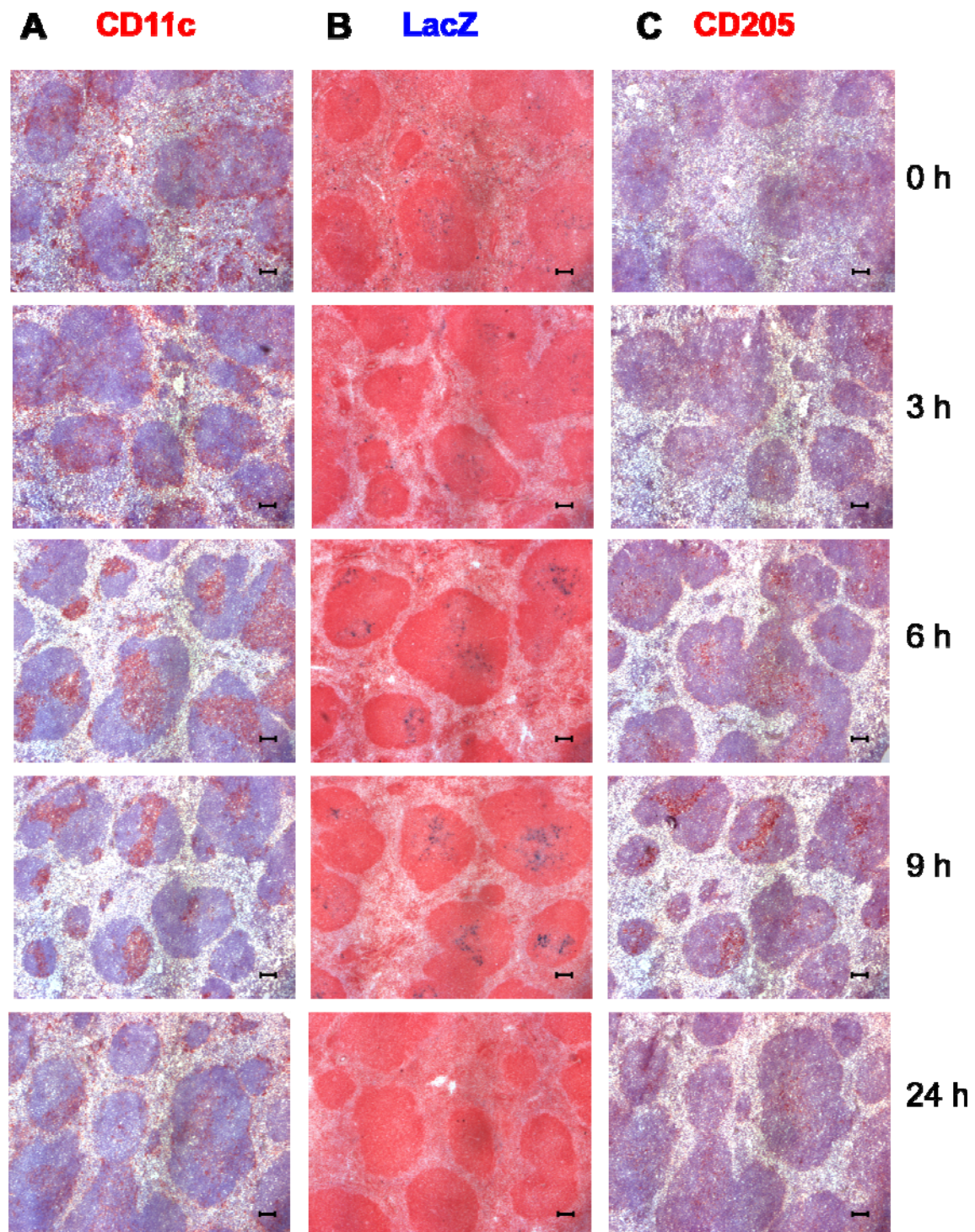


Fig. 11: CD8⁺ DC translocate to the T cell zone in the spleen after LPS injection

25 μ g LPS was injected i.v. into B6.XCR1-LacZ^{+/+} mice and after different time points (0, 3, 6, 9, and 24 h) cryostat sections from spleens were prepared. (A) CD11c staining using the peroxidase immunostaining protocol, CD11c in red, nuclear counterstaining using haematoxylin. (B) β -galactosidase activity using X-gal staining, XCR1 in blue, nuclear counterstaining with Neutral Red. (C) CD205 staining using the peroxidase immunostaining protocol, CD205 in red, counterstaining with haematoxylin. Scale bar corresponds to 50 μ m.

3.2.2 localization of XCR1⁺ cells after ATAC application

An *in vitro* chemotaxis assay showed that ATAC induces chemotaxis selectively in CD8⁺ DC from B6.XCR1-LacZ^{+/-} heterozygous mice but not from homozygous mice. To test the effect of ATAC on the translocation of CD8⁺ DC *in vivo*, 1×10^6 300-19-wt or 300-19-ATAC transfectant cells were injected i.v. into B6.XCR1-LacZ^{+/-} recipient mice which express one XCR1 allele. After 6 h, spleen cryosections were prepared and subjected to X-gal histostaining. In heterozygous B6.XCR1-LacZ^{+/-} mice injected with PBS or 300-19-wt, the XCR1⁺ cells were present in the red pulp, marginal zone and very few cells were detected in the T cell zones. After injection of the ATAC transfectant, the XCR1⁺ cells location were mainly localized in the T cell zones and very few cells were left in the red pulp or marginal zone (Fig. 12). Although not all experiments showed the same results, we observed that XCR1⁺ cells had a tendency to translocate after application of ATAC transfectant cells *in vivo*. This effect were not observed in B6.XCR1-LacZ^{+/+} (data not shown).

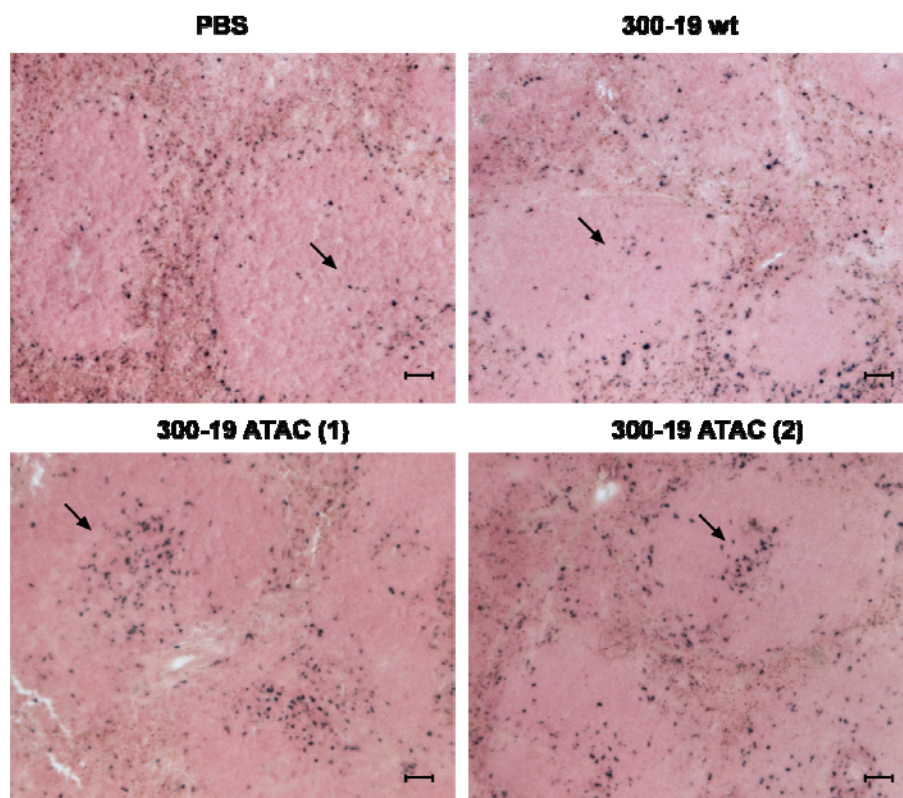


Fig. 12: ATAC induces an increase of the XCR1 signal in the T cell area

300-19-wt or 300-19-ATAC transfectant cells were injected i.v. into heterozygous B6.XCR1-LacZ^{+/-} recipient mice. After 6 h, cryosections of spleens from recipient mice were prepared for X-gal histostaining. XCR1 signal in blue, nuclear counterstaining with Neutral Red. Scale bar corresponds to 50 μ m.

3.3 Uptake of allogeneic cells by APC

Phagocytic cells such as macrophages and DC are responsible for the clearance of necrotic and apoptotic cells. Depending on the type of cell death, DC induce either an immune response or tolerance. The selective capability of CD8⁺ DC to take up live allogeneic cells has been described before (Iyoda et al., 2002). Next we wanted to investigate the possible role of XCR1 on CD8⁺ DC in the uptake of an allogeneic cell line.

3.3.1 In vivo uptake of allogeneic splenocytes or cell line

To test whether there are differences in the uptake of allogeneic versus syngeneic splenocytes, CFSE-labeled splenocytes prepared from B6 or BALB/c donor mice were injected i.v. into B6 recipient mice. Splenic DC from the recipient mice were analyzed by flow cytometry to determine if they have taken up CFSE⁺ cells (Fig. 13 A).

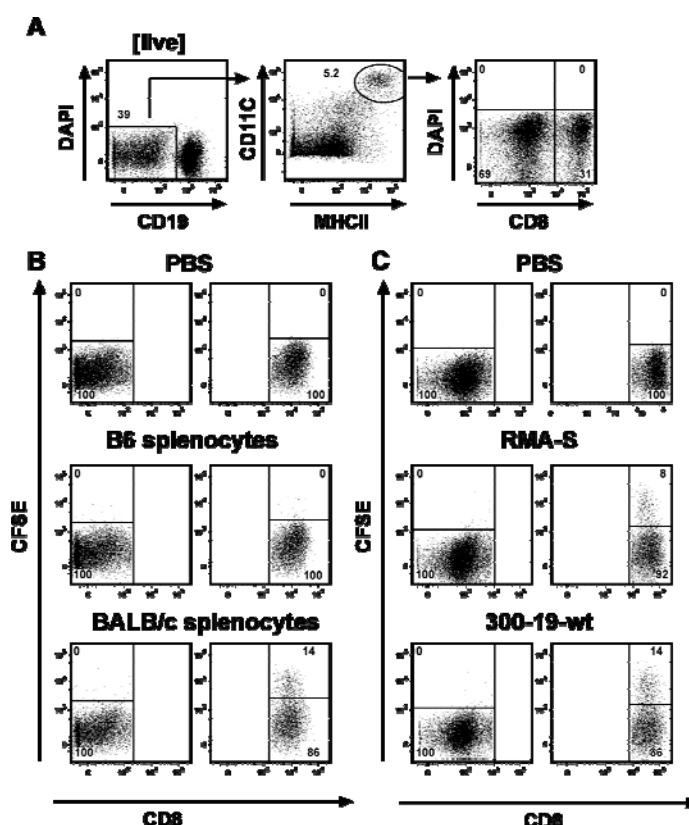


Fig. 13: Uptake of allogeneic cells by CD8⁺ DC

CFSE-labeled cells (10×10^6) or PBS were injected i.v. into B6 recipient mice. After 12 h, CFSE⁺ cells were detected in the spleen by flow cytometry. (A) Gating of DC subsets using the markers CD19, CD11c, MHC-II, and CD8. (B) Uptake of CFSE⁺ cells in the various DC subsets in spleen after injection of splenocytes from B6 or BALB/c mice (C) Uptake of CFSE⁺ cells in the various DC subsets in spleen after injection of an allogeneic cell line. The inset numbers represent percentages of positive cells.

Syngeneic splenocytes from B6 donor mice were not taken up by DC. Only allogeneic splenocytes from BALB/c donor mice were taken up by CD8⁺ DC but not by CD8⁻ DC (Fig. 13 B). The same uptake-experiment was performed with CFSE-labeled allogeneic cell lines (300-19-wt or RMA-S). Again, only splenic CD8⁺ DC showed uptake of the allogeneic cells (Fig. 13 C).

3.3.2 Kinetics of the uptake of an allogeneic cell line by CD8⁺ DC

To analyze the uptake kinetics of allogeneic cell lines by CD8⁺ DC, CFSE-labeled 300-19-wt cells were injected i.v. into B6 recipient mice. At different time points (0.5, 4, 14, and 20 h) CFSE⁺ cells were analyzed in the spleen by flow cytometry. As shown in Fig. 14, the uptake starts after 30 min and increases with time up to 14 h. After 20 h, the percentage of CFSE⁺ CD8⁺ DC decreases again.

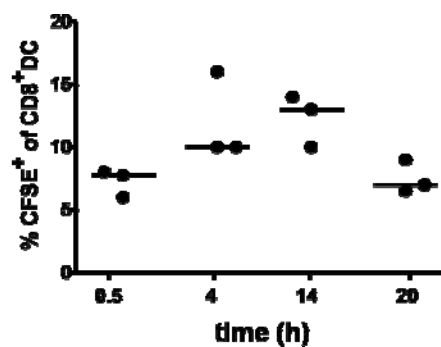
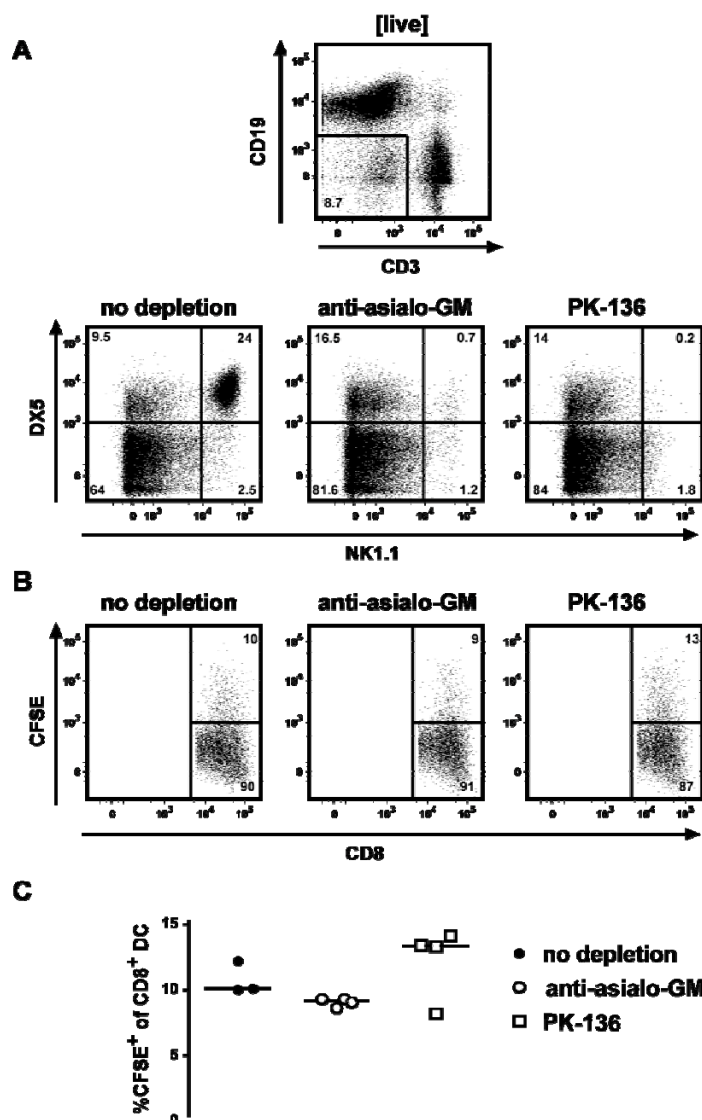


Fig. 14: Uptake kinetics of the allogeneic cell line 300-19-wt

CFSE-labeled 300-19-wt allogeneic cells (10×10^6) were injected i.v. into B6 recipient mice. After 0.5, 4, 14, and 20 h the percentages of CD8⁺ DC which have taken up CFSE⁺ cells in spleen was analyzed by flow cytometry.

3.3.3 NK cell depletion has no effect on the uptake of allogeneic cell lines

It has been described that NK cell depletion leads to an inhibition of the uptake of an allogeneic cell line by DC (Iyoda et al., 2002). To test whether NK cells play a role in the uptake of allogeneic cell lines, we depleted NK cells *in vivo* in B6 recipient mice using mAb PK136 or anti-asialo serum (Wako Pure Chemical Industries Ltd.) as detailed in Materials and Methods (Chap. 2.9.4). NK cells were defined as CD3⁻ CD19⁻ DX5⁺ NK1.1⁺, a depletion >98 % was observed with either PK136 antibody or anti-asialo serum (Fig. 15 A).



Thus, NK depletion using either PK136 monoclonal antibody or anti-asialo serum did not affect the uptake of CFSE⁺ allogeneic cells by CD8⁺ DC in our experiments

3.3.4 Only XCR1⁺ CD8⁺ splenic DC take up live allogeneic cell

DC are not the only phagocytic cells present in the mouse. Other professional phagocytes like macrophages or neutrophils were reported as very efficient at internalizing particles (Aderem and Underhill, 1999). So it was important to test whether these cells are involved in the uptake of allogeneic cells. CFSE-labeled 300-19-wt were injected i.v. into B6 recipient mice and after 12 h splenocytes were prepared. The CFSE signal in the different cell subsets was detected by flow cytometry (Fig. 16).

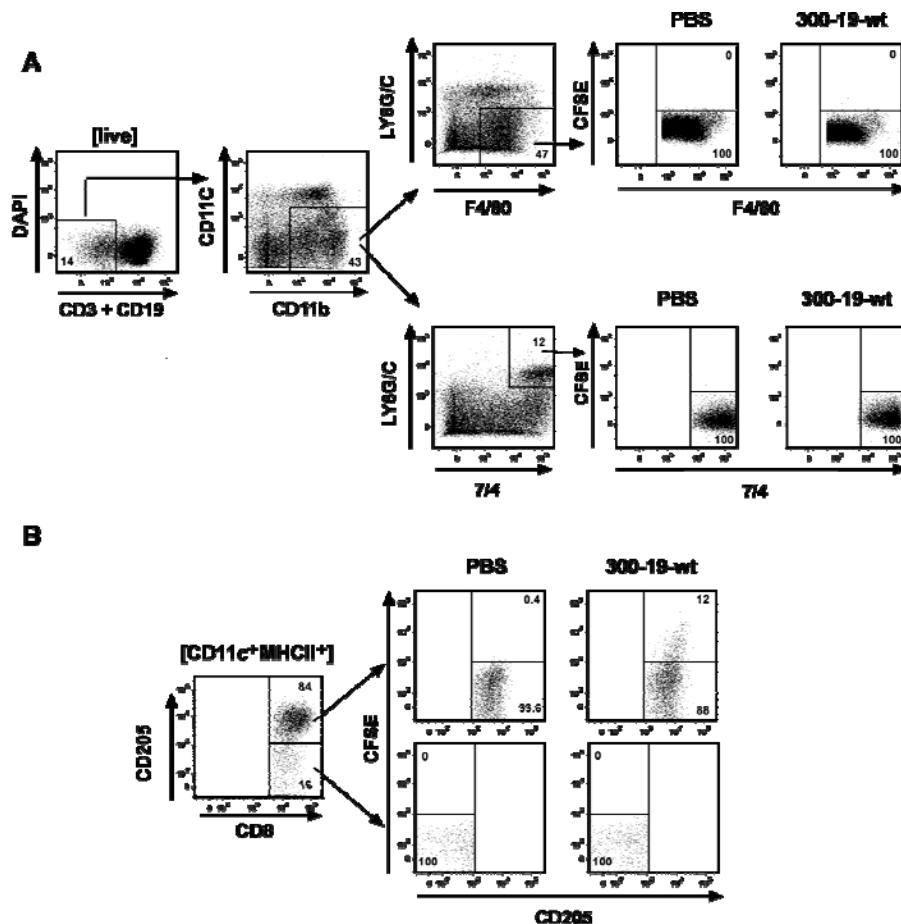


Fig. 16: 300-19 allogeneic cells are selectively taken up by XCR1⁺ CD8⁺ DC

Spleen cell subsets were analyzed by flow cytometry 12 h after injecting B6 mice with PBS or 10×10^6 CFSE-labeled 300-19-wt cells. (A) Dot plots of macrophages (CD11b⁺ F4/80⁺) and neutrophils (CD11b⁺ 7/4⁺) gated on CD19⁻ CD3⁺ CD11c⁻ cells. (B) Dot plots of either CD205⁺ CD8⁺ DC or CD205⁻ CD8⁺ DC subsets in spleen gated on DC. The inset numbers represent percentages of positive cells.

Allogeneic cells were not taken up by macrophages ($CD11b^+F4/80^+$) or neutrophils ($CD11b^+7/4^+$). At least at this time point, neither macrophages nor neutrophils seemed to play a role in the uptake of allogeneic cell lines in the spleen (Fig. 16 A). In the same experimental setup, the uptake of allogeneic cells by $XCR1^+CD8^+$ DC versus $XCR1^-CD8^+$ DC was tested using CD205. Direct staining of XCR1 in this experimental setup using FDG was technically not possible due to the overlap between the FDG and CFSE spectrum. It was found that $CD8^+CD205^+$ DC cells were the only subpopulation responsible for the uptake of allogeneic cells and not $CD8^+CD205^-$ DC (Fig. 16 B). As a final conclusion, we could demonstrate that only $CD205^+XCR1^+CD8^+$ DC subpopulation in the spleen is responsible for the uptake of allogeneic cell lines.

3.3.5 ATAC/XCR1 interaction increases the uptake of allogeneic cells by $CD8^+$ DC

Next we investigated the question if ATAC/XCR1 interaction could have an effect on the uptake of allogeneic cells. To this end we used either a CFSE-labeled 300-19-ATAC transfectant or 300-19-wt controls to test for differences in the uptake of these cells by $CD8^+$ DC. B6.ATAC-KO as recipient mice were used instead of B6 mice to avoid any involvement of endogenous ATAC. CFSE-labeled cells were injected i.v. into B6.ATAC-KO or B6.XCR1-LacZ^{+/+} mice, respectively. The uptake of the cell line by $CD8^+$ DC was tested in the spleen after 12 h using flow cytometry (Fig. 17).

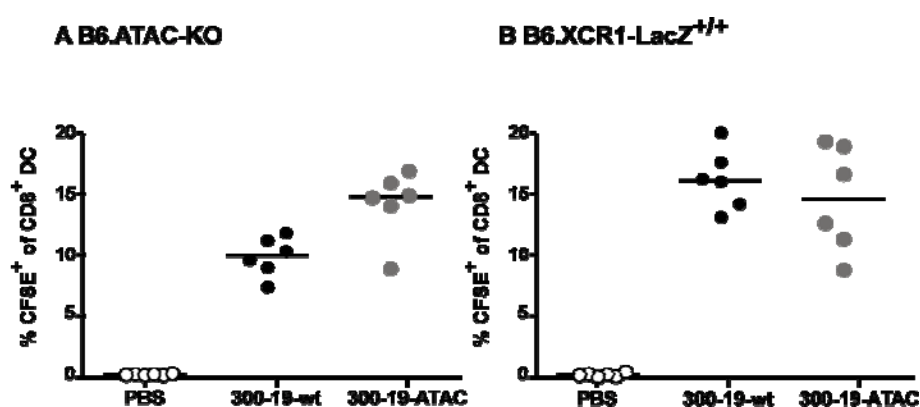


Fig. 17: Increase in the uptake of the 300-19 cell line expressing ATAC by $CD8^+$ DC

Percentage of CFSE⁺ $CD8^+$ DC in the spleen 12 h after i.v. injection of either 10×10^6 300-19-wt or 300-19-ATAC into (A) B6.ATAC-KO or (B) B6.XCR1-LacZ^{+/+}. Horizontal lines indicate the median value for all animals within one experimental group. One representative experiment out of 4 is shown (6 mice per group).

An increase in the uptake of the allogeneic cell line in B6.ATAC-KO recipient mice injected with ATAC transfectant was found compared to the wt control cell line (Fig. 17 A). In the case of B6.XCR1-LacZ^{+/+} there was no difference between the wt cell line and the ATAC transfectant (Fig. 17 B).

These results suggest that the increased uptake of cells by CD8⁺ DC was due to the presence of ATAC and not caused by any other differences between the wt and the transfected cell line.

3.3.6 ATAC binds to the cell membrane of apoptotic cell lines

Chemokines bind to GAG molecules associated with proteins in the extracellular matrix and on cell surfaces (Rot and von Andrian, 2004). It was reported that ATAC adopts two distinct structures in equilibrium: one conformation specifically recognizing XCR1 and the other binding to the GAG-containing molecule heparin (Tuinstra et al., 2008; Volkman et al., 2009). One possible explanation for the increased uptake of ATAC-expressing cells is that ATAC binds to the surface of cells in addition to its binding to XCR1. In our first experiment we observed a possible binding of ATAC on the cell surface of apoptotic cells and not live cells. For this reason, we further tested whether ATAC can bind to the surface of live, early apoptotic, late apoptotic and dead cells *in vitro*. To achieve this, 300-19-wt cells were incubated for 15 min at 46° C and then further cultured for 6 h at 37° C to induce a mixture of live and apoptotic cells. Heat-shocked 300-19-wt cells (1×10^6) were incubated for 1 h with 1 µg/ml synthetic ATAC (Dictagene, Lausanne, Switzerland) at RT. After washing, cells were stained with anti-ATAC mAb (MTAC-311) and with Annexin V to discriminate between live and apoptotic cells. ATAC specifically bound *in vitro* to the cell surface of late apoptotic cells (DAPI⁺ Annexin V⁺) and not to early apoptotic (DAPI⁻ Annexin V⁺), live (DAPI⁻ Annexin V⁻) or dead cells (DAPI⁺ Annexin V⁻) (Fig. 18). The same result was also observed with heat-shocked, apoptotic primary cells from B6 mice (data not shown).

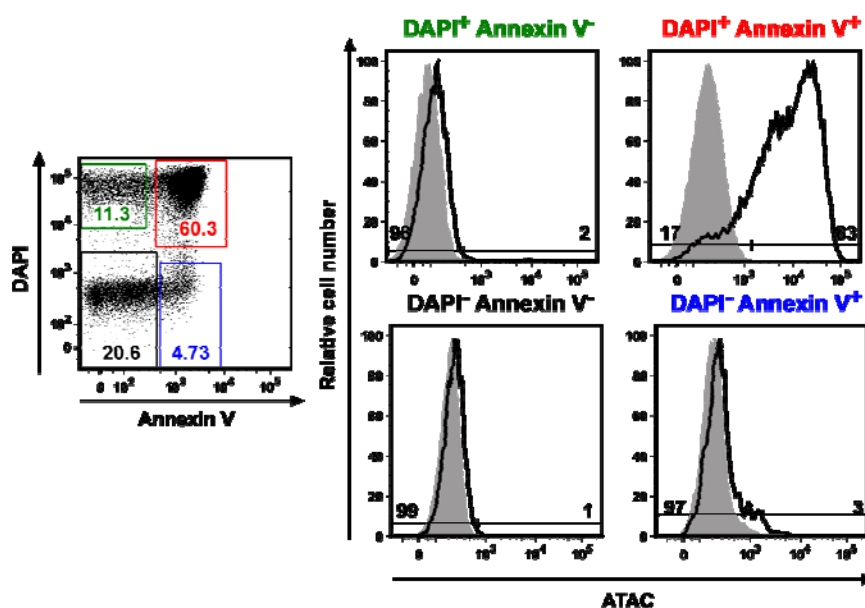


Fig. 18: ATAC binds on the cell surface to apoptotic cell

Heat-shocked 300-19-wt cells (1×10^6) were incubated with 1 $\mu\text{g/ml}$ synthetic ATAC (Dictagene) for 1 h at 37 °C. After washing two times with PBS, live or apoptotic cell were distinguished by staining with Annexin V for apoptotic cells and DAPI for dead cells. ATAC (open black curve) was detected on the cell surface using MTAC-311 mAb coupled to PE in flow cytometry. Background staining without ATAC incubation is also shown (filled grey curve).

3.4 Antigen targeting to CD8⁺ DC leads to cellular but not to humoral immunity

CD8⁺ DC efficiently endocytose extracellular antigen, cross-present it in the context of MHC-I and potently induce cytotoxic T lymphocytes. We started to investigate the biological consequences after antigen delivery to XCRI⁺ CD8⁺ DC *in vivo*. Cell-associated ovalbumin (OVA) was generated and used to deliver OVA to CD8⁺ DC. A delta OVA-YFP-pcDNA3 vector was constructed and transfected into the murine pre-B cell line 300-19-wt (Chap. 2.6.2). The delta OVA sequence lacked the first 137 N-terminal amino acids and thus produces a protein variant that could only be expressed intracellularly. This gives the advantage of targeting the cell-associated OVA selectively to CD8⁺ DC and not any other APC. Stable clones expressing delta OVA were selected in culture by resistance against Geneticin (G418, Invitrogen). Flow cytometric analysis was used to test positive clones expressing YFP. Clone A5 showed a strong YFP expression and therefore was selected for further *in vivo* antigen targeting experiments (Fig. 19).

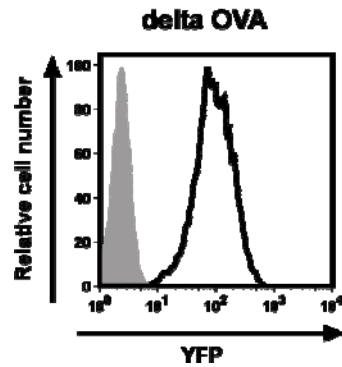


Fig. 19: Delta OVA-YFP transfected cell line

YFP expression in transfectant cell lines was analyzed using flow cytometry for the selection of the stable clone. 300-19-delta OVA-YFP clone A5 (open black curve) and negative control 300-19-wt cell line (filled grey curve).

In this model, the capacity of delta OVA expressing allogeneic cells to induce antigen-specific T cell or humoral immune responses was investigated (Fig. 20).

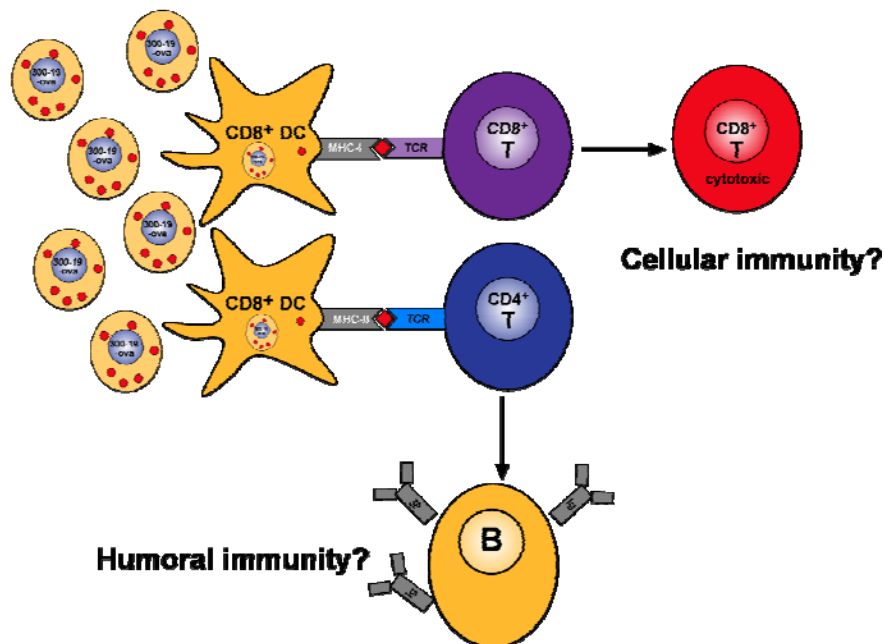


Fig. 20: Model of the immune response using an allogeneic cell line that targets antigen to CD8⁺ DC

To determine the generation of OVA-specific antibodies, B6 recipient mice were immunized i.v. with 300-19-delta OVA \pm LPS, 300-19-wt cells were used as a negative control. Mice were immunized either at days 1, 3, and 14 (analysis was at day 28), or at days 1, 3, 14, and 30 (analysis was at day 48). The serum of immunized mice was collected by puncture of the

retro-bulbar vein and the presence of OVA-specific immunoglobulin (Ig) in the serum was analyzed by ELISA (Chap. 2.10.1). Mice immunized with 300-19-delta OVA, when compared to mice immunized with 300-19-wt showed no OVA-specific Ig production, and the addition of LPS did not lead to any change (Fig. 21).

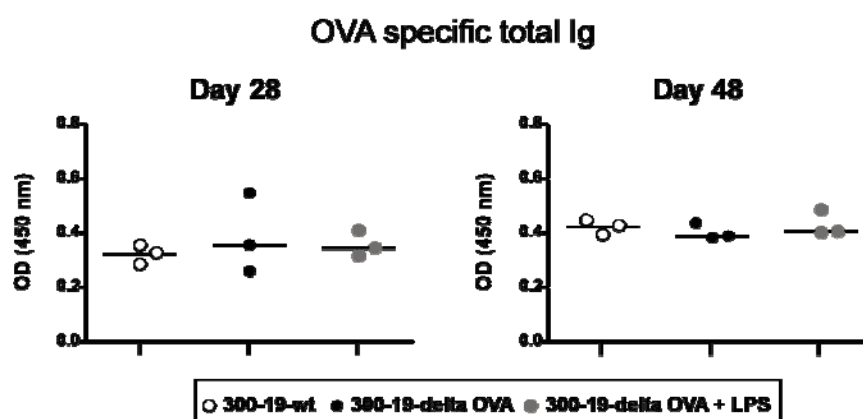


Fig. 21: OVA-specific immunoglobulin production

B6 recipient mice were immunized i.v. with 3×10^6 300-19-delta OVA cells \pm 3 μ g LPS (control: 3×10^6 300-19-wt). At days 28 or 48 after immunization, serum levels of OVA-specific Ig were determined by ELISA and are represented as optical density (OD) values at 450 nm (3 mice per group).

To determine the generation of OVA-specific cytotoxicity, the B6 recipient mice tested above for the production of OVA-specific Ig, were once more immunized at day 60. After another 6 days, a mixture of 10×10^6 CFSE^{low} unpulsed splenocytes and 10×10^6 CFSE^{high} SIINFEKL-peptide-pulsed B6 splenocytes were adoptively transferred into the differently immunized mice. Spleen cells of recipient mice were prepared 18 h later to evaluate the percentage of specific killing (Chap. 2.4.6). Dot plots of all CFSE⁺ cells gated on live cells are presented, which are further subdivided into CFSE^{low} and CFSE^{high} (Fig 22 A). Percentage target cell killing was calculated according to the ratio between CFSE^{low} and CFSE^{high} in immunized and control groups. In mice immunized with 300-19-delta OVA 60 % specific target cell killing was found. The addition of LPS lead to a slight increase in the killing percentage (Fig 22 B). These data show that targeting of antigen to CD8⁺ DC using the cell line 300-19-delta OVA induces strong cytotoxicity but no antigen-specific antibodies.

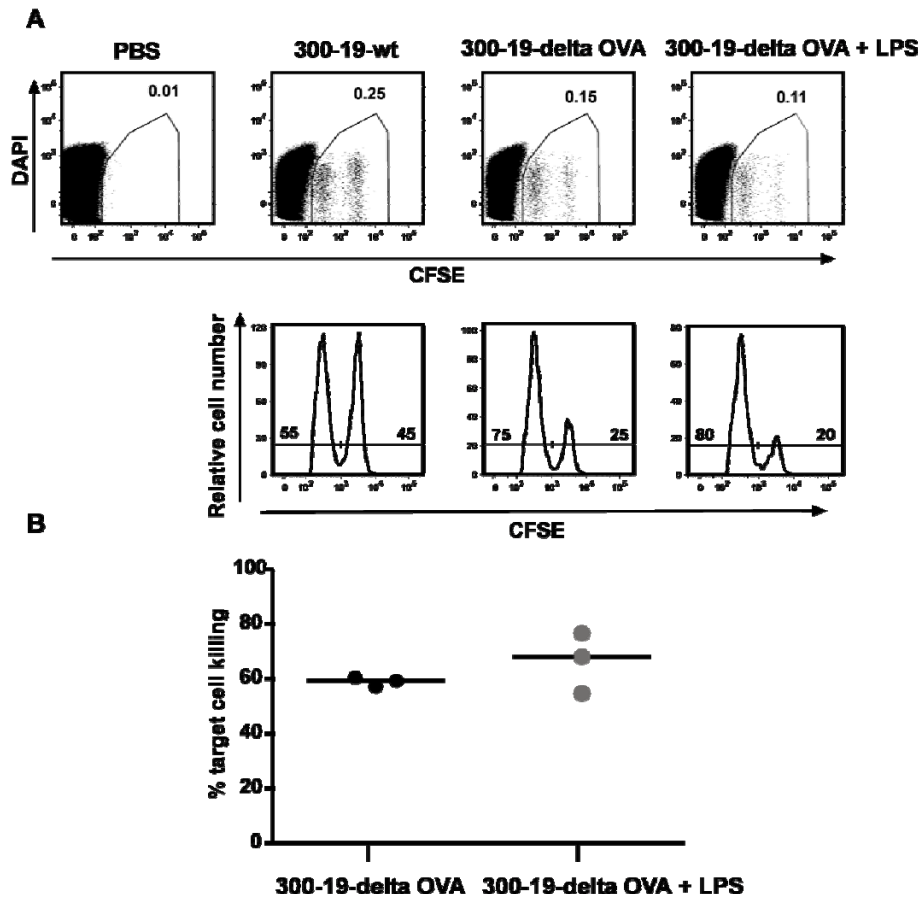


Fig 22: *In vivo* CTL activity against SIINFEKL-loaded B6 splenocytes

B6 recipient mice were immunized i.v with 3×10^6 300-19-delta OVA cells \pm 3 μ g LPS (control: 3×10^6 300-19-wt) at days 1, 3, 14, 30, and 60. After further 6 days a 1:1 mixture of unpulsed CFSE^{low} and peptide-pulsed CFSE^{high} naive B6 spleen cells was adoptively transferred into the immunized mice. (A) 18 h later, CFSE signals gated on live cells were analyzed by flow cytometry. (B) Percentage of specific targeting killing. Injection of 300-19-wt cells never resulted in a cytotoxic activity against SIINFEKL-loaded syngeneic target cells.

3.5 Influence of ATAC secretion on the development of cytotoxicity

Antigen targeting to CD8⁺ DC initiates a strong immune response and the induction of antigen-specific cytotoxic T cell. In addition, activated CD8⁺ T cell were reported to express ATAC. The role of XCRI⁺ CD8⁺ DC *in vivo* was investigated using CTL assay as a suitable read out to test the interaction between CD8⁺ DC expressing XCR1 and CD8⁺ T cell expressing ATAC.

3.5.1 Induction of cytotoxicity after adoptive transfer

OVA contains at amino acids positions 257-264 and 323-339 well defined binding sequences for MHC class I and class II in B6 mice, respectively. OVA was used as model antigen for T cell activation assays using TCR transgenic mice that are specific for OVA peptide presented either onto the MHC class I (OT-I mice) or class II epitope (OT-II mice) (Diebold et al., 2001).

At first, we investigated whether after injection of 300-19-delta OVA, splenic $CD8^+$ DC present OVA to OVA-specific transgenic $CD8^+$ T cells or $CD4^+$ T cells, or both. CFSE-labeled OT-I or OT-II cells were adoptively transferred into B6 mice at day -1. At day 0, the recipient mice were immunized with different cell number of the 300-19-delta OVA transfectant. After 3 days, the frequency and the percentage of divided transgenic T cells was analyzed by flow cytometry. As shown in Fig. 23, OT-I transgenic $CD8^+$ T cells strongly expanded and almost all the cells had divided even with the lower numbers of the transferred 300-19-delta OVA. In the case of OT-II transgenic $CD4^+$ T cells, no expansion was observed regardless of the number of transferred cells. A small increase of the percentages of divided OT-II transgenic $CD4^+$ T cells was observed only after injection of higher cell numbers.

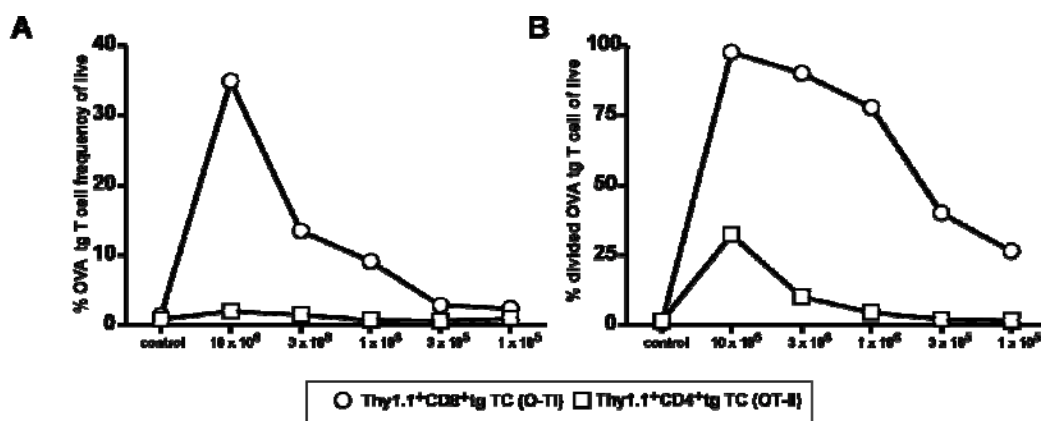


Fig. 23: Presentation of intracellular OVA to OT-I but not OT-II transgenic T cells

B6 mice were adoptively transferred with 4×10^6 OT-I or OT-II OVA transgenic T cells on day -1. On day 0, the mice were i.v. immunized with different 300-19-delta OVA cell numbers (1×10^5 , 3×10^5 , 1×10^6 , 3×10^6 and 10×10^6), negative control: 3×10^6 300-19-wt. After 3 days, (A) the frequency of $Thy1.1^+ CD8^+$ T cells or $Thy1.1^+ CD4^+$ T cells, and (B) the percentages of $Thy1.1^+ CD8^+$ T cells or $Thy1.1^+ CD4^+$ T cells that have undergone division was determined by flow cytometry analysis, of splenic cells.

Apparently, CD8⁺ DC efficiently presented cell-associated OVA antigen and induced the activation of OVA-specific CD8⁺ T cells even at lower antigen dose, while in the case of OVA-specific CD4⁺ T cells very low activation was observed only with the high antigen load.

3.5.1.1 ATAC/XCR1 interaction increases the cytotoxicity activity of CD8⁺ T cells

While we could show that antigen delivered specifically to XCR1⁺ CD8⁺ DC induces an efficient cytotoxic response (see above), it was still unclear whether in this situation the interaction of ATAC and XCR1 influences the expansion and induction of cytotoxic CD8⁺ T cells. To answer this question, we used different experimental settings: we either adoptively transferred B6.OT-I T cells in wild type (B6) and XCR1-deficient (B6.XCR1-LacZ^{+/+}) recipients or we transferred ATAC-deficient OT-I cells in ATAC-deficient (B6.ATAC-KO) recipients (Fig. 24). The animals were injected 24 h later with 300-19-delta OVA cells. On day 6 after antigen delivery, the frequency and CTL activity of the transgenic T cells were tested.

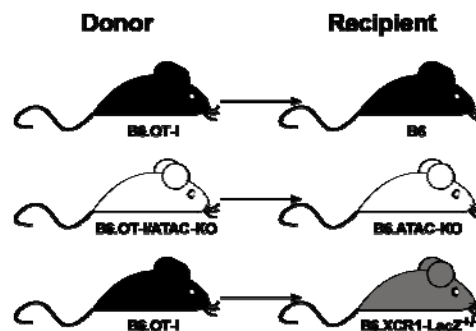


Fig. 24: Overview of the adoptive transfer system used to test the influence of ATAC/XCR1 interaction on the induction of CTL.

When both ATAC and XCR1 were present, the frequencies of transferred T cells strongly expanded by a factor of about 4 after activation. This expansion was clearly reduced in the absence of XCR1 and completely abolished in the absence of ATAC (Fig. 25 A). A comparable effect was observed after analysis of the cytotoxic activity. Interruption of the ATAC/XCR1 interaction reduced the percentage of target cell killing from 80% to 60% or

40%, respectively (Fig. 25 B). These results show that the induction of strong cytotoxic T lymphocytes is only optimal in B6 mice in which the ATAC/XCR1 interaction is possible.

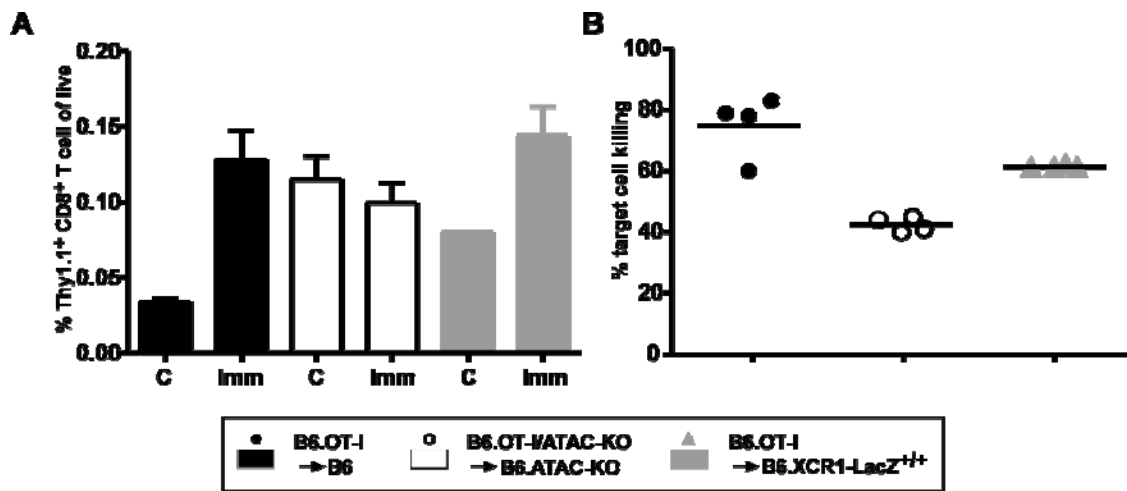


Fig. 25: Influence of ATAC/XCR1 interaction on the differentiation of CD8⁺ T cells into effector cells

1×10^6 B6.OT-I T cells were adoptively transferred into wild type B6 or B6.XCR1-LacZ^{+/+} recipients and 1×10^6 B6.OT-I/ATAC-KO cells into B6.ATAC-KO recipients. Animals were injected 24 h later with 3×10^6 allogeneic 300-19-delta OVA cells (negative controls were immunized with 300-19-wt). (A) The frequency of Thy1.1⁺ CD8⁺ T cells gated on live cells, and (B) percentage of specific targeting killing were determined on day 6. Horizontal lines indicate the mean value for all animals within one experimental group.

To exclude the influence of other endogenous cell populations secreting ATAC (like NK and NK T cells), an experiment was performed in which B6.OT-I/ATAC-KO cells were transferred into B6 or B6.ATAC-KO recipients. Transfer of B6.OT-I cells in B6 recipients served as a control (Fig. 26). CTL activity was analyzed at day 6 and 12.

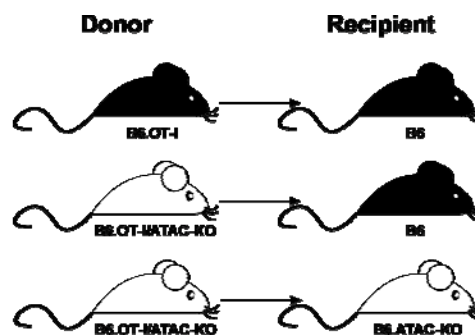


Fig. 26: Overview of the adoptive transfer system used to test CTL induction in the same recipient mice.

At day 6, no significant differences were observed concerning the frequency of OT-I T cells in all experimental settings. However, the cytotoxic activity was slightly reduced when ATAC was absent both in the transferred T cells and the recipient (Fig. 27 A and B). At day 12, the presentation of specific antigen increased OT-I frequency and CTL activity only when B6.OT-I cells were transferred into B6 recipients. In the absence of ATAC, the expansion of the transferred T cell population was severely diminished and the cytotoxic activity reduced by about 50% (Fig. 27 A and B). Thus, the ATAC/XCR1 interaction strongly increases the survival of antigen-specific T cells and enhances the development of cytotoxicity.

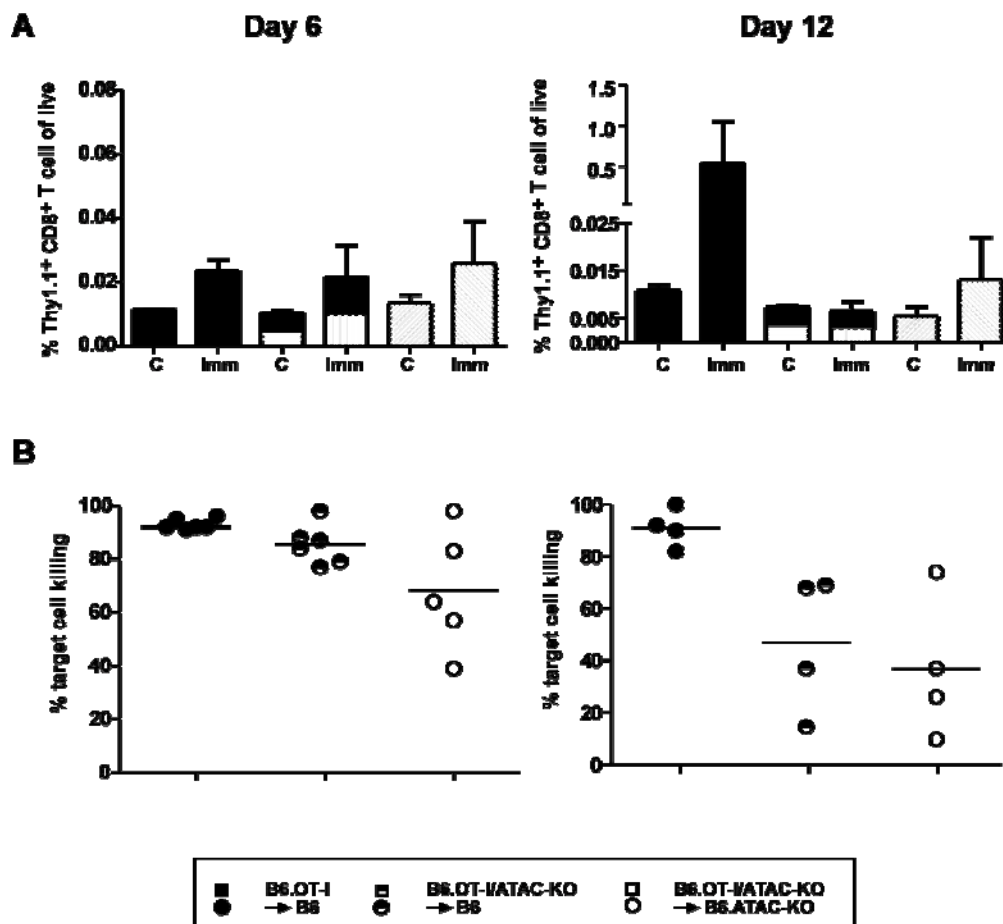


Fig. 27: CTL induction in B6 recipient mice after transfer of B6 OT-I versus B6.OT-I/ATAC-KO

B6.OT-I T cells (1×10^6) were adoptively transferred into wild type B6 and 1×10^6 B6.OT-I/ATAC-KO cells into B6 or B6.ATAC-KO recipients. 24 h later, mice were immunized with 3×10^6 allogeneic 300-19-delta OVA cells (controls were immunized with 300-19-wt). (A) The frequency of Thy1.1⁺ CD8⁺ T cells gated on live cells, and (B) percentage of specific targeting killing were determined on day 6 and 12 (Horizontal lines indicate the mean value for all animals within one experimental group).

3.5.2 Induction of endogenous cytotoxicity

Using an adoptive transfer system does not reflect all aspects of the physiological situation because the starting frequency of antigen-specific T cells is strongly enhanced. To test whether the observed contribution of endogenous ATAC-secreting cells to the cytotoxic activity of transferred OT-I T cells (Fig. 27 A) is also relevant in a more physiological situation, we induced cytotoxicity of an endogenous T cell population in B6 versus B6.ATAC-KO or B6.XCR1-LacZ^{+/+} mice by injecting 3×10^6 300-19-delta OVA cells (Tab. 8).

Tab. 8: Immunization for the induction of endogenous cytotoxicity

Exp. no.	Immunization (day)	CTL analysis (day)
1	1	12
2	1, 3, and 14	20
3	1, 3, and 14	45
4	1, 3, 14 and 30	36
5	1, 3, 14, 30 and 50	56

At days 12, 20, and 45 the percentage of specific targeting killing was low in all immunized mice, however in B6 mice we observed a slightly increased cytotoxicity compared to B6.ATAC-KO mice. At day 36, these differences were more pronounced while no differences were detected at day 56. In B6.XCR1-LacZ^{+/+} mice, we could not detect a significantly reduced cytotoxic activity compared to B6 mice (Fig. 28).

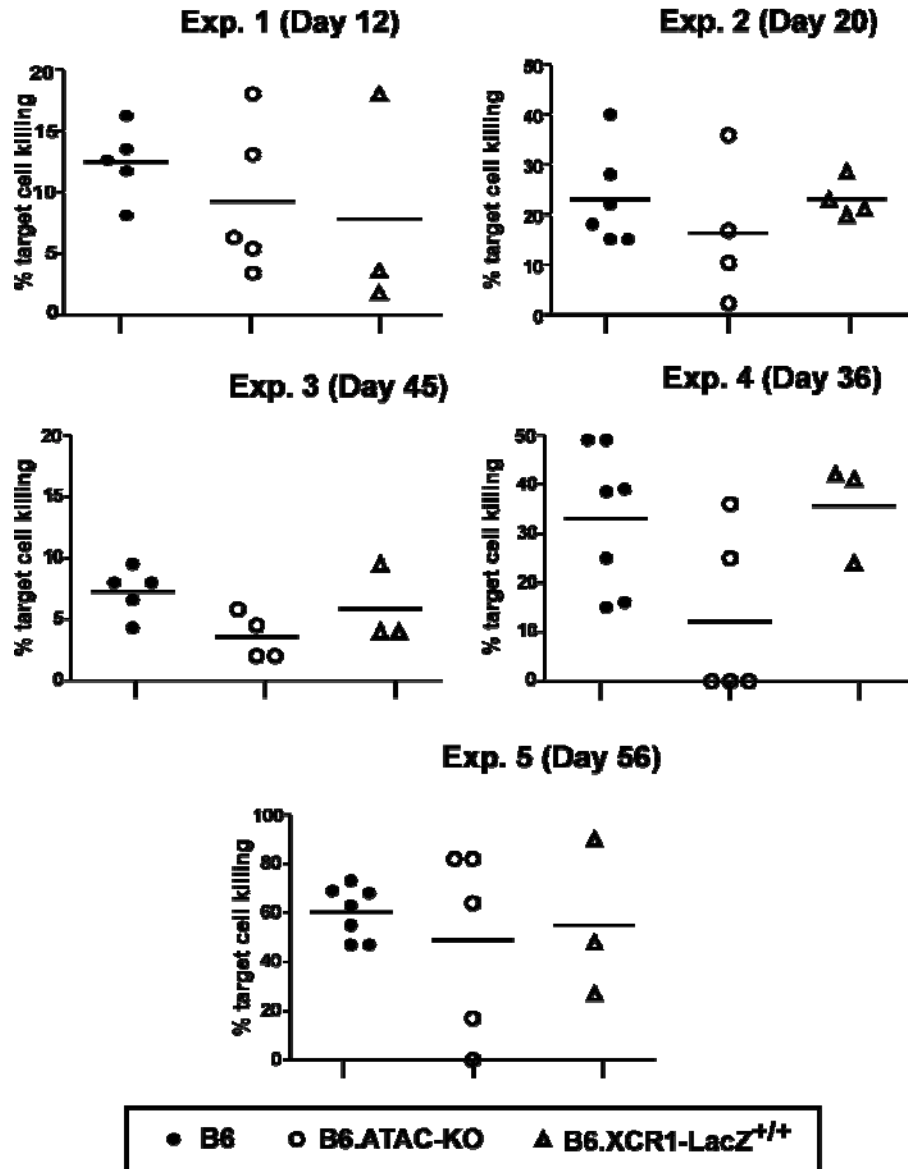


Fig. 28: The development of endogenous OVA-specific cytotoxic activity

B6, B6.ATAC-KO or B6.XCR1-LacZ^{+/+} recipient mice were immunized with 3×10^6 300-19-delta OVA or 300-19-wt cell line as described in (Tab. 8). Exp. no. showing the percentage of specific targeting killing. Horizontal lines indicate the mean value for all animals within one experimental group.

4 Discussion

In the presented thesis, the expression and the function of the chemokine receptor XCR1 was analyzed *in vivo*. We could demonstrate for the first time with LacZ reporter mice the XCR1 expression in the different tissues and also the exclusive expression of XCR1 in CD8⁺ DC. In addition, we could exactly phenotype these cells. The translocation of these specific cell subsets in the spleen from the MZ and red pulp to the T cell area was shown after application of an inflammatory stimulus or ATAC transfected allogeneic cells. At the functional level, XCR1⁺ CD8⁺ DC selectively endocytose allogeneic cell lines which can be enhanced by transfection with ATAC. ATAC/XCR1 interaction in B6 mice induces a potent CTL response.

4.1 Detection of XCR1 expression in murine tissues and cell subsets

The cloned 7-TM receptor GPR5 (Heiber et al., 1995) was renamed about 10 years ago to XCR1 because it was shown that ATAC is the only ligand for this receptor (Yoshida et al., 1999). At the beginning of this work, many contradictory data were published on the expression of murine or human XCR1 in different immune cell subtypes or tissues. All published data were based on standard RT-PCR assays performed on total RNA extracted from whole tissues or defined cell subsets.

We first planned to generate a mAb against murine XCR1 to avoid the problems encountered by using RT-PCR detection systems. Unfortunately, we did not succeed to produce a mAb against murine XCR1. In the past, mAbs could be generated against a variety of chemokine receptors, but still the creation of mAbs against chemokine receptors remains very challenging. One of the main difficulties is that chemokine receptors are 7-TM proteins where only 30 % of the receptor is accessible on the cell surface. The second factor is the high similarity between the different chemokine receptors (Ponath et al., 2000; Kremer and Marquez, 2004). We therefore used an antibody-independent strategy for the characterization of XCR1 expression in order to understand the role of XCR1 for the murine immune system. It was shown that LacZ can be used in mice as a reporter gene for the activity of a given promoter (Schmidt et al., 1998). In this work, XCR1 expression was characterized in the B6.XCR1-LacZ^{+/+} reporter mouse which expresses β -galactosidase under the control of the XCR1 promoter.

We could detect for the first time XCR1 expression in the different murine tissues represented by β -galactosidase enzyme activity. The XCR1 signal was present in a wide

range of murine lymphoid organs like spleen, thymus, and lymph nodes. XCR1 was also detected in non-lymphoid organs like liver, lung, and testis, but at a lower frequency (Tab. 6). XCR1⁺ cells in the spleen were found in the red pulp, the marginal zones and central areas of the T cell zone (Fig. 6). This is in accordance with recent reports while CD8⁻ DC are present in the red pulp and in B cell areas of the white pulp (McLellan et al., 2002; Shortman and Liu, 2002; Idoyaga et al., 2009). In the peripheral organs, the appearance of the few XCR1⁺ cells and the anatomical location suggests that these cells are DC. In addition, a characterization of cell subsets expressing XCR1 was performed in histological section using a newly established double staining protocol. We could demonstrate in all lymphoid tissues that XCR1⁺ cells represent a subset of CD11c⁺ or CD8⁺ cells (Fig. 8).

Due to the inherent difficulties in interpreting double staining data, the characterization of cell subsets expressing XCR1 in spleen and LN was performed by also flow cytometry. This was achieved using FDG, a substrate for LacZ cells in B6.XCR1-LacZ^{+/+} reporter mice. The XCR1 expression in spleen and LN was detected on a large majority of CD8⁺ DC and on very few CD4⁻ CD8⁻ DC. All other cell subsets tested showed no XCR1 expression (Fig. 9). Thus, in contrast to the published data showing XCR1 expression on T, B, and NK cells (Cairns et al., 2001; Huang et al., 2001; Yoshida et al., 1999), we found a selective expression of XCR1 on splenic CD8⁺ DC. These results were supported by recent findings in our group using a highly specific, quantitative PCR approach (Dorner et al., 2009). Many surface markers like CD205, CD103, CD207 and CD24 were demonstrated to be preferentially expressed on CD8⁺ DC and responsible for diverse functions (McLellan et al., 2002; Idoyaga et al., 2009; Qiu et al., 2009). We found that all XCR1⁺ cells are strictly correlated with CD205 in spleen and LN, however not all CD205⁺ cells were also positive for XCR1 (Fig. 10). Similar results were obtained with CD24 and CD103 (data not shown). Recently, CD103 or CD207 were described as good markers to localize CD8⁺ DC in the spleen (Idoyaga et al., 2009; Qiu et al., 2009). A major problem for the histological detection of CD8⁺ DC using the above mentioned surface markers is the wide expression of these molecules on other cell subsets (like Langerhans DC or T cells). Our flow cytometry data, when taken together with the histological results, demonstrated that XCR1 expression in the mouse is essentially restricted to CD8⁺ DC. These results makes XCR1 a useful candidate for the simple detection of the low percentage CD8⁺ DC in lymphoid tissues instead of complicated histostaining with different markers that are also expressed on other cell subtypes (like macrophages, B cells or T cells).

4.2 Localization and migration of CD8⁺ DC expressing XCR1

Migratory DC are well known for their migration from the periphery to the lymphoid organs. CD8⁺ DC are resident cDC already present in lymphoid organs and which do not migrate to other organs. However, it was demonstrated that during infection or inflammation, splenic DC translocate from the marginal zone to the T cell area for optimal interactions with T lymphocytes (Ato et al., 2006; Alvarez et al., 2008). In this work, XCR1 was used as a specific marker to test the localization of CD8⁺ DC in spleen section after application of LPS or ATAC.

We could clearly show that LPS injection into B6.XCR1-LacZ^{+/+} induces the translocation of XCR1⁺ cells after 3 – 9 h from the marginal zone and red pulp to the T cell area. Migration of CD11c⁺ cells and CD205⁺ cells was comparable to the migration of XCR1⁺ cells (Fig. 11). Similar results were reported recently on CD207⁺ CD205⁺ CD8⁺ DC in BALB/c mice after systemic application of LPS (Idoyaga et al., 2009). Previously, it was reported that microbial agonists like LPS or CpG lead to the redistribution of CD11c⁺ DC from the MZ to the T cell area and then to cell death (De Smedt et al., 1998). In our study after 24 h, there was no XCR1 signal left after LPS injection, whereas CD11c signal was still detectable. The differences between XCR1 signal and CD11c signal after 24 h can be explained in several ways. One possibility could be that the LacZ protein is no longer produced, since we observed that LPS rapidly downregulates XCR1 expression (data not shown). Another possibility could be that XCR1⁺ CD8⁺ DC are more sensitive to apoptosis than other DC subtypes after injection of LPS, possibly due to higher expression level of TLR4 (De Trez C. et al., 2005). Although the migration of XCR1⁺ CD8⁺ DC from the marginal zone to the T cell area after LPS application is independent of XCR1, nevertheless XCR1 is a suitable marker to localize CD8⁺ DC in sections of an intact spleen.

ATAC chemoattraction was demonstrated before on cell populations like T cells, B cells, NK cells in many publications (Kelner et al., 1994; Kennedy et al., 1995; Hedrick et al., 1997; Huang et al., 2001). However, these published results were disputed by other groups (Bleul et al., 1996; Dorner et al., 1997; Yoshida et al., 1998; Johnston et al., 2003)

Recently in our group we could show that ATAC induced *in vitro* selective migration of CD8⁺ DC from B6.XCR1-LacZ^{+/-} heterozygous mice (containing one intact XCR1 allele), whereas CD8⁺ DC from homozygous B6.XCR1-LacZ^{+/+} mice (lacking XCR1) no longer responded (Dorner et al., 2009). In the present work, the consequence of ATAC application

on XCR1⁺ CD8⁺ DC was tested *in vivo* using a transfectant secreting ATAC (300-19-ATAC). Six h after ATAC application into B6.XCR1-LacZ^{+/-} recipient mice, in tendency the numbers of XCR1⁺ cells in T cells areas increased whereas XCR1⁺ cells numbers were reduced in the red pulp and marginal zone (Fig. 12). This effect could not be detected in the B6.XCR1-LacZ^{+/+} homozygous mice (data not shown).

All chemokines are functionally classified into subfamilies termed inflammatory (e.g. CXCR1 and CCR5) and homeostatic (e.g. CXCR4 and CCR7). Inflammatory chemokines are regulated by inflammatory stimuli and are involved mainly in the orchestration of innate and adaptive immune responses whereas homeostatic chemokines are expressed constitutively and are involved primarily in the organization of lymphoid tissue. Homeostatic chemokines knockout mice show many abnormalities in the development of the immune system (Murphy et al., 2000; Moser et al., 2004). It was shown in the CXCR4^{-/-} knockout mice that B-lymphopoiesis and myelopoiesis were impaired (Ma et al., 1998). XCR1-deficient mice did not exhibit any abnormalities in organ development, immune cell composition, and immune cell localization which suggests that ATAC/XCR1 belongs to inflammatory chemokines. In addition, CD8⁺ DC are a DC population which does not leave secondary lymphoid organs (Shortman and Naik, 2007; Wu and Liu, 2007). Taking our results regarding the localization and the translocation of XCR1⁺ CD8⁺ DC to the T cell areas suggest that ATAC/XCR1 interactions mainly occur at short distances within organs. According to the data mentioned above on the selective XCR1 expression on CD8⁺ DC, it is very unlikely that ATAC has a chemotactic effect on other populations unless one would postulate a second receptor for ATAC. Originally, ATAC and XCR1 have been recognized as a monogamous ligand-receptor system (Yoshida et al., 1998; Shan et al., 2000). To date, there is no evidence for a second receptor.

4.3 XCR1 and the uptake of allogeneic cells

The nature of the immune response to cell death depends on how the cells die and which cells are responsible for the uptake of these dying cells. DC play a central role in the uptake of dying or dead cells and may direct the immune response either toward tolerance (cells dying without inflammatory signals or in the presence of immunosuppressive cytokines) or immunity (cells dying in the presence of DAMPs or PAMPs) (Kono and Rock, 2008; Green et al., 2009).

In vitro studies show that both immature DC and macrophages are efficient phagocytic cells but only DC cross-present cell-associated antigens to CD8⁺ T cells (Albert et al., 1998;

Schulz and Reis e Sousa, 2002). In the present work the role of XCR1 on the uptake of allogeneic cells by CD8⁺ DC was investigated.

Uptake of cells by DC was extensively studied *in vivo* by Iyoda (2002). They show that CD8⁺ DC are selectively responsible for the uptake of live allogeneic cells or apoptotic cells but not for live syngeneic cells. They also found that CD8⁻ DC, marginal zone macrophages and red pulp macrophages are not involved in the uptake of allogeneic cells. In accordance with Iyoda (2002), we could show that systemically applied allogeneic primary cells or a cell line are taken up *in vivo* by splenic CD8⁺ DC but not CD8⁻ DC (Fig. 13). Other phagocytic cells like macrophages or neutrophils did not appear to participate in the uptake of allogeneic cells (Fig. 16 A). However, to firmly exclude an involvement of macrophages also early time points would have to be analyzed in addition. Kerksiek (2005) reported that the special capability of CD8⁺ DC to take up apoptotic cells depends on Rac1 GTPase (member of the Rac family of GTPases) (Kerksiek et al., 2005).

Iyoda (2002) reported that the uptake of live allogeneic cells depends on the presence of NK cells. In contrast, we found that NK cells are not required for the uptake of allogeneic cells by CD8⁺ DC *in vivo* (Fig. 15). In the Iyoda (2002) study they used primary allogeneic B cells from BALB/c mice while in this work we used an allogeneic pre B cell line (300-19). This could be one possible explanation for the discrepancy between the data concerning NK cell involvement. Other cell types like macrophages or neutrophils could be responsible for the killing of the allogeneic cells *in vivo* via complement-dependent cytotoxicity (CDC), or Ab-dependent cell-mediated cytotoxicity (ADCC) (Okuda and Tachibana, 1992; Valerius et al., 1997).

We could show that allogeneic cells injected in B6 mice are taken up selectively by splenic CD205⁺ XCR1⁺ CD8⁺ DC and not by the CD205⁻ XCR1⁻ CD8⁺ DC (Fig. 16 B). Compatible results were published recently on the dominant role of splenic CD103⁺ CD8⁺ DC present in the marginal zone versus CD103⁻ CD8⁺ DC for the uptake of blood-borne apoptotic cells (Qiu et al., 2009). It was also shown that transient depletion of this population inhibits the induction of tolerance to cell-associated antigen (Qiu et al., 2009).

It was important to test if the presence of ATAC plays a role in the uptake of allogeneic cells by the XCR1⁺ CD8⁺ DC subset. To achieve this, the uptake of allogeneic cell expressing ATAC versus wt control was tested in ATAC-KO or B6.XCR1-LacZ^{+/+} mice. In ATAC-KO mice an increased uptake of the cell line expressing ATAC by XCR1⁺ CD8⁺ DC was demonstrated compared to the wt control (Fig. 17). This effect could not be observed in B6.XCR1-LacZ^{+/+} mice which suggests that the results shown are specific for ATAC and not

caused by any other effect in the ATAC transfectant cells. A role in the uptake of allogeneic cells *in vivo* was not observed to date by any other chemokine. The increased endocytosis of allogeneic cells expressing ATAC by XCR1⁺ CD8⁺ DC could be due to the attraction of more XCR1⁺ CD8⁺ DC to the cells expressing ATAC.

4.4 ATAC binds to the cell surface of late apoptotic cells

It is well established that chemokine receptors undergo endocytosis after stimulation by their specific ligands (Arai et al., 1997). It was also reported that mutations in the GAG binding sites of CCL2, CCL4, and CCL5 retain their chemotactic activity *in vitro*, however these mutant chemokines were unable to recruit cells when administered *in vivo* (Proudfoot et al., 2003). A similar observation was reported for ATAC mutants with altered heparin binding sites showing less potent chemoattractant activity for leukocytes *in vivo* (Peterson et al., 2004). It was also demonstrated that ATAC adopts two distinct structures in equilibrium under physiological solution conditions (Tuinstra et al., 2007). One conformation specifically recognizes XCR1 on the surface of a target cell and the other one bind to GAG molecule heparin. These binding sites by ATAC were speculated to be essential for the biological role of ATAC to maintain a chemotactic concentration gradient (Tuinstra et al., 2008).

Specific interaction of ATAC with XCR1 expressed on the surface of CD8⁺ DC may not be the only possible explanation for the increased uptake of ATAC expressing cells. Considering the published data on different ATAC conformations, the possible binding of ATAC to the surface of live, early apoptotic, late apoptotic and dead cells was investigated. To achieve this, heat shocked 300-19 cells were incubated with ATAC. We could show for the first time that ATAC specifically binds *in vitro* to the cell surface of late apoptotic cells and not to live or dead cells (Fig. 18), the same result was also observed with splenocytes prepared from B6 mice (data not shown). The possible candidate on the apoptotic cell surface that binds to ATAC is unknown and needs to be characterized in the future. Certain glycoproteins like HERDS (heterogeneous ectopic ribonucleoprotein-derived structures) translocate to the cell surface of late apoptotic cells and could be responsible for the specific binding of ATAC on the cell surface (Radic et al., 2006). Several DAMPs like (fragments of the extracellular matrix, heat shock proteins, phosphatidylserine (PS), and DNA fragments) were reported to be released from dying cells and constructs an “eat-me” could be also a candidate for ATAC (Kono and Rock, 2008; Green et al., 2009).

Taking together the *in vivo* data showing the increased uptake of a cell line expressing ATAC

and the *in vitro* data dealing with the binding of ATAC on the cell surface of late apoptotic cells, lead to the following scenario. ATAC secreted by activated NK or CD8⁺ T cells decorates dying cells and thus targets them to XCR1⁺ CD8⁺ DC *in vivo* to facilitate their clearance. XCR1⁺ CD8⁺ DC clearance of apoptotic cells leads to the induction of either tolerance in the case of tolerogenic cell death or immune response in the case of immunogenic cell death.

4.5 Antigen targeting to CD8⁺ DC using an allogeneic cell line *in vivo*

The role of CD8⁺ DC in the generation of cytotoxic T lymphocyte responses against cell-associated antigens was demonstrated in several publications (den Haan et al., 2000; Iyoda et al., 2002; Schulz and Reis e Sousa, 2002). To study the function of XCR1⁺ CD8⁺ DC *in vivo*, we used 300-19-delta OVA transfected allogeneic cells to target antigen selectively to this DC subsets.

It was of interest in such a system to test whether this type of specific antigen targeting leads to the induction of antigen-specific T cell or B cell immune responses. We could show *in vivo* after targeting of XCR1⁺ CD8⁺ DC using 300-19-delta OVA that cell-associated antigens were efficiently presented onto MHC-I generating cytotoxic CD8⁺ T cells (Fig 22). The addition of LPS did not induce any differences in the killing activity which indicates that allogeneic cells could act at the same time as an adjuvant. In the tested serum of the immunized mice we could not detect any OVA-specific Ig production (Fig. 21). This could be due to the lower presentation of cell associated antigen in the context of MHC-II which would result in a reduction of CD4⁺ T cells help for antibody production by B cells, or because the antigen was not accessible for B cells. Several *in vitro* studies using sorted DC subtypes incubated with OT-I or OT-II OVA specific T cells showed that CD8⁺ DC can present cell-associated OVA to both CD8⁺ and CD4⁺ T cells (Schnorrer et al., 2006; Iyoda et al., 2002). In contrast to these data, we found that CD8⁺ DC were able to cross present cell-associated OVA efficiently in the context of MHC-I to OT-I transferred cells and present antigen to a very lower level in the context of MHC-II to OT-II transferred cells (Fig. 23). Similar result were reported on the effective stimulation of MHC-I restricted CD8⁺ T with CD8⁺ DC only while an effective MHC-II restricted CD4⁺ T cell response was obtained with CD8⁻ DC only (Pooley et al., 2001). Taking together, we could show that our cell-associated

antigen targeting model leads to efficiently antigen presentation in the context of MHC-I to induce effector CD8⁺ T cells.

4.6 Role of ATAC/XCR1 interaction in the induction of cytotoxic CD8⁺ T cells

In this work it was demonstrated that an allogeneic cell line was selectively taken up by XCR1⁺ CD8⁺ DC. In addition, published data show that ATAC is expressed by activated NK cells, CD8 T cells, and CD4 Th1 cells after intracellular infection (*Listeria* or MCMV) (Müller et al., 2003; Dorner et al., 2004). *In vivo* antigen targeting to XCR1⁺ CD8⁺ DC, which induced cytotoxic CD8⁺ T cells as described above was used as a suitable read-out to test the interaction effect of XCR1⁺ CD8⁺ DC and CD8⁺ T cell expressing ATAC on the induction of CTL in the different mouse strains (B6, B6.ATAC-KO or B6.XCR1-LacZ^{+/+}). Using an adoptive transfer system and after single immunization with 300-19-delta OVA, we found at day 6 a significantly increased killing activity in B6 mice compared to B6.ATAC-KO or B6.XCR1-LacZ^{+/+} mice (Fig. 25). The increased starting frequencies of OVA-specific T cells in the adoptive transfer system do not reflect all the aspects of the physiological differentiations of CD8⁺ T cells. Further experiments were therefore performed in the different mouse strains without adoptive transfer. We could show an increased endogenous killing in B6 mice versus B6.ATAC-KO mice (Fig. 28).

In vivo studies show a positive correlation between the duration of initial antigen encounter and the magnitude of primary CD8⁺ T cell expansion (Prlic et al., 2006; Tewari et al., 2006). A possible explanation for the strong CTL responses in B6 mice observed before could be the chemotactic effect of ATAC on XCR1 which increases the recognition chances between CD8⁺ DC presenting antigen and CD8⁺ T cells. This interaction substantially increases the number of surviving antigen-specific T cells and induces effective cytotoxicity. In the future, *in vivo* imaging experiments are planned to show the interaction between XCR1⁺ CD8⁺ DC and CD8⁺ T cells expressing ATAC directly.

Another possible hypothesis explaining the differences in the pool size of CD8⁺ effectors T cells and the strong CTL responses seen in B6 mice but not B6.ATAC-KO or B6.XCR1-LacZ^{+/+} mice could be that, ATAC/XCR1 interaction lead to an intracellular signals that modulate antigen processing by CD8⁺ DC. The data in this work show the possible role of XCR1⁺CD8⁺ DC for cross-presentation of cell-associated antigen. Further experiments are planned to differentiate between XCR1⁺ DC and XCR1⁻ DC for the

investigation of the role of XCR1 on CD8⁺ DC in cross-presentation. Recently it has been shown that CLEC9A (also known as DNGR-1) expressed on CD8⁺ DC cross-present cell-associated antigens to CD8⁺ T cells. Blocking of CLEC9A does not impair uptake of dying cells but reduces cross-presentation of antigens associated with dead cells (Sancho et al., 2008; Sancho et al., 2009).

Several studies were published on antigen targeting to dendritic cells *in vitro* or *in vivo* as a new model for vaccination or therapy trials (Yang et al., 2008; Shortman et al., 2009). It was reported that vaccination with bone-marrow derived DC primed before with tumor antigen *in vitro* mediate regression of tumor in mice (Strome et al., 2002). This type of *in vitro* loading studies are difficult to interpret since DC maturation cannot be controlled and specific antigen loading in culture may not reflect the normal physiological contact between DC and antigen *in vivo*. Recently, antigen coupled to mAb against several cell surface molecules like DEC-205, DCIR2, MR, and CD11c on different DC subsets were used for antigen targeting *in vivo*. It was also shown that this type of *in vivo* antigen targeting on different DC plus maturation stimulus induce strong CTL responses (Bonifaz et al., 2004; Dudziak et al., 2007; Soares et al., 2007; He et al., 2007; Castro et al., 2008). However, these surface molecules are widely expressed on diverse DC or other cell subsets and thus lack the required target specificity. Because loading of antigen exquisite specificity, antigen targeting to CD8⁺ DC via XCR1 may be advantageous to develop potent cellular immunity against certain pathogens and also tumors. Conventional vaccines using soluble protein mainly induce protective antibodies, but fail to induce cytotoxic immune responses (Figdor et al., 2002). We are in the process to develop ATAC fusion proteins coupled to antigens of interest for targeting CD8⁺ DC via XCR1 as a relevant strategy for the development of new vaccines. XCR1⁺ cells in the human that correspond to the CD8⁺ DC in the mice will be of a great importance as a new target for ATAC fusion antigens. This approach may be a helpful for future clinical vaccination aimed to induce cytotoxic T cells against viruses and other intracellular pathogens.

Reference List

- Aderem, A. and Underhill, D.M. (1999). Mechanisms of phagocytosis in macrophages. *Annu. Rev. Immunol.* *17*, 593-623.
- Agrewala, J.N., Suvas, S., Singh, V., and Vohra, H. (2003). Delivery of antigen in allogeneic cells preferentially generates CD(4+) Th1 cells. *Clin. Exp. Immunol.* *134*, 13-22.
- Albert, M.L., Pearce, S.F., Francisco, L.M., Sauter, B., Roy, P., Silverstein, R.L., and Bhardwaj, N. (1998). Immature dendritic cells phagocytose apoptotic cells via alphavbeta5 and CD36, and cross-present antigens to cytotoxic T lymphocytes. *J. Exp. Med.* *188*, 1359-1368.
- Allen, S.J., Crown, S.E., and Handel, T.M. (2007). Chemokine: receptor structure, interactions, and antagonism. *Annu. Rev. Immunol.* *25*, 787-820.
- Alt, F., Rosenberg, N., Lewis, S., Thomas, E., and Baltimore, D. (1981). Organization and reorganization of immunoglobulin genes in A-MULV-transformed cells: rearrangement of heavy but not light chain genes. *Cell* *27*, 381-390.
- Alvarez, D., Vollmann, E.H., and von Andrian, U.H. (2008). Mechanisms and consequences of dendritic cell migration. *Immunity.* *29*, 325-342.
- Arai, H., Monteclaro, F.S., Tsou, C.L., Franci, C., and Charo, I.F. (1997). Dissociation of chemotaxis from agonist-induced receptor internalization in a lymphocyte cell line transfected with CCR2B. Evidence that directed migration does not require rapid modulation of signaling at the receptor level. *J. Biol. Chem.* *272*, 25037-25042.
- Arase, H., Saito, T., Phillips, J.H., and Lanier, L.L. (2001). Cutting edge: the mouse NK cell-associated antigen recognized by DX5 monoclonal antibody is CD49b (alpha 2 integrin, very late antigen-2). *J. Immunol.* *167*, 1141-1144.
- Ato, M., Maroof, A., Zubairi, S., Nakano, H., Kakiuchi, T., and Kaye, P.M. (2006). Loss of dendritic cell migration and impaired resistance to *Leishmania donovani* infection in mice deficient in CCL19 and CCL21. *J. Immunol.* *176*, 5486-5493.
- Austyn, J.M. and Gordon, S. (1981). F4/80, a monoclonal antibody directed specifically against the mouse macrophage. *Eur. J. Immunol.* *11*, 805-815.
- Barnden, M.J., Allison, J., Heath, W.R., and Carbone, F.R. (1998). Defective TCR expression in transgenic mice constructed using cDNA-based alpha- and beta-chain genes under the control of heterologous regulatory elements. *Immunol. Cell Biol.* *76*, 34-40.
- Bedoui, S., Whitney, P.G., Waithman, J., Eidsmo, L., Wakim, L., Caminschi, I., Allan, R.S., Wojtasiak, M., Shortman, K., Carbone, F.R., Brooks, A.G., and Heath, W.R. (2009). Cross-presentation of viral and self antigens by skin-derived CD103+ dendritic cells. *Nat. Immunol.* *10*, 488-495.
- Belz, G.T., Shortman, K., Bevan, M.J., and Heath, W.R. (2005). CD8alpha+ dendritic cells selectively present MHC class I-restricted noncytolytic viral and intracellular bacterial antigens in vivo. *J. Immunol.* *175*, 196-200.
- Bhattacharya, A., Dorf, M.E., and Springer, T.A. (1981). A shared alloantigenic determinant on Ia antigens encoded by the I-A and I-E subregions: evidence for I region gene duplication. *J. Immunol.* *127*, 2488-2495.
- Bleul, C.C., Fuhlbrigge, R.C., Casasnovas, J.M., Aiuti, A., and Springer, T.A. (1996). A highly efficacious lymphocyte chemoattractant, stromal cell-derived factor 1 (SDF-1). *J. Exp. Med.* *184*, 1101-1109.
- Bonifaz, L., Bonnyay, D., Mahnke, K., Rivera, M., Nussenzweig, M.C., and Steinman, R.M. (2002). Efficient targeting of protein antigen to the dendritic cell receptor DEC-205 in the steady state leads to antigen presentation on major histocompatibility complex class I products and peripheral CD8+ T cell tolerance. *J. Exp. Med.* *196*, 1627-1638.

Reference List

- Bonifaz,L.C., Bonnyay,D.P., Charalambous,A., Darguste,D.I., Fujii,S., Soares,H., Brimnes,M.K., Moltedo,B., Moran,T.M., and Steinman,R.M. (2004). In vivo targeting of antigens to maturing dendritic cells via the DEC-205 receptor improves T cell vaccination. *J. Exp. Med.* 199, 815-824.
- Boscardin,S.B., Hafalla,J.C., Masilamani,R.F., Kamphorst,A.O., Zebroski,H.A., Rai,U., Morrot,A., Zavala,F., Steinman,R.M., Nussenzweig,R.S., and Nussenzweig,M.C. (2006). Antigen targeting to dendritic cells elicits long-lived T cell help for antibody responses. *J. Exp. Med.* 203, 599-606.
- Cairns,C.M., Gordon,J.R., Li,F., Baca-Estrada,M.E., Moyana,T., and Xiang,J. (2001). Lymphotactin expression by engineered myeloma cells drives tumor regression: mediation by CD4+ and CD8+ T cells and neutrophils expressing XCR1 receptor. *J. Immunol.* 167, 57-65.
- Cambi,A., Koopman,M., and Figdor,C.G. (2005). How C-type lectins detect pathogens. *Cell Microbiol.* 7, 481-488.
- Caminschi,I., Lahoud,M.H., and Shortman,K. (2009). Enhancing immune responses by targeting antigen to DC. *Eur. J. Immunol.* 39, 931-938.
- Castro,F.V., Tutt,A.L., White,A.L., Teeling,J.L., James,S., French,R.R., and Glennie,M.J. (2008). CD11c provides an effective immunotarget for the generation of both CD4 and CD8 T cell responses. *Eur. J. Immunol.* 38, 2263-2273.
- Chaussabel,D., Pajak,B., Vercruysse,V., Bisseye,C., Garze,V., Habib,M., Goldman,M., Moser,M., and Vray,B. (2003). Alteration of migration and maturation of dendritic cells and T-cell depletion in the course of experimental Trypanosoma cruzi infection. *Lab Invest* 83, 1373-1382.
- Corbett,A.J., Caminschi,I., McKenzie,B.S., Brady,J.L., Wright,M.D., Mottram,P.L., Hogarth,P.M., Hodder,A.N., Zhan,Y., Tarlinton,D.M., Shortman,K., and Lew,A.M. (2005). Antigen delivery via two molecules on the CD8- dendritic cell subset induces humoral immunity in the absence of conventional "danger". *Eur. J. Immunol.* 35, 2815-2825.
- De Smedt,T., Pajak,B., Klaus,G.G., Noelle,R.J., Urbain,J., Leo,O., and Moser,M. (1998). Antigen-specific T lymphocytes regulate lipopolysaccharide-induced apoptosis of dendritic cells in vivo. *J. Immunol.* 161, 4476-4479.
- De Trez C., Pajak,B., Brait,M., Glaichenhaus,N., Urbain,J., Moser,M., Lauvau,G., and Muraille,E. (2005). TLR4 and Toll-IL-1 receptor domain-containing adapter-inducing IFN-beta, but not MyD88, regulate Escherichia coli-induced dendritic cell maturation and apoptosis in vivo. *J. Immunol.* 175, 839-846.
- De,T.C., Brait,M., Leo,O., Aebischer,T., Torrentera,F.A., Carlier,Y., and Muraille,E. (2004). Myd88-dependent in vivo maturation of splenic dendritic cells induced by Leishmania donovani and other Leishmania species. *Infect. Immun.* 72, 824-832.
- del Rio,M.L., Rodriguez-Barbosa,J.I., Kremmer,E., and Forster,R. (2007). *C. J. Immunol.* 178, 6861-6866.
- den Haan,J.M., Lehar,S.M., and Bevan,M.J. (2000). CD8(+) but not CD8(-) dendritic cells cross-prime cytotoxic T cells in vivo. *J. Exp. Med.* 192, 1685-1696.
- Dialynas,D.P., Quan,Z.S., Wall,K.A., Pierres,A., Quintans,J., Loken,M.R., Pierres,M., and Fitch,F.W. (1983). Characterization of the murine T cell surface molecule, designated L3T4, identified by monoclonal antibody GK1.5: similarity of L3T4 to the human Leu-3/T4 molecule. *J. Immunol.* 131, 2445-2451.
- Diebold,S.S., Cotten,M., Koch,N., and Zenke,M. (2001). MHC class II presentation of endogenously expressed antigens by transfected dendritic cells. *Gene Ther.* 8, 487-493.
- Dong,C., Chua,A., Ganguly,B., Krensky,A.M., and Clayberger,C. (2005). Glycosylated recombinant human XCL1/lymphotactin exhibits enhanced biologic activity. *J. Immunol. Methods.*

Dorner,B., Muller,S., Entschladen,F., Schroder,J.M., Franke,P., Kraft,R., Friedl,P., Clark-Lewis,I., and KroczeK,R.A. (1997). Purification, structural analysis, and function of natural ATAC, a cytokine secreted by CD8(+) T cells. *J. Biol. Chem.* 272, 8817-8823.

Dorner,B.G., Scheffold,A., Rolph,M.S., Huser,M.B., Kaufmann,S.H., Radbruch,A., Flesch,I.E., and KroczeK,R.A. (2002). MIP-1alpha, MIP-1beta, RANTES, and ATAC/lymphotactin function together with IFN-gamma as type 1 cytokines. *Proc. Natl. Acad. Sci. U. S. A* 99, 6181-6186.

Dorner,B.G., Smith,H.R., French,A.R., Kim,S., Poursine-Laurent,J., Beckman,D.L., Pingel,J.T., KroczeK,R.A., and Yokoyama,W.M. (2004). Coordinate expression of cytokines and chemokines by NK cells during murine cytomegalovirus infection. *J. Immunol.* 172, 3119-3131.

Brigitte G. Dorner, Martin B. Dorner, Xuefei Zhou, Corinna Opitz, Ahmed Mora, Steffen Güttler, Andreas Hutloff, Hans W. Mages, Katja Ranke, Michael Schaefer, Robert S. Jack, Volker Henn & Richard A. KroczeK. (2009). Selective expression of the chemokine receptor XCR1 on cross-presenting dendritic cells determines cooperation with CD8+ T cells. *Immunity* 31, 1-11.

Dudziak,D., Kamphorst,A.O., Heidkamp,G.F., Buchholz,V.R., Trumfheller,C., Yamazaki,S., Cheong,C., Liu,K., Lee,H.W., Park,C.G., Steinman,R.M., and Nussenzweig,M.C. (2007). Differential antigen processing by dendritic cell subsets in vivo. *Science* 315, 107-111.

Engering,A., Geijtenbeek,T.B., van Vliet,S.J., Wijers,M., van,L.E., Demareux,N., Lanzavecchia,A., Fransen,J., Figdor,C.G., Piguet,V., and van,K.Y. (2002). The dendritic cell-specific adhesion receptor DC-SIGN internalizes antigen for presentation to T cells. *J. Immunol.* 168, 2118-2126.

Erbacher,A., Gieseke,F., Handgretinger,R., and Muller,I. (2009). Dendritic cells: functional aspects of glycosylation and lectins. *Hum. Immunol.* 70, 308-312.

Figdor,C.G., van,K.Y., and Adema,G.J. (2002). C-type lectin receptors on dendritic cells and Langerhans cells. *Nat. Rev. Immunol.* 2, 77-84.

Fijak,M. and Meinhardt,A. (2006). The testis in immune privilege. *Immunol. Rev.* 213, 66-81.

Fleming,T.J., Fleming,M.L., and Malek,T.R. (1993). Selective expression of Ly-6G on myeloid lineage cells in mouse bone marrow. RB6-8C5 mAb to granulocyte-differentiation antigen (Gr-1) detects members of the Ly-6 family. *J. Immunol.* 151, 2399-2408.

Gallatin,W.M., Weissman,I.L., and Butcher,E.C. (1983). A cell-surface molecule involved in organ-specific homing of lymphocytes. *Nature* 304, 30-34.

Green,D.R., Ferguson,T., Zitvogel,L., and Kroemer,G. (2009). Immunogenic and tolerogenic cell death. *Nat. Rev. Immunol.* 9, 353-363.

Hanahan,D., Jessee,J., and Bloom,F.R. (1991). Plasmid transformation of Escherichia coli and other bacteria. *Methods Enzymol.* 204, 63-113.

Hao,X., Kim,T.S., and Braciale,T.J. (2008). Differential response of respiratory dendritic cell subsets to influenza virus infection. *J. Virol.* 82, 4908-4919.

Hautamaa,D., Merica,R., Chen,Z., and Jenkins,M.K. (1997). Murine lymphotactin: gene structure, post-translational modification and inhibition of expression by CD28 costimulation. *Cytokine* 9, 375-382.

He,L.Z., Crocker,A., Lee,J., Mendoza-Ramirez,J., Wang,X.T., Vitale,L.A., O'Neill,T., Petromilli,C., Zhang,H.F., Lopez,J., Rohrer,D., Keler,T., and Clynes,R. (2007). Antigenic targeting of the human mannose receptor induces tumor immunity. *J. Immunol.* 178, 6259-6267.

Heath,W.R., Belz,G.T., Behrens,G.M., Smith,C.M., Forehan,S.P., Parish,I.A., Davey,G.M., Wilson,N.S., Carbone,F.R., and Villadangos,J.A. (2004). Cross-presentation, dendritic cell subsets, and the generation of immunity to cellular antigens. *Immunol. Rev.* 199, 9-26.

Reference List

- Hedrick, J.A., Saylor, V., Figueroa, D., Mizoue, L., Xu, Y., Menon, S., Abrams, J., Handel, T., and Zlotnik, A. (1997). Lymphotoxin is produced by NK cells and attracts both NK cells and T cells in vivo. *J. Immunol.* *158*, 1533-1540.
- Heiber, M., Docherty, J.M., Shah, G., Nguyen, T., Cheng, R., Heng, H.H., Marchese, A., Tsui, L.C., Shi, X., George, S.R., and . (1995). Isolation of three novel human genes encoding G protein-coupled receptors. *DNA Cell Biol.* *14*, 25-35.
- Hernandez, M.G., Shen, L., and Rock, K.L. (2007). CD40-CD40 ligand interaction between dendritic cells and CD8+ T cells is needed to stimulate maximal T cell responses in the absence of CD4+ T cell help. *J. Immunol.* *178*, 2844-2852.
- Hirsch, S. and Gordon, S. (1983). Polymorphic expression of a neutrophil differentiation antigen revealed by monoclonal antibody 7/4. *Immunogenetics* *18*, 229-239.
- Hogquist, K.A., Jameson, S.C., Heath, W.R., Howard, J.L., Bevan, M.J., and Carbone, F.R. (1994). T cell receptor antagonist peptides induce positive selection. *Cell* *76*, 17-27.
- Huang, H., Bi, X.G., Yuan, J.Y., Xu, S.L., Guo, X.L., and Xiang, J. (2005). Combined CD4+ Th1 effect and lymphotoxin transgene expression enhance CD8+ Tc1 tumor localization and therapy. *Gene Ther.* *12*, 999-1010.
- Huang, H., Li, F., Cairns, C.M., Gordon, J.R., and Xiang, J. (2001). Neutrophils and B cells express XCR1 receptor and chemotactically respond to lymphotoxin. *Biochem. Biophys. Res. Commun.* *281*, 378-382.
- Idoyaga, J., Suda, N., Suda, K., Park, C.G., and Steinman, R.M. (2009). Antibody to Langerin/CD207 localizes large numbers of CD8alpha+ dendritic cells to the marginal zone of mouse spleen. *Proc. Natl. Acad. Sci. U. S. A* *106*, 1524-1529.
- Iwasaki, A. and Medzhitov, R. (2004). Toll-like receptor control of the adaptive immune responses. *Nat. Immunol.* *5*, 987-995.
- Iyoda, T., Shimoyama, S., Liu, K., Omatsu, Y., Akiyama, Y., Maeda, Y., Takahara, K., Steinman, R.M., and Inaba, K. (2002). The CD8+ dendritic cell subset selectively endocytoses dying cells in culture and in vivo. *J. Exp. Med.* *195*, 1289-1302.
- Jakubzick, C., Tacke, F., Ginhoux, F., Wagers, A.J., van, R.N., Mack, M., Merad, M., and Randolph, G.J. (2008). Blood monocyte subsets differentially give rise to CD103+ and CD103- pulmonary dendritic cell populations. *J. Immunol.* *180*, 3019-3027.
- Johansson, C. and Kelsall, B.L. (2005). Phenotype and function of intestinal dendritic cells. *Semin. Immunol.* *17*, 284-294.
- Johnson, Z., Schwarz, M., Power, C.A., Wells, T.N., and Proudfoot, A.E. (2005). Multi-faceted strategies to combat disease by interference with the chemokine system. *Trends Immunol.* *26*, 268-274.
- Johnston, B., Kim, C.H., Soler, D., Emoto, M., and Butcher, E.C. (2003). Differential chemokine responses and homing patterns of murine TCR alpha beta NKT cell subsets. *J. Immunol.* *171*, 2960-2969.
- Karre, K., Ljunggren, H.G., Piontek, G., and Kiessling, R. (1986). Selective rejection of H-2-deficient lymphoma variants suggests alternative immune defence strategy. *Nature* *319*, 675-678.
- Kearney, J.F., Radbruch, A., Liesegang, B., and Rajewsky, K. (1979). A new mouse myeloma cell line that has lost immunoglobulin expression but permits the construction of antibody-secreting hybrid cell lines. *J. Immunol.* *123*, 1548-1550.
- Kelner, G.S., Kennedy, J., Bacon, K.B., Kleyensteuber, S., Largaespada, D.A., Jenkins, N.A., Copeland, N.G., Bazan, J.F., Moore, K.W., Schall, T.J., and . (1994). Lymphotoxin: a cytokine that represents a new class of chemokine. *Science* *266*, 1395-1399.

- Kennedy,J., Kelner,G.S., Kleyensteuber,S., Schall,T.J., Weiss,M.C., Yssel,H., Schneider,P.V., Cocks,B.G., Bacon,K.B., and Zlotnik,A. (1995). Molecular cloning and functional characterization of human lymphotactin. *J. Immunol.* *155*, 203-209.
- Kerksiek,K.M., Niedergang,F., Chavrier,P., Busch,D.H., and Brocker,T. (2005). Selective Rac1 inhibition in dendritic cells diminishes apoptotic cell uptake and cross-presentation in vivo. *Blood* *105*, 742-749.
- Kloetzel,P.M. and Ossendorp,F. (2004). Proteasome and peptidase function in MHC-class-I-mediated antigen presentation. *Curr. Opin. Immunol.* *16*, 76-81.
- Kono,H. and Rock,K.L. (2008). How dying cells alert the immune system to danger. *Nat. Rev. Immunol.* *8*, 279-289.
- Koo,G.C. and Peppard,J.R. (1984). Establishment of monoclonal anti-Nk-1.1 antibody. *Hybridoma* *3*, 301-303.
- Kraal,G., Breel,M., Janse,M., and Bruin,G. (1986). Langerhans' cells, veiled cells, and interdigitating cells in the mouse recognized by a monoclonal antibody. *J. Exp. Med.* *163*, 981-997.
- Kremer,L. and Marquez,G. (2004). Generation of monoclonal antibodies against chemokine receptors. *Methods Mol. Biol.* *239*, 243-260.
- Krop,I., de Fougerolles,A.R., Hardy,R.R., Allison,M., Schlissel,M.S., and Fearon,D.T. (1996). Self-renewal of B-1 lymphocytes is dependent on CD19. *Eur. J. Immunol.* *26*, 238-242.
- Kuloglu,E.S., McCaslin,D.R., Kitabwalla,M., Pauza,C.D., Markley,J.L., and Volkman,B.F. (2001). Monomeric solution structure of the prototypical 'C' chemokine lymphotactin. *Biochemistry* *40*, 12486-12496.
- Lanzavecchia,A. (1996). Mechanisms of antigen uptake for presentation. *Curr. Opin. Immunol.* *8*, 348-354.
- Lata,S. and Raghava,G.P. (2009). Prediction and classification of chemokines and their receptors. *Protein Eng Des Sel* *22*, 441-444.
- Ledbetter,J.A., Rouse,R.V., Mickle,H.S., and Herzenberg,L.A. (1980). T cell subsets defined by expression of Lyt-1,2,3 and Thy-1 antigens. Two-parameter immunofluorescence and cytotoxicity analysis with monoclonal antibodies modifies current views. *J. Exp. Med.* *152*, 280-295.
- Leisewitz,A.L., Rockett,K.A., Gumedé,B., Jones,M., Urban,B., and Kwiatkowski,D.P. (2004). Response of the splenic dendritic cell population to malaria infection. *Infect. Immun.* *72*, 4233-4239.
- Lin,M.L., Zhan,Y., Villadangos,J.A., and Lew,A.M. (2008). The cell biology of cross-presentation and the role of dendritic cell subsets. *Immunol. Cell Biol.* *86*, 353-362.
- Locati,M., Otero,K., Schioppa,T., Signorelli,P., Perrier,P., Baviera,S., Sozzani,S., and Mantovani,A. (2002). The chemokine system: tuning and shaping by regulation of receptor expression and coupling in polarized responses. *Allergy* *57*, 972-982.
- Logdberg,L., Gunter,K.C., and Shevach,E.M. (1985). Rapid production of monoclonal antibodies to T lymphocyte functional antigens. *J. Immunol. Methods* *79*, 239-249.
- Lüttichau,H.R. (2008). The herpesvirus 8 encoded chemokines vCCL2 (vMIP-II) and vCCL3 (vMIP-III) target the human but not the murine lymphotactin receptor. *Virology* *5*, 50.
- Ma,Q., Jones,D., Borghesani,P.R., Segal,R.A., Nagasawa,T., Kishimoto,T., Bronson,R.T., and Springer,T.A. (1998). Impaired B-lymphopoiesis, myelopoiesis, and derailed cerebellar neuron migration in C. *Proc. Natl. Acad. Sci. U. S. A* *95*, 9448-9453.
- MacGregor,G.R., Mogg,A.E., Burke,J.F., and Caskey,C.T. (1987). Histochemical staining of clonal mammalian cell lines expressing E. coli beta galactosidase indicates heterogeneous expression of the bacterial gene. *Somat. Cell Mol. Genet.* *13*, 253-265.

Reference List

- Mackay,C.R. (2001). Chemokines: immunology's high impact factors. *Nat. Immunol.* 2, 95-101.
- Matsuyoshi,H., Senju,S., Hirata,S., Yoshitake,Y., Uemura,Y., and Nishimura,Y. (2004). Enhanced priming of antigen-specific CTLs in vivo by embryonic stem cell-derived dendritic cells expressing chemokine along with antigenic protein: application to antitumor vaccination. *J. Immunol.* 172, 776-786.
- McLellan,A.D., Kapp,M., Eggert,A., Linden,C., Bommhardt,U., Brocker,E.B., Kammerer,U., and Kampgen,E. (2002). Anatomic location and T-cell stimulatory functions of mouse dendritic cell subsets defined by CD4 and CD8 expression. *Blood* 99, 2084-2093.
- Metlay,J.P., Witmer-Pack,M.D., Agger,R., Crowley,M.T., Lawless,D., and Steinman,R.M. (1990). The distinct leukocyte integrins of mouse spleen dendritic cells as identified with new hamster monoclonal antibodies. *J. Exp. Med.* 171, 1753-1771.
- Moser,B., Wolf,M., Walz,A., and Loetscher,P. (2004). Chemokines: multiple levels of leukocyte migration control. *Trends Immunol.* 25, 75-84.
- Müller,K., Bischof,S., Sommer,F., Lohoff,M., Solbach,W., and Laskay,T. (2003). Differential production of macrophage inflammatory protein 1gamma (MIP-1gamma), lymphotactin, and MIP-2 by CD4(+) Th subsets polarized in vitro and in vivo. *Infect. Immun.* 71, 6178-6183.
- Müller,S., Dorner,B., Korthauer,U., Mages,H.W., D'Apuzzo,M., Senger,G., and Kroczeck,R.A. (1995). Cloning of ATAC, an activation-induced, chemokine-related molecule exclusively expressed in CD8+ T lymphocytes. *Eur. J. Immunol.* 25, 1744-1748.
- Murphy,P.M., Baggiolini,M., Charo,I.F., Hebert,C.A., Horuk,R., Matsushima,K., Miller,L.H., Oppenheim,J.J., and Power,C.A. (2000). International union of pharmacology. XXII. Nomenclature for chemokine receptors. *Pharmacol. Rev.* 52, 145-176.
- Nakano,H., Yanagita,M., and Gunn,M.D. (2001). CD11c(+)B220(+)Gr-1(+) cells in mouse lymph nodes and spleen display characteristics of plasmacytoid dendritic cells. *J. Exp. Med.* 194, 1171-1178.
- Nakayama,M., Akiba,H., Takeda,K., Kojima,Y., Hashiguchi,M., Azuma,M., Yagita,H., and Okumura,K. (2009). Tim-3 mediates phagocytosis of apoptotic cells and cross-presentation. *Blood* 113, 3821-3830.
- Niess,J.H. and Reinecker,H.C. (2006). Dendritic cells in the recognition of intestinal microbiota. *Cell Microbiol.* 8, 558-564.
- Okuda,T. and Tachibana,T. (1992). The role of complement receptors in tumor cell destruction. *Tohoku J. Exp. Med.* 168, 417-420.
- Olson,T.S. and Ley,K. (2002). Chemokines and chemokine receptors in leukocyte trafficking. *Am. J. Physiol Regul. Integr. Comp Physiol* 283, R7-28.
- Peterson,F.C., Elgin,E.S., Nelson,T.J., Zhang,F., Hoeger,T.J., Linhardt,R.J., and Volkman,B.F. (2004). Identification and characterization of a glycosaminoglycan recognition element of the C chemokine lymphotactin. *J. Biol. Chem.* 279, 12598-12604.
- Pillarisetty,V.G., Shah,A.B., Miller,G., Bleier,J.I., and DeMatteo,R.P. (2004). Liver dendritic cells are less immunogenic than spleen dendritic cells because of differences in subtype composition. *J. Immunol.* 172, 1009-1017.
- Plitas,G., Burt,B.M., Stableford,J.A., Nguyen,H.M., Welles,A.P., and DeMatteo,R.P. (2008). Dendritic cells are required for effective cross-presentation in the murine liver. *Hepatology* 47, 1343-1351.
- Ponath,P.D., Kassam,N., and Qin,S. (2000). Monoclonal antibodies to chemokine receptors. *Methods Mol. Biol.* 138, 231-242.

- Pooley,J.L., Heath,W.R., and Shortman,K. (2001). Cutting edge: intravenous soluble antigen is presented to CD4 T cells by CD8- dendritic cells, but cross-presented to CD8 T cells by CD8+ dendritic cells. *J. Immunol.* *166*, 5327-5330.
- Porstmann,T. and Kiessig,S.T. (1992). Enzyme immunoassay techniques. An overview. *J. Immunol. Methods* *150*, 5-21.
- Prlic,M., Hernandez-Hoyos,G, and Bevan,M.J. (2006). Duration of the initial TCR stimulus controls the magnitude but not functionality of the CD8+ T cell response. *J. Exp. Med.* *203*, 2135-2143.
- Proudfoot,A.E., Handel,T.M., Johnson,Z., Lau,E.K., LiWang,P., Clark-Lewis,I., Borlat,F., Wells,T.N., and Kosco-Vilbois,M.H. (2003). Glycosaminoglycan binding and oligomerization are essential for the in vivo activity of certain chemokines. *Proc. Natl. Acad. Sci. U. S. A* *100*, 1885-1890.
- Qiu,C.H., Miyake,Y., Kaise,H., Kitamura,H., Ohara,O., and Tanaka,M. (2009). Novel subset of CD8{alpha}+ dendritic cells localized in the marginal zone is responsible for tolerance to cell-associated antigens. *J. Immunol.* *182*, 4127-4136.
- Radbruch,A. (2000). *Flow Cytometry and Cell Sorting* (2nd) Edition). Springer-Verlag.
- Radic,M.Z., Shah,K., Zhang,W., Lu,Q., Lemke,G., and Hilliard,G.M. (2006). Heterogeneous nuclear ribonucleoprotein P2 is an autoantibody target in mice deficient for Mer, Axl, and Tyro3 receptor tyrosine kinases. *J. Immunol.* *176*, 68-74.
- Rock,K.L. and Shen,L. (2005). Cross-presentation: underlying mechanisms and role in immune surveillance. *Immunol. Rev.* *207*, 166-183.
- Romano,M., Denis,O., D'Souza,S., Wang,X.M., Ottenhoff,T.H., Brulet,J.M., and Huygen,K. (2004). Induction of in vivo functional Db-restricted cytolytic T cell activity against a putative phosphate transport receptor of *Mycobacterium tuberculosis*. *J. Immunol.* *172*, 6913-6921.
- Rosen,H. and Gordon,S. (1987). Monoclonal antibody to the murine type 3 complement receptor inhibits adhesion of myelomonocytic cells in vitro and inflammatory cell recruitment in vivo. *J. Exp. Med.* *166*, 1685-1701.
- Rot,A. and von Andrian,U.H. (2004). Chemokines in innate and adaptive host defense: basic chemokine grammar for immune cells. *Annu. Rev. Immunol.* *22*, 891-928.
- Rothman,J.E. (1994). Mechanisms of intracellular protein transport. *Nature* *372*, 55-63.
- Rumsaeng,V., Vliagoftis,H., Oh,C.K., and Metcalfe,D.D. (1997). Lymphotactin gene expression in mast cells following Fc(epsilon) receptor I aggregation: modulation by TGF-beta, IL-4, dexamethasone, and cyclosporin A. *J. Immunol.* *158*, 1353-1360.
- Sancho,D., Joffre,O.P., Keller,A.M., Rogers,N.C., Martinez,D., Hernanz-Falcon,P., Rosewell,I., and Reis e Sousa (2009). Identification of a dendritic cell receptor that couples sensing of necrosis to immunity. *Nature* *458*, 899-903.
- Sancho,D., Mourao-Sa,D., Joffre,O.P., Schulz,O., Rogers,N.C., Pennington,D.J., Carlyle,J.R., and Reis e Sousa (2008). Tumor therapy in mice via antigen targeting to a novel, DC-restricted C-type lectin. *J. Clin. Invest* *118*, 2098-2110.
- Sander,B., Andersson,J., and Andersson,U. (1991). Assessment of cytokines by immunofluorescence and the paraformaldehyde-saponin procedure. *Immunol. Rev.* *119*, 65-93.
- Sanes,J.R., Rubenstein,J.L., and Nicolas,J.F. (1986). Use of a recombinant retrovirus to study post-implantation cell lineage in mouse embryos. *EMBO J.* *5*, 3133-3142.
- Schmidt,A., Tief,K., Foletti,A., Hunziker,A., Penna,D., Hummler,E., and Beermann,F. (1998). LacZ transgenic mice to monitor gene expression in embryo and adult. *Brain Res. Brain Res. Protoc.* *3*, 54-60.

Reference List

- Schnorrer,P., Behrens,G.M., Wilson,N.S., Pooley,J.L., Smith,C.M., El-Sukkari,D., Davey,G., Kupresanin,F., Li,M., Maraskovsky,E., Belz,G.T., Carbone,F.R., Shortman,K., Heath,W.R., and Villadangos,J.A. (2006). The dominant role of CD8+ dendritic cells in cross-presentation is not dictated by antigen capture. *Proc. Natl. Acad. Sci. U. S. A* *103*, 10729-10734.
- Schulz,O. and Reis e Sousa (2002). Cross-presentation of cell-associated antigens by CD8alpha+ dendritic cells is attributable to their ability to internalize dead cells. *Immunology* *107*, 183-189.
- Serbina,N.V., Salazar-Mather,T.P., Biron,C.A., Kuziel,W.A., and Pamer,E.G. (2003). TNF/iNOS-producing dendritic cells mediate innate immune defense against bacterial infection. *Immunity*. *19*, 59-70.
- Shan,L., Qiao,X., Oldham,E., Catron,D., Kaminski,H., Lundell,D., Zlotnik,A., Gustafson,E., and Hedrick,J.A. (2000). Identification of viral macrophage inflammatory protein (vMIP)-II as a ligand for GPR5/XCR1. *Biochem. Biophys. Res. Commun.* *268*, 938-941.
- Shklovskaya,E. and Fazekas de St.G.B. (2007). Balancing tolerance and immunity: the role of dendritic cell and T cell subsets. *Methods Mol. Biol.* *380*, 25-46.
- Shortman,K. (1968). The separation of different cell classes from lymphoid organs. II. The purification and analysis of lymphocyte populations by equilibrium density gradient centrifugation. *Aust. J. Exp. Biol. Med. Sci.* *46*, 375-396.
- Shortman,K., Lahoud,M.H., and Caminschi,I. (2009). Improving vaccines by targeting antigens to dendritic cells. *Exp. Mol. Med.* *41*, 61-66.
- Shortman,K. and Liu,Y.J. (2002). Mouse and human dendritic cell subtypes. *Nat. Rev. Immunol.* *2*, 151-161.
- Shortman,K. and Naik,S.H. (2007). Steady-state and inflammatory dendritic-cell development. *Nat. Rev. Immunol.* *7*, 19-30.
- Smith,C.M., Belz,G.T., Wilson,N.S., Villadangos,J.A., Shortman,K., Carbone,F.R., and Heath,W.R. (2003). Cutting edge: conventional CD8 alpha+ dendritic cells are preferentially involved in CTL priming after footpad infection with herpes simplex virus-1. *J. Immunol.* *170*, 4437-4440.
- Soares,H., Waechter,H., Glaichenhaus,N., Mougneau,E., Yagita,H., Mizenina,O., Dudziak,D., Nussenzweig,M.C., and Steinman,R.M. (2007). A subset of dendritic cells induces CD4+ T cells to produce IFN-gamma by an IL-12-independent but CD70-dependent mechanism in vivo. *J. Exp. Med.* *204*, 1095-1106.
- Springael,J.Y., Urizar,E., and Parmentier,M. (2005). Dimerization of chemokine receptors and its functional consequences. *Cytokine Growth Factor Rev.* *16*, 611-623.
- Steinman,R.M. and Cohn,Z.A. (1973). Identification of a novel cell type in peripheral lymphoid organs of mice. I. Morphology, quantitation, tissue distribution. *J. Exp. Med.* *137*, 1142-1162.
- Stievano,L., Piovan,E., and Amadori,A. (2004). C and CX3C chemokines: cell sources and physiopathological implications. *Crit Rev. Immunol.* *24*, 205-228.
- Strome,S.E., Voss,S., Wilcox,R., Wakefield,T.L., Tamada,K., Flies,D., Chapoval,A., Lu,J., Kasperbauer,J.L., Padley,D., Vile,R., Gastineau,D., Wettstein,P., and Chen,L. (2002). Strategies for antigen loading of dendritic cells to enhance the antitumor immune response. *Cancer Res.* *62*, 1884-1889.
- Tacke,P.J., de,V., I, Torensma,R., and Figdor,C.G. (2007). Dendritic-cell immunotherapy: from ex vivo loading to in vivo targeting. *Nat. Rev. Immunol.* *7*, 790-802.
- Tagliani,E., Guernonprez,P., Sepulveda,J., Lopez-Bravo,M., Ardavin,C., Amigorena,S., Benvenuti,F., and Burrone,O.R. (2008). Selection of an antibody library identifies a pathway to induce immunity by targeting CD36 on steady-state CD8 alpha+ dendritic cells. *J. Immunol.* *180*, 3201-3209.
- Tewari,K., Walent,J., Svaren,J., Zamoyska,R., and Suresh,M. (2006). Differential requirement for Lck during primary and memory CD8+ T cell responses. *Proc. Natl. Acad. Sci. U. S. A* *103*, 16388-16393.

- Toes, R.E., Blom, R.J., van, d., V, Offringa, R., Melief, C.J., and Kast, W.M. (1996). Protective antitumor immunity induced by immunization with completely allogeneic tumor cells. *Cancer Res.* 56, 3782-3787.
- Tomonari, K. (1988). A rat antibody against a structure functionally related to the mouse T-cell receptor/T3 complex. *Immunogenetics* 28, 455-458.
- Tuinstra, R.L., Peterson, F.C., Elgin, E.S., Pelzek, A.J., and Volkman, B.F. (2007). An engineered second disulfide bond restricts lymphotactin/XCL1 to a chemokine-like conformation with XCR1 agonist activity. *Biochemistry* 46, 2564-2573.
- Tuinstra, R.L., Peterson, F.C., Kutlesa, S., Elgin, E.S., Kron, M.A., and Volkman, B.F. (2008). Interconversion between two unrelated protein folds in the lymphotactin native state. *Proc. Natl. Acad. Sci. U. S. A.*
- Valerius, T., Wurflein, D., Stockmeyer, B., Repp, R., Kalden, J.R., and Gramatzki, M. (1997). Activated neutrophils as effector cells for bispecific antibodies. *Cancer Immunol. Immunother.* 45, 142-145.
- Villadangos, J.A. and Schnorrer, P. (2007). Intrinsic and cooperative antigen-presenting functions of dendritic-cell subsets in vivo. *Nat. Rev. Immunol.* 7, 543-555.
- Villadangos, J.A. and Young, L. (2008). Antigen-presentation properties of plasmacytoid dendritic cells. *Immunity* 29, 352-361.
- Volkman, B.F., Liu, T.Y., and Peterson, F.C. (2009). Chapter 3. Lymphotactin structural dynamics. *Methods Enzymol.* 461, 51-70.
- Vondenhoff, M.F., Desanti, G.E., Cupedo, T., Bertrand, J.Y., Cumano, A., Kraal, G., Mebius, R.E., and Golub, R. (2008). Separation of splenic red and white pulp occurs before birth in a LTalphabeta-independent manner. *J. Leukoc. Biol.* 84, 152-161.
- Wang, C.R., Liu, M.F., Huang, Y.H., and Chen, H.C. (2004). Up-regulation of XCR1 expression in rheumatoid joints. *Rheumatology. (Oxford)* 43, 569-573.
- Wilson, N.S., El-Sukkari, D., and Villadangos, J.A. (2004). Dendritic cells constitutively present self antigens in their immature state in vivo and regulate antigen presentation by controlling the rates of MHC class II synthesis and endocytosis. *Blood* 103, 2187-2195.
- Wu, L. and Liu, Y.J. (2007). Development of dendritic-cell lineages. *Immunity* 26, 741-750.
- Yang, L., Yang, H., Rideout, K., Cho, T., Joo, K.I., Ziegler, L., Elliot, A., Walls, A., Yu, D., Baltimore, D., and Wang, P. (2008). Engineered lentivector targeting of dendritic cells for in vivo immunization. *Nat. Biotechnol.* 26, 326-334.
- Yoshida, T., Imai, T., Kakizaki, M., Nishimura, M., Takagi, S., and Yoshie, O. (1998). Identification of single C motif-1/lymphotactin receptor XCR1. *J. Biol. Chem.* 273, 16551-16554.
- Yoshida, T., Imai, T., Kakizaki, M., Nishimura, M., and Yoshie, O. (1995). Molecular cloning of a novel C or gamma type chemokine, SCM-1. *FEBS Lett.* 360, 155-159.
- Yoshida, T., Ishikawa, I., Ono, Y., Imai, T., Suzuki, R., and Yoshie, O. (1999) A. An activation-responsive element in single C motif-1/lymphotactin promoter is a site of constitutive and inducible DNA-protein interactions involving nuclear factor of activated T cell. *J. Immunol.* 163, 3295-3303.
- Yoshida, T., Izawa, D., Nakayama, T., Nakahara, K., Kakizaki, M., Imai, T., Suzuki, R., Miyasaka, M., and Yoshie, O. (1999) B. Molecular cloning of mXCR1, the murine SCM-1/lymphotactin receptor. *FEBS Lett.* 458, 37-40.
- Zhang, H., Jiang, G.P., Zheng, S.S., Wu, L.H., Zhu, F., and Yang, Z.L. (2004). Lymphotactin enhances the in-vitro immune efficacy of dendritoma formed by dendritic cells and mouse hepatocellular carcinoma cells. *J. Zhejiang. Univ. Sci.* 5, 1255-1261.

Reference List

Zlotnik,A. and Yoshie,O. (2000). Chemokines: a new classification system and their role in immunity. *Immunity*. *12*, 121-127.

Abbreviations

A 647/700	Alexa Fluor 647/700
Ab	antibody
AEC	3-Amino-9-Ethylcarbazol
ATAC	Activation-induced, T cell-derived And Chemokine related molecules
BSA	bovine serum albumin
CD	cluster of differentiation
cDC	conventional DC
cDNA	complementary DNA
CFSE	5,6-Carboxyfluorescein Diacetat Succinimidyl Ester
cfu	colony forming unit
CTL	cytotoxic lymphocytes
Cy5	Cyanin 5
Da	Dalton
DAPI	4',6-Diamidino-2-Phenylindol
DAMPs	Damage associated molecular patterns
DC	Dendritic cells
DMSO	Dimethylsulfoxide
DNA	Deoxyribonucleic acid
E. coli	Escherichia coli
EDTA	ethylenediaminetetraacetic acid
ELISA	Enzyme Linked Immuno Sorbant Assay
ER	endoplasmic reticulum
FACS	Fluorescence Activated Cell Sorting
FCS	fetal calf serum
FITC	fluorescein isothiocyanate

Abbreviations

GAG	Glycosaminoglycans
GPCRs	G Protein-Coupled Receptors
HERDs	Heterogenous ectopic ribonucleoprotein derived structures
HIV-1	Human Immunodeficiency Virus type 1
HSV-1	Herpes simplex Virus type 1
Ig	immunoglobulin
IFN	Interferon
i.v.	intravenous
i.p.	intraperitoneal
LCs	Langerhans Cells
LN	Lymph Node
LPS	Lipopolysaccharides
mAb	Monoclonal Antibodies
MBL	Mannose Binding Receptors
MHC	Major histocompatibility complex
MHC-I	MHC class I
MHC-II	MHC class II
MLN	Mesenteric Lymph Node
MR	Mannose Receptor
mRNA	messenger ribonucleic acid
MZ	Marginal Zone
NMR	nuclear magnetic resonance
NK	Natural Killer cells
PALS	Periarteriolar Lymphoid Sheath
PAMPs	Pathogen associated molecular patterns
PBS	phosphate buffered saline

PCR	Polymerase Chain Reaction
pDC	Plasmacytoid DC
PE	Phycoerythrin
PI	Propidiumiodid
PMA	Phorbol-12 Myristate-13-Aceteate
PPs	Peyer's patch
PS	Pohsphatidylserine
qRT-PCR	quantitative Reverse transcriptase polymerase chain reaction
RANTES	Regulated on activation of normal T cell expressed & secreted
RNA	Ribonucleic acid
RNase A	Riboneclease
RT	Room temperature
TAP	Transporter associated with antigen presentation
TLR	Toll like Receptors
7-TM	7-Transmembrane
TNF	Tumor Necrosis Factor
YFP	yellow fluorescent protein
wt	wild type
β-ME	β-Mercaptoethanol

Acknowledgements

First of all, I would like to thank the Egyptian government and the El Azhar University for the scholarship program that gave me the opportunity to accomplish my PhD project in Germany.

I would like to thank all the people who supported me during my PhD project that was carried out at the Robert Koch-Institute in Berlin.

.My special thank to Prof. Dr. Richard A. KroczeK for proposing the interesting topic of this work and for the helpful discussions.

I would like to thank Prof. Dr. Peter M. Kloetzel at the Humboldt University in Berlin for his co-supervision.

Furthermore, I acknowledge Dr. Hans-Werner Mages and Dr. Volker Henn at the Robert Koch-Institute for their support in planning the experiments and analysing the data, as well as critical discussions.

A special thank to Dr. Andreas Hutloff, Dr. Stephanie Gurka, Dr. Sylvia Worbs, and Dr. Timo Lischke for constructive discussion and helpful technical advice.

I appreciate the great support provided by our technical assistants Ewa Kowalczyk, Katja Ranke, Petra Jahn und Monika Jaensch. A special thank to the entire P21 group for creating a good working atmosphere, and especially to Xuefei Zhou and Stefen Güttler for helping me in the lab.

I would like to thank the animal keepers in the Robert Koch Institute in Berlin for the reliable care of the mice, especially Frau Annette Dietrich, who was responsible for the LacZ mice breeding.

Finally, I would like to thank my family for the support and encouragement during my work.

Publications

Original publications

Brigitte G. Dorner, Martin B. Dorner, Xuefei Zhou, Corinna Opitz, **Ahmed Mora**, Steffen Güttler, Andreas Hutloff, Hans W. Mages, Katja Ranke, Michael Schaefer, Robert S. Jack, Volker Henn & Richard A. KroczeK; Selective expression of the chemokine receptor XCR1 on cross-presenting dendritic cells determines cooperation with CD8⁺ T cells. *Immunity* 2009. in press.

Conferences

A. Mora, X. Zhou, A. Bachem, H.W. Mages, V. Henn, R. A. KroczeK; Highly specific antigen targeting to CD8⁺ DC via the chemokine receptor XCR1. *2nd European Congress of Immunology*, 13.-16. September 2009 Berlin (poster)

X. Zhou, **A. Mora**, S. Güttler, H.W. Mages, V. Henn, R.A. KroczeK; Selective expression of the chemokine receptor XCR1 on CD8⁺ dendritic cells determines cooperation with CD8⁺ T cells. *2nd European Congress of Immunology*, 13.-16. September 2009, Berlin (poster)

C. Opitz, B. Dorner, M. Dorner, **A. Mora**, R.A. KroczeK; ATAC is an inflammatory chemokine with selective action on XCR1-expressing CD8⁺ dendritic cells. *2nd European Congress of Immunology*, 13.-16. September 2009, Berlin (poster/presentation)

Eidesstattliche Erklärung

Hiermit versichere ich, Ahmed Mora, geb. 27.12.1978 in Lyon, an Eides statt, die vorliegende Arbeit selbstständig und ohne unerlaubte Hilfe angefertigt zu haben und alle verwendeten Hilfsmittel und Quellen als solche ausgewiesen zu haben. Des Weiteren versichere ich, dass die vorliegende Arbeit nie in dieser oder anderer Form Gegenstand eines früheren Promotionsverfahrens war.

Die dem angestrebten Promotionsverfahren an der Mathematisch-Naturwissenschaftlichen Fakultät I der Humboldt-Universität zu Berlin zugrunde liegende Promotionsordnung ist mir bekannt.

Berlin, 16. November 2009